MULTI-SCALE DRIVERS OF WILDFIRE DANGER IN TEMPERATE EUROPE

ASSESSING WILDFIRE DANGER REQUIRES A MULTI-SCALE UNDERSTANDING OF DRIVERS AND DECISION-MAKING NEEDS

Kerryn Elizabeth Little

A thesis submitted to the University of Birmingham for the degree of DOCTOR OF PHILOSOPHY

School of Geography, Earth, and Environmental Sciences

College of Life and Environmental Sciences

University of Birmingham

December 2023

ABSTRACT

Wildfire danger is increasing within temperate ecosystems that have not historically been prone to extreme wildfires. To date, assessments of wildfire danger have typically been constrained to coarse spatial scales using systems that were developed within traditionally fire prone regions. However, the processes controlling wildfire danger operate across spatiotemporal scales, supporting the need for a more holistic approach to assessing wildfire danger that recognises the multi-scale requirements of different decision-making needs. An understanding of the underlying controls on components of wildfire danger is especially needed in understudied, emerging fire prone landscapes like the peatlands and heathlands of temperate Europe, where fine-scale heterogeneity can be important for wildfire danger and fuels differ to those in traditionally fire prone landscapes.

This PhD thesis examined the multi-scale drivers of wildfire danger in temperate Europe at the synoptic, landscape, and plot scales through four research papers, finding: (1) Europe-wide, extreme fire weather and wildfires are more likely to occur during persistent, anomalous atmospheric blocking. (2) Fuel moisture content is highly variable at the landscape level, creating on/off thresholding of live fuel availability for wildfire spread and vulnerability of the organic layer to smouldering combustion associated with landscape controls. (3) This cross-landscape fuel moisture variability significantly impacts simulated wildfire behaviour. (4) Among-sampler variability is a relevant source of measurement error in fuel moisture campaigns that is important to consider and account for to isolate fuel moisture dynamics at broad spatial scales.

This PhD thesis contributes to our understanding of the multi-scale processes controlling wildfire danger in temperate ecosystems by demonstrating that weather patterns at large spatial extents have a key impact on wildfire occurrence and surface fire weather in the synoptic temporal range. However, there is a clear need to understand landscape-level fuel moisture dynamics that are masked using current regional estimates. This is shown to be relevant for improving fire behaviour predictions in the dominant fuel types in temperate fire prone ecosystems by indicating that fire behaviour models are sensitive to fine-scale landscape fuel moisture variability. Finally, in a drive to scale-up fuel moisture field campaigns using measurements collected from different samplers, it has been possible to isolate the likely measurement error within intensive fuel measurement campaigns that are essential for understanding spatiotemporal fuel moisture dynamics. The results of this thesis have implications for wildfire preparedness, land and fire management decision-making, embedding citizen science into wildfire research, and understanding future wildfire risk. A holistic approach to wildfire danger research will ultimately allow for the development of fuel models, fire behaviour models, and wildfire danger rating systems that meet the diversity of decision-making needs and spatial complexity of wildfire danger both in temperate emerging fire prone regions and beyond.

ACKNOWLEDGEMENTS

I started this journey putting out fires. It is only fitting that the first people I thank are those who have taken on a similar role (figuratively) during my PhD. Thank you to my supervisors Prof Nick Kettridge and Dr Laura Graham for all their guidance and support in developing the research in this thesis, including fun research discussions, stats advice, for instilling the importance of doing ‘good research with good people’, and for including me in many research opportunities.

Thank you to those I have been lucky enough to work with over the past three years. There are too many of you to name, which I think reflects the sort of genuine, collaborative people you are. Special mention must go to the UK FDRS group, Mike Flannigan’s research group in Canada, and the PyroLife ESRs.

Thank you to the volunteers who assisted with field fuel sampling campaigns, and to the landowners, land managers, and gamekeepers across the North Yorkshire Moors who hosted field sites. Thank you to PyroLife Innovative Training Network (funded by the European Union’s Horizon 2020 research and innovation programme under the Marie Sklodowska-Curie grant agreement No 860787) for the funding and support I received to complete this PhD.

Thank you to Matt, for your unwavering support. I am sorry you lived in fear of being asked to help take down field equipment for the past three years. Finally, thank you to my family. Doing this from across the other side of the world to you has been the most challenging part of all, thank you for always encouraging me to follow my interests, wherever they might take me.

TABLE OF CONTENTS

LIST OF FIGURES

LIST OF TABLES

CANDIDATE'S CONTRIBUTION

Chapters 2–5 of this thesis contain the results of collaborative research. The specific contributions of the candidate are outlined below:

CHAPTER ONE: INTRODUCTION

Completed by the candidate.

CHAPTER TWO: PERSISTENT POSITIVE ANOMALIES IN GEOPOTENTIAL HEIGHT DRIVE ENHANCED WILDFIRE ACTIVITY ACROSS EUROPE

Authors: <u>Little, K</u>., Castellanos-Acuna, D., Jain, P., Graham, L., Kettridge, N. and Flannigan, M.

Status: Manuscript under review for special issue 'Novel Fire Regimes under Climate Changes and Human Influences: Impacts, Ecosystem Responses, and Feedbacks' of *Philosophical Transactions of the Royal Society B*

Candidate's contribution: The candidate conceived the research question, collected and analysed the data, interpreted the results, and wrote the manuscript. DC assisted with data collation and analysis. MF, PJ, NK, LG helped develop the research question, interpreted the results, and reviewed the draft manuscript.

CHAPTER THREE: LANDSCAPE CONTROLS ON FUEL MOISTURE VARIABILITY IN FIRE PRONE PEATLAND AND HEATHLAND LANDSCAPES

Authors: <u>Little, K.</u>, Graham, L., Flannigan, M., Belcher, C. and Kettridge, N.

Status: Published in *Fire Ecology* January 2024. The published manuscript can be found at https://doi.org/10.1186/s42408-024-00248-0.

Candidate's contribution: The candidate designed the experiment, collected and analysed the data, interpreted the results, and wrote the manuscript. LG and NK helped design the experiment, collected the data, advised on statistical analysis, and reviewed the draft manuscript. MF and CB reviewed the draft manuscript. Two anonymous peer-reviewers of *Fire Ecology* provided feedback on the manuscript during the submission process.

CHAPTER FOUR: DO CROSS-LANDSCAPE FUEL MOISTURE DIFFERENCES IMPACT EXPECTED FIRE BEHAVIOUR?

Authors: <u>Little, K.</u>, Graham, L., Ivison, K., Stoof, C., Belcher, C., Kettridge, N. and Cardil, A.

Status: Manuscript under review for *International Journal of Wildland Fire*

Candidate's contribution: The candidate conceived the research questions, analysed the data, interpreted the results, and wrote the manuscript. AC, NK, LG helped develop the methodology, interpreted the results, and reviewed the draft manuscript. KI, CS, CB made suggestions to present the results and reviewed the draft manuscript.

CHAPTER FIVE: ACCOUNTING FOR AMONG-SAMPLER VARIABILITY IMPROVES CONFIDENCE IN FUEL MOISTURE CONTENT ESTIMATES

Authors: <u>Little, K.</u>, Graham, L. and Kettridge, N.

Status: Published in *International Journal of Wildland Fire* December 2023. The published manuscript can be found at https://www.publish.csiro.au/wf/WF23078.

Candidate's contribution: The candidate designed the experiment, analysed the data, interpreted the results, and wrote the manuscript. NK and LG helped design the experiment, interpreted the results, and reviewed the draft manuscript. *International Journal of Wildland Fire* Editor-in-chief Stefan Doerr, Associate Editor Ali Bentley, and two anonymous peer-reviewers provided feedback on the manuscript during the submission process.

CHAPTER SIX: DISCUSSION

Completed by the candidate.

1

1 INTRODUCTION

1.1 EMERGING WILDFIRE PRONE LANDSCAPES

Fire is a natural part of most ecosystems and plays a critical role in maintaining ecosystem health (McLauchlan *et al.* 2020). However, recent years have seen an increase in wildfire risk associated with global climate and land use change, intensifying ecosystem, carbon, health, and societal impacts (Shuman *et al.* 2022). One aspect of this has been the emergence of increasing wildfire risk in temperate regions that have not historically been prone to large wildfires (Belcher *et al.* 2021).

Peatlands and heathlands are temperate landscapes that currently experience larger wildfires and frequent fire activity that does not map onto weather drivers, posing a threat to populations and a society with low wildfire awareness (Gazzard *et al.* 2016; Belcher *et al.* 2021; Cardíl *et al.* 2023). Temperate peatlands and heathlands are particularly vulnerable to wide-ranging environmental impacts under increased fire activity because they contain globally critical carbon stores (Page and Baird 2016; Kirkland *et al.* 2023). Peatlands store 550 gigatons of organic soil carbon globally, and approximately 0.19–0.88 million km^2 of these peatlands are found in the temperate latitudes (30–50 degrees) (Batjes 1996; Yu 2012).

Severe wildfires can result in smouldering combustion within peat soils and the release of carbon sequestered over a millennia into the atmosphere (Page and Baird 2016).

Emerging fire prone regions such as Northwestern Europe have been understudied compared to traditionally fire prone regions like Mediterranean Europe, Canada, and Australia. Current and future fire regimes in emerging fire prone regions are not well understood, and operational tools are being applied outside of the fuels and fire regimes they were originally developed for. Fire prevention, management capacity, and wildfire-specific policy is also underdeveloped, further compounding increases in wildfire risk under changing climate (Pandey *et al.* 2023). Many areas of Northwestern Europe have a large rural–urban interface, meaning that fires do not necessarily need to be large to have a significant impact on populations. Climate projections suggest that temperate environments will continue to experience increased wildfire activity associated with drier and warmer weather and drier fuels (Perry *et al.* 2022). It is essential to understand the controls on wildfire danger in these regions to develop wildfire prevention strategies.

1.2 WILDFIRE DANGER

Wildfire danger is defined as the combination of factors affecting the initiation, spread, and ease of control of a wildfire (Natural Resources Canada 2021). It is influenced by characteristics of fuels, topography, weather, and human-risk factors (Figure 1.1). By understanding the underlying controls on components of wildfire danger (as explored in this thesis, Figure 1.1), we can develop models that better reflect real-life systems.

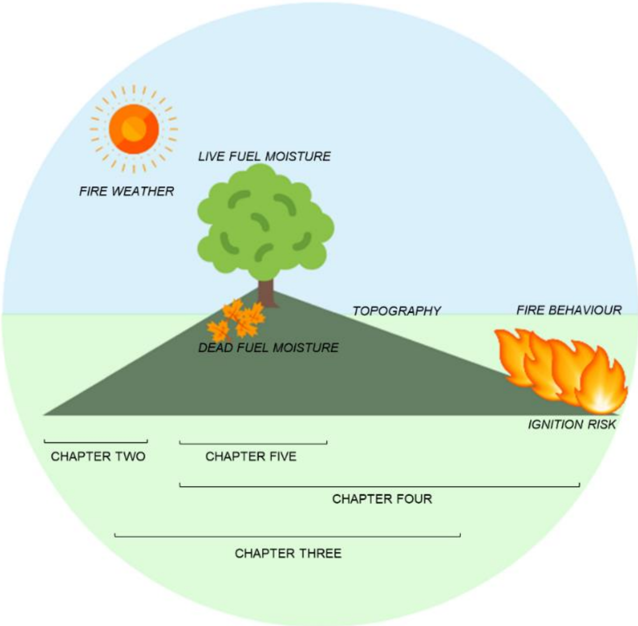

Figure 1.1 Key factors that control wildfire danger and the contribution of this thesis towards understanding the drivers of wildfire danger.

Fire behaviour describes how a fuel ignites and the development and consequent characteristics of the fire's spread. It is therefore an important component of assessing wildfire danger. The behaviour of a fire is influenced by fuels, weather, and topography, and fire behaviour models use simplified inputs of these to generate outputs of potential fire behaviour, including rate of spread (ROS), flame length, and fireline intensity (Finney *et al.* 2021). ROS is the speed at which a fire travels across surface fuels, and the maximum ROS refers to the speed at the head of the fire. Flame length is measured as the length from the midpoint within the active flame to the average flame point. Fireline intensity is the heat energy release per unit time (Andrews 2014).

Fuels are a key component of wildfire danger. Differences in plant species, arrangement, amount (fuel load), proportion of living to dead material, and moisture content can all influence fuel flammability, ignition probability, and fire behaviour (Matthews 2014; Scarff *et al.* 2021). In particular, fuel moisture content, i.e., the amount of water in vegetation as a percentage, is critical for determining whether an ignition will occur and spread. Dead fuel moisture describes the water content of dead vegetation, such as fallen twigs or litter. It reflects drying and wetting cycles and responds to the relative humidity of the air and unlike live vegetation, it is unable to regulate its moisture content (Matthews 2014). Live fuel moisture describes the water content of living vegetation and is also impacted by plant physiological responses and carbon dynamics (Dickman *et al.* 2023). Live vegetation is an important component of fuel availability in temperate environments. This is particularly true for peatland and heathland landscapes where live fuel moisture can strongly influence ignitability during certain seasons, for example it is typically lowest in spring, where these ecosystems see increased fire frequency (Belcher *et al.* 2021).

The fuel, weather, topographic, and human-risk factors that influence wildfire danger are core components of wildfire danger rating systems (FDRS), which can be used to predict fire weather, fire occurrence, and fire behaviour, and provide a quantitative and qualitative assessment of potential wildfire danger (Natural Resources Canada 2021). FDRS are important tools for communicating wildfire danger to the public and informing decision-making within policy and the fire management sector (Zacharakis and Tsihrintzis 2023). Research into understanding the underlying controls on wildfire danger can be translated into developing tailored FDRS.

Empirical models have been developed to capture the factors impacting wildfire danger, but these have largely been developed in fire prone forested landscapes where meteorological drivers dominate (Matthews *et al.* 2019; Natural Resources Canada 2021; Zacharakis and Tsihrintzis 2023). In lieu of fully integrated FDRS, Fire Weather Indices (FWIs) that are based on fuel moisture and antecedent weather conditions have been explored for regions with different fuel types, including the United Kingdom, to capture meteorological wildfire danger (de Jong *et al.* 2016). For example, the Met Office Fire Severity Index (MOFSI) is largely based around the Canadian FWI (Met Office 2023), and others have used FWIs to forward prediction aspects of wildfire risk in the UK (Arnell *et al.* 2021; Perry *et al.* 2022). However, indices based on meteorological controls do not capture spring wildfire danger well as phenological, landscape, and ecohydrological controls are also likely important to consider in these environments (Davies and Legg 2008; Belcher *et al.* 2021). There are opportunities to apply lessons learned from countries with a longer fire history to emerging fire prone regions. However, there is a need to understand the underlying science to inform what can be applied from other regions, what needs to be adapted first, and what needs to be tailored.

1.3 WILDFIRE DANGER ACROSS SPATIAL SCALES

Perhaps due to the development of FDRS in traditionally fire prone regions, wildfire danger is typically considered at the coarse spatial resolution that existing tools have been designed for (Matthews *et al.* 2019). This demonstrates the conflation between what existing wildfire danger models are currently capable of and real-life system processes. This discrepancy is particularly relevant in the context of emerging fire prone environments, where fine resolution landscape heterogeneity can be relevant for fire behaviour. We do not yet fully understand the processes controlling wildfire danger to be able to develop functional models for decision making (Belcher *et al.* 2021).

In this PhD thesis, I present a multi-scale conceptual framework for considering wildfire danger, recognising that different spatial scales may be required for different user needs—assessing wildfire danger is not a 'one size fits all' approach (Figure 1.2). Considering controls at multiple spatial scales provides a more holistic understanding of the processes driving wildfire danger. Such an approach will aid the development of functional wildfire danger assessments that better reflect real-life processes. Furthermore, understanding the benefits and pitfalls of applying systems at particular spatial scales will help to use fit-for-purpose systems to answer research questions, make management decisions, and communicate wildfire danger.

Within this PhD thesis, synoptic scale refers to upper air atmospheric circulation conditions that vary spatially across 1000's of km and in the temporal range of several days to weeks (Barry and Carleton 2001). Landscape scale is defined as the scale that encompasses the range of variability in topographic, soil, and land cover characteristics within a given regional climate. Within this PhD thesis, plot scale refers to the fine-scale 20 x 20 m extent of homogeneous vegetation stands that were defined by previous land management activities. Within-plot variability in the age, structure, and management of plants as well as landscape characteristics is minimised in favour of exploring fine-scale fuel moisture dynamics that are masked at coarser resolutions.

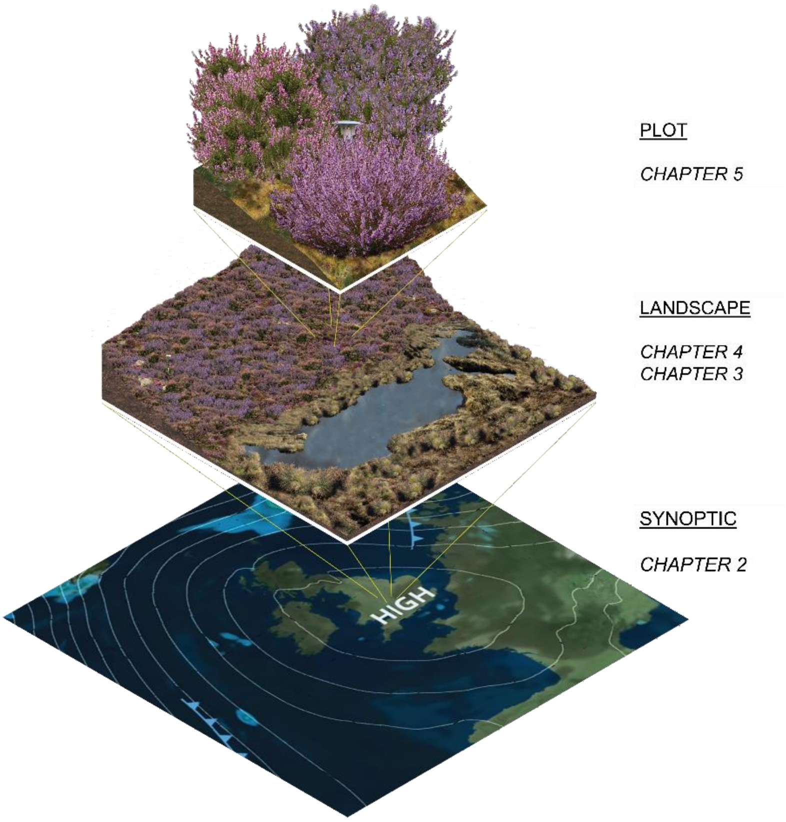

Figure 1.2 The spatial scales at which controls on wildfire danger are examined in this thesis.

Synoptic scale

The high spatiotemporal variability of point-to-point surface fire weather observations makes it difficult to generate reliable forecasts beyond the short term (4–7 days). Longer-varying synoptic-scale circulation patterns by contrast can be more reliably predicted in the medium range (+10 days) as they do not include the complexity of land surface and boundary layer effects (Hohenegger and Schär 2007). Understanding how synoptic circulation patterns like atmospheric blocking impact surface fire weather and wildfire activity may therefore open opportunities to improve near-term forecasting of wildfire dangerous conditions (Pfahl and Wernli 2012; Papavasileiou and Giannaros 2023). Improved forecast lead times aid effective decision making, including wildfire preparedness and resource allocation/movement during extended, extensive periods of extreme fire weather that may overwhelm suppression resources (Bloem *et al.* 2022).

Landscape scale

Existing regional-scale wildfire danger assessments do not capture the high spatial variability in fuel moisture content at the landscape scale. Consequently, wildfire danger assessments do not account for fuel-driven within-landscape vulnerability to wildfires and may not reflect local conditions (Nyman *et al.* 2018; Matthews *et al.* 2019). Furthermore, fire behaviour predictions based on a single regional average fuel moisture estimate could underpredict expected fire behaviour and create dangerous situations for those suppressing wildfires or increase the risk of escaped managed burns (Duane *et al.* 2021; Dickman *et al.* 2023).

Understanding the drivers of fuel moisture variability at the landscape scale provides opportunities to enhance the spatial resolution of regional fuel moisture estimates using downscaling techniques (Nyman *et al.* 2014). Cross-landscape differences in fire behaviour and wildfire danger are particularly relevant to consider in emerging fire prone landscapes, where fire behaviour, including wildfire spread through live fuels and smouldering combustion of organic soils, can be influenced by fine-scale spatial heterogeneity in landscape characteristics (Finney *et al.* 2021). It is therefore important to understand fuel moisture dynamics at the landscape scale to develop appropriate fuel models for inclusion in wildfire danger assessments in temperate ecosystems.

Plot scale

Extensive direct fuel moisture measurement campaigns across broad spatial extents are necessary to capture the spatiotemporal complexity of fuel moisture dynamics for developing fuel models, especially in emerging fire prone regions where cross-scale fuel moisture dynamics are not fully understood. Such campaigns require multiple people to cover the spatial extent of sampling required, but this introduces systematic differences in measurements between samplers (Bird *et al.* 2014; August *et al.* 2020). Plot-scale field campaigns can be used to experimentally quantify sources of variability in fuel moisture in order to improve our scientific understanding of fuel moisture dynamics and our ability to isolate spatial fuel moisture variability from other sources of measurement error (Little *et al.* 2023). Furthermore, understanding fuel moisture variability associated with among-sampler differences at the plot scale allows us to capitalise on citizen science opportunities to understand fuel moisture dynamics at broad spatiotemporal scales that cannot be captured by traditional, controlled field experiments (Dickinson *et al.* 2010; Arazy and Malkinson 2021).

1.4 RESEARCH GAPS

There is a need to develop a multi-scale understanding of the processes influencing components of wildfire danger. This underlying science is needed to develop functional models for decision making needs at relevant spatial scales. This research is especially needed in emerging fire prone regions where wildfire danger is less understood, and fuels and fire regimes differ to traditionally fire prone regions. Examining the multi-scale controls on wildfire danger will allow us to understand where existing systems fall short and why, as well as what information is needed to develop systems that are functional for the variety of purposes and users they serve.

The following are identified as key research areas for wildfire danger research across spatiotemporal scales (detailed literature reviews given in Chapters 2–5).

1. The extent to which persistent anomalous atmospheric blocking patterns are important for surface fire weather and wildfire activity across the diverse fire regimes and human-dominated ignitions within Europe is relatively unknown. Disentangling synoptic–fire relationships offer opportunities to develop medium-range forecasting of wildfire dangerous conditions and understand future wildfire risk under climate change (Chapter 2).
2. Fuel moisture content is highly spatially variable, but the extent and drivers of this variability within landscapes are unknown. Capturing fuel moisture complexity is especially important in peatland and heathland landscapes where spatial discontinuity can impact fire behaviour. Cross-landscape direct fuel moisture campaigns are rare and have not been conducted in temperate peatlands and heathlands. Current understanding of the landscape controls on fuel moisture content is mainly limited to forested fuels and landscapes (Chapter 3).
3. Understanding of the extent to which cross-landscape fuel moisture variability impacts simulated fire behaviour in operational fire behaviour models is limited. The ability of existing temperate fuel models and fire behaviour models to adequately capture landscape complexity is also questionable. Research is needed to understand

fire behaviour across the observed range of fuel moisture conditions in peatland/heathland landscapes (Chapter 4).

4. Systematic differences in fuel moisture content measurements between samplers is a relevant source of measurement error in broad spatial scale field measurement campaigns seeking to capture fuel moisture dynamics. The extent of uncertainty in measured fuel moisture related to among-sampler variability is unknown and currently limits the potential to optimise citizen science in fuel-related wildfire research (Chapter 5).

1.5 AIMS AND OBJECTIVES

This PhD thesis aims to assess the multi-scale drivers of wildfire danger from synoptic scale controls on surface fire weather and wildfires across Europe (Chapter 2) to the controls on fuel moisture variability in a temperate peatland and heathland landscape (Chapters 3–5). To address the overarching aim, each chapter also comprises their own specific aims:

Chapter 2 aims to examine the association between PPAs and surface fire weather and wildfire activity across Europe between March and August 2001–2021.

Chapter 3 aims to assess the range of variability in the live and dead fuel moisture content of *Calluna vulgaris* across a temperate fire prone landscape and examine the relative contributions of landscape and micrometeorological drivers of fuel moisture variability at the landscape scale.

Chapter 4 aims to examine the impact of cross-landscape fuel moisture variation on predicted fire behaviour across a temperate peatland and heathland landscape using direct fuel moisture content measurements in BehavePlus simulations.

Chapter 5 aims to determine the magnitude and variability of among-sampler variability in measured fuel moisture at the plot scale within a *Calluna vulgaris* dominated temperate fire prone landscape.

1.6 THESIS LAYOUT

This thesis is laid out as a series of research papers. Chapters 2–5 address individual research questions and can be read in isolation from the other chapters. Each chapter contains an introduction to the relevant literature and research gaps, methodology, results, discussion, and conclusions. Chapter 6 synthesises the key findings of the preceding chapters in the thesis and outlines future research directions. The References and Supplementary Materials for all chapters are presented at the end of the thesis.

2

2 PERSISTENT POSITIVE ANOMALIES IN GEOPOTENTIAL HEIGHT DRIVE ENHANCED WILDFIRE ACTIVITY ACROSS EUROPE

ABSTRACT

Persistent positive anomalies in 500 hPa geopotential height (PPAs) are upper-air circulation patterns associated with surface heatwaves, drought, and consequently fuel aridity, elevated fire weather, and active wildfires. I examined the association between PPA events and surface fire weather and burned area at a pan-European level. Europe-wide, extreme fire weather and wildfires were on average 4.3 and 2.7 times more likely to occur concurrently with a PPA, respectively. PPAs were associated with 28% of pan-European area burned between March and August 2001–2021, and there was a latitudinal increase in the percentage of area burned during PPAs up to 49% over Northern Europe. Burned area was highest in the three days following PPA presence, and fuel moisture indices from the Canadian Fire Weather Index System lagged behind peak PPA strength, demonstrating the role of PPAs in pre-drying fuels. PPAs have been associated with significant wildfire events experienced across Europe, including the 2017 Portugal wildfires, the 2018 UK, Sweden, and Finland wildfires, and the 2021 Greece wildfires. My findings demonstrate opportunities for

developing early warning systems of wildfire danger, having implications for wildfire awareness and preparedness, informing policy, and wildfire management decisions like early mobilisation and resource sharing initiatives within and across Europe.

2.1 INTRODUCTION

Global climate change is increasing the risk of co-occurring fire weather extremes across large geographic regions (Abatzoglou *et al.* 2021). Recent extreme wildfire seasons across Europe have demonstrated how long duration synoptic weather patterns promote synchronous surface fire weather extremes that can strain firefighting resources and even overwhelm response capabilities (Bloem *et al.* 2022).

In the Northern Hemisphere mid-latitudes, surface weather is driven by the west to east progression of synoptic-scale weather systems. Anticyclonic blocking highs and ridges disrupt the usual zonal airflow for an extended period, leading to hot, dry surface weather (Rex 1950). Where these systems persist, they can lead to extreme events such as heatwaves and drought (Pfahl and Wernli 2012; Tuel *et al.* 2022; Rousi *et al.* 2022). Persistent Positive Anomalies in 500 hPa geopotential height (PPAs) are associated with a range of such blocking patterns, characterised by weakened or reversed zonal flow and persistent, large anticyclonic anomalies (Elliott and Smith 1949; Dole and Gordon 1983). Clear-sky radiative forcing, atmospheric subsidence, and associated adiabatic warming during PPAs results in extreme surface temperatures, which may be amplified by land–atmosphere feedbacks including soil moisture deficits and snow cover changes (Pfahl and Wernli 2012; Tuel *et al.* 2022; Rousi *et al.* 2022). PPAs have been associated with notable heatwaves and droughts throughout Europe, including the 2003 heatwave that led to an estimated 70,000 deaths in Europe (Robine *et al.* 2008).

PPAs are also important for wildfires. Associated extremes in surface fire weather create conditions conducive to the pre-drying of fuels, sustained ignition of wildfires, and their subsequent behaviour (Skinner *et al.* 2002; Zhao and Liu 2019; Sharma *et al.* 2022). Moreover, atmospheric subsidence can lead to poor surface air quality from wildfire smoke trapped at the surface, with the potential to impact densely populated regions such as the air pollution events in Russia during the 2010 heatwave (Konovalov *et al.* 2011). PPAs have recently been directly associated with wildfire activity in western North America (Sharma *et al.* 2022). Wildfires were on average seven times more likely to start during PPAs and were even more likely at higher latitudes (eight-fold increase above 50°N). Whether these relationships also hold for the diversity of fire behaviour and human-dominated ignitions across Europe have to date been unknown.

Weather can influence fire occurrence and behaviour at different spatiotemporal scales. Relationships between surface fire weather and wildfire regimes have been well documented at global (Ellis *et al.* 2022) and regional levels (Fernandes 2019). While the Canadian Fire Weather Index System (CFWIS) is used widely across Europe to assess fire weather, this system is not as effective for some of the emerging fire prone regions of Europe with different fuels the system was not developed for (Taylor *et al.* 2021). Assessing synoptic indicators of wildfire activity in addition to surface fire weather indices may prove more insightful for forecasting fire weather.

Operationally, surface weather observations are used to monitor wildfire danger; however, their high spatiotemporal variability makes it difficult for numerical weather prediction systems to generate reliable forecasts beyond the short term (4–7 days). Longer-varying synoptic-scale circulation patterns by contrast can be more reliably predicted in the medium range (+10 days) as they do not include the complexity of land surface and boundary layer effects. Previous research found that the predictability error of a 10-day synoptic forecast was equivalent to a one-day convective-scale forecast (Hohenegger and Schär 2007). Understanding how PPAs impact wildfire across Europe may therefore open opportunities to improve our near-term forecasting of wildfire dangerous conditions. Improved forecast lead times aid effective decision making, including wildfire preparedness and resource allocation/movement. Advanced warnings of elevated wildfire risk are useful both within and across agencies and countries.

Studies linking synoptic-scale circulation patterns directly to wildfire activity have mainly focused on specific wildfire events and seasons (Papavasileiou and Giannaros 2023; Rodrigues *et al.* 2023) or weather typing for specific regions (Drobyshev *et al.* 2021; Rodrigues). Giannaros and Papavasileiou (2023) recently related extreme fire weather to blocking over northern Europe and subtropical ridging over southern Europe. Their findings highlighted the importance of positive upper air geopotential height (Z500) anomalies at a continental scale. There is therefore a need to narrow in on the specific synoptic circulation drivers of surface wildfire activity across Europe. Moreover, the exact mechanisms by which these systems influence surface wildfire activity are still debated, including the role of the position of the anomaly and event breakdown (Shepherd 2014). There is scope for a pan-European analysis of the role of PPAs in driving wildfires, as the large spatial and temporal nature of PPAs may constrain wildfire response capabilities across political borders for an extended period. Such a scenario occurred during the exceptional 2023 wildfire season in Canada that experienced persistent blocking ridges in both the west and east, stretching firefighting resources beyond their limits across the country (Barnes *et al.* 2023). Across Europe, the European Civil Protection Pool and RescEU reserve pool of firefighting assets provide shared resources where national resources are overwhelmed, including firefighting appliances, aircraft, and ground crews. Resource sharing is coordinated by the European Union Civil Protection Mechanism (ICF 2014; Bloem *et al.* 2022). Understanding the spatiotemporal extent of PPAs across Europe can provide insights for coordinating pan-European wildfire response and resource allocation.

There is significant uncertainty surrounding how large-scale synoptic weather patterns will be affected by future changes in climate. There is some evidence that the conditions conducive to PPA formation will become more common in the future with weakening of the jet stream (Francis and Vavrus 2015). High-latitude anthropogenic warming during summer may lead to increased occurrence of double jets between atmospheric blocks (Rousi *et al.* 2022). However, whether we are currently observing a weakened jet stream is still actively debated (Blackport and Screen 2020). Other models predict a decrease in blocking frequency (Davini and D'Andrea 2020). Representation of atmospheric dynamics such as PPAs in climate models is poor, and the physical mechanisms of PPA response to anthropogenic warming are still debated (Shepherd 2014; Manning *et al.* 2023). As such, it is critical to first understand how atmospheric circulation patterns like PPAs drive wildfire activity in the present.

I examine the association between PPAs and burned area across Europe between March and August 2001—2021 by addressing the following research questions: (1) what are the characteristics of European PPA events? And (2) to what extent are PPAs associated with surface fire weather and wildfire activity across Europe?

2.2 METHODS

2.2.1 STUDY REGION

I applied a bounding box of 30°N to 75°N and -50°E to 60°E to detect and track PPA events at a pan-European level. Dijkstra *et al.* (2022) estimated ca. 96.5 ± 0.9% of burned area across Europe is started by anthropogenic activities, while lightning ignitions can be regionally important, such as for the high latitudes of Scandinavia. Fire regimes (area burned and seasonality) within Europe are spatially variable (Figure 2.1a; Figure S2.1), but climate and land use change are impacting wildfire occurrence and behaviour across the continent (Fernandez-Anez *et al.* 2021; Galizia *et al.* 2023). Southern European countries are traditionally fire prone but are experiencing new fire phenomena and extremes associated with climate, land use, and social change (Fernandez-Anez *et al.* 2021). The temperate and boreal regions of Western and Northern Europe are emerging fire prone regions that contain globally critical carbon stores and are experiencing increasing wildfire risk (Belcher *et al.* 2021; Cardíl *et al.* 2023).

I present PPA–fire associations by four geographical regions: Northern, Southern, Eastern, and Western Europe (Figure 2.1b). I use these broad geographically grouped regions to capture synoptic-scale patterns that are spatially contiguous. In doing so, I aim to capture the synoptic signal of PPA–fire relationships, despite the variability of wildfire occurrence across Europe associated with local effects like vegetation cover, fire management strategies and policies, and ignition sources. In addition to the main regional analyses, I include PPA–fire associations by country in the Supplementary Material to help understand country-level patterns within the four geographical regions. I excluded three far Eastern European countries (Republic of Türkiye, Ukraine, and Belarus) from my analyses due to the large number of agricultural fires that could not be accounted for within the scope of this research (Boschetti *et al.* 2019; Hall *et al.* 2021).

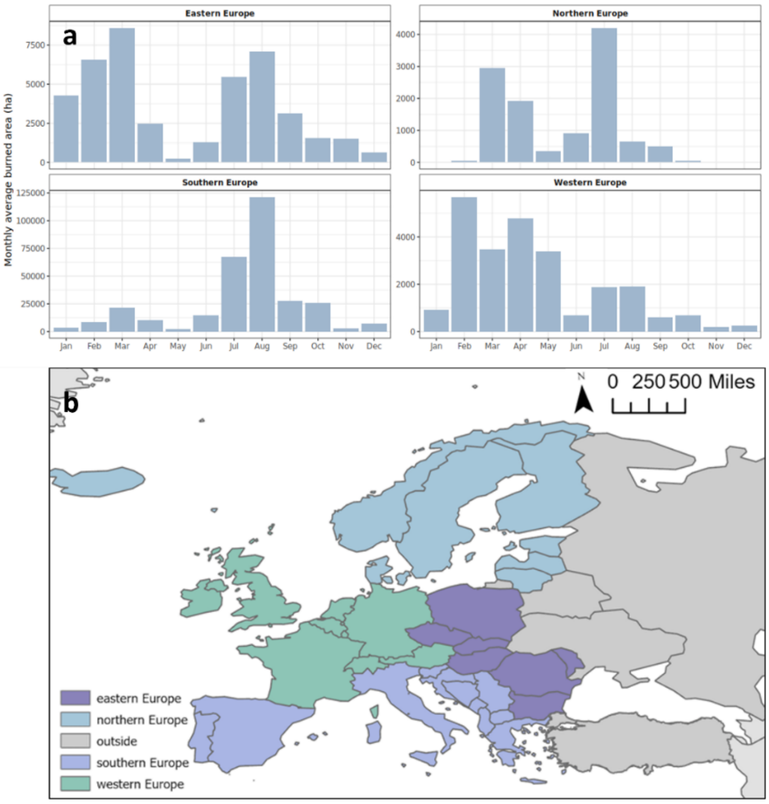

Figure 2.1 Average monthly burned area by region (a). Map of Europe and the four geographical regions used to associate PPAs with surface fire weather and burned area (b). Countries with no 2001–2021 MODIS wildfire records were excluded from the regional analyses of PPA–burned area associations. 'Outside' refers to areas where surface fire weather and wildfire activity were not examined in these analyses.

2.2.2 DATA

<u>Atmospheric data</u>

I used gridded 500 hPa geopotential height (Z500) and surface variables from the European Centre for Medium-Range Weather Forecasts (ERA5) global reanalysis dataset, extracted for the study area between the calendar spring and summer (March–August) 2001–2021 (Hersbach *et al.* 2020). Hourly surface variables included were accumulated precipitation, 2-

m air temperature and relative humidity, and 10-m meridional and zonal wind components. From these data I calculated vapour pressure deficit (VPD). Midday (local grid-cell time zone) values of the ERA5 surface variables were extracted to calculate the Canadian Fire Weather Indices (Van Wagner 1987). The Canadian Fire Weather Index System (CFWIS) describes the effects of fuel moisture and weather on fire behaviour and outputs comprise the fine fuel moisture code (FFMC), duff moisture code (DMC), drought code (DC), initial spread index (ISI), build up index (BUI), and the fire weather index (FWI). The first three codes refer to the moisture conditions of the litter, top organic layer, and deeper soil layer with increasing equilibrium drying times of 16-h, 2-weeks, and 53 days, respectively. The last three codes are fire behaviour indices, describing the expected rate of spread (ISI), amount of fuel available (BUI), and an overall rating of fire intensity (FWI). I defined extreme fire weather (FWIx) as days exceeding the 95th percentile of FWI values for each grid cell for the fire season, as this definition has been widely used in fire–climate research to characterise extreme fire weather and large wildfires have been found to occur under such extremes (Richardson *et al.* 2021; Jain *et al.* 2022; Sharma *et al.* 2022; Giannaros and Papavasileiou 2023).

ERA5 atmospheric variables were aggregated from 0.25x0.25 to 1x1 degree spatial and daily average temporal resolutions as synoptic patterns, including PPAs, are sufficiently resolved at this resolution (Barnes *et al.* 2012; Liu *et al.* 2018; Sharma *et al.* 2022). Anomalies of surface variables were calculated by subtracting daily values from the long-term climatological mean for the study period (2001–2021).

Wildfire data

I obtained burned area records for my study region from the database provided by the European Forest Fire Information System (EFFIS) for the period March–August 2001–2021 (EFFIS 2023). In selecting this time window, I capture the peak rates of cumulative number of wildfires and burned area for spring and summer Europe-wide (San-Miguel-Ayanz *et al.* 2023), though I recognise this may exclude late summer wildfires and winter wildfires that can occur outside of this primary window of interest (Resco de Dios *et al.* 2022). EFFIS burned area polygons are mapped by the Moderate Resolution Imaging Spectroradiometer (MODIS) on the TERRA and AQUA satellites at 500 m resolution twice daily and have been further refined by Sentinel-2 imagery since 2018 to 250 m. The database captures wildfires greater than 30 ha across Europe, representing ca. 95% of the total annual burned area in the European Union, making it suitable for analysing large wildfires at the pan-European level (San-Miguel-Ayanz *et al.* 2012). I summed daily burned area polygons within each 1x1 degree grid cell, where the date used is the initial date of the wildfire detection and burned area is total burned area (in hectares; ha) per grid cell. I did not apply a burned area threshold to my main analyses (aside from the size detectable by MODIS) due to the lower total number of available records and smaller overall wildfire size in some regions. I acknowledge this may result in some biases at the lowest burned areas depending on detection efficiency and the presence of false negatives.

2.2.3 PPA IDENTIFICATION

I used the PPA algorithm of Sharma *et al.* 2022 (adapted from Miller *et al.* 2020) to detect and track PPA events, adjusting the minimum size from 80,000 km^2 to 40,000 km^2 to fit the smaller land area covered by the study area. A brief description of the algorithm is as follows (for full details see Sharma *et al.* 2022). I first calculated daily Z500 anomalies for each grid cell and applied a 5-day moving mean and latitude correction factor to properly account for atmospheric energy dispersion (Dole and Gordon 1983). Because I am most interested in PPA events during the main wildfire seasons when pressure gradients are weaker compared to winter, I used the daily varying mean standard deviation of the geopotential height anomaly in a 4-week moving window to define a seasonally-varying threshold for magnitude. Grid cells that exceeded a given threshold for both magnitude and duration criteria were identified as PPA grid cells. Here I used a minimum magnitude of 1x standard deviation and minimum duration threshold of five days. Subsequently, the geometric centroid of spatially contiguous PPA grid cells were tracked until they reached a size of 40,000 km^2, at which point they were labelled as an individual PPA event. I also assessed the sensitivity of the algorithm to different thresholds. While the algorithm was relatively insensitive to magnitude and size, it was affected most by the duration, so I selected five days to exclude shorter events (Table S2.1).

2.2.4 PPA–FIRE CLASSIFICATION

I categorized each day as either PPA–fire, PPA–nofire, noPPA–fire, or noPPA–nofire for each grid cell in my spatial domain (Table 2.1) as follows. I defined PPA–fire days as the presence of a PPA during or up to five days prior to a wildfire event (initial day of burned area recorded) for each grid cell, with the lag accounting for the role of PPA conditions in pre-drying fuels that may subsequently ignite. I used the same approach to define PPA–extreme fire weather days as PPA–FWIx, PPA–noFWIx, noPPA–FWIx, or noPPA–noFWIx for each grid cell; however, I confined PPA–FWIx days to presence of a PPA on the same day as extreme FWI recorded (i.e., zero time lag).

Table 2.1 Each daily grid cell record is categorised as a PPA–fire, PPA–nofire, noPPA–fire, or noPPA–nofire day to define PPA-fire associations, and a PPA–FWIx, PPA–noFWIx, noPPA–FWIx, or noPPA–noFWIx day to define PPA-FWIx associations.

Category	Definition
PPA–fire	Presence of a PPA during or up to five days prior to a wildfire event.
PPA–nofire	The presence of a PPA in a grid cell is not coincident with a wildfire event during or up to five days following a PPA.
noPPA–fire	A wildfire event is recorded but is not associated with the presence of a PPA.
noPPA–nofire	There is no PPA or wildfire activity recorded.
PPA–FWIx	Presence of a PPA coincident with extreme surface FWI values (above the 95th percentile).
PPA–noFWIx	The presence of a PPA in a grid cell is not coincident with extreme FWI values.
noPPA–FWIx	Extreme FWI is recorded but not associated with the presence of a PPA.
noPPA–noFWIx	There is no PPA or extreme FWI recorded.

2.2.5 STATISTICAL ANALYSES

I used linear regression models for each grid cell by month to examine differences in surface weather anomalies between PPA and non-PPA days. In these models the surface weather anomaly was the dependent variable, and the independent variable was a 2-level categorical variable detailing whether a day is PPA or non-PPA. The residuals of the models were normally distributed, as assessed visually by Q-Q plots, and did not display heteroscedasticity. I presented the monthly average t-statistic for the regression slope from the linear model for each grid cell, where positive values depict larger surface anomalies on PPA days. I chose the t-statistic of the slope, rather than the slope itself because this means the values are comparable.

I examined the lead-lag relationship between maximum PPA strength and daily surface anomalies to examine the response of surface conditions to PPAs. The PPA area on the day of maximum PPA strength was used for calculating spatially averaged surface anomalies, for 15 days prior to and following the day of maximum strength. I calculated PPA strength as the daily summed area-weighted magnitude. This differs slightly from Sharma *et al.* 2022's definition, as I explicitly incorporate the effect of latitude on grid cell area from mid to high latitudes in my calculation.

I generated descriptive statistics to summarise PPA events in Europe and their association with wildfire activity as per Sharma *et al.* (2022). The odds ratio (OR) is a measure of the likelihood that an outcome (extreme fire weather or wildfire activity) will occur given the presence of an exposure (PPA), compared to the likelihood of the outcome occurring without an exposure (Agresti 1999). I calculated the odds ratio to determine the association between PPAs and wildfire activity, where a = PPA–fire, b = PPA–nofire, c = noPPA–fire, and d = noPPA–nofire (Equation 2.1). Using the same equation, I calculated the OR for the association between PPAs and extreme fire weather, where a = PPA–FWIx, b = PPA–noFWIx, c = noPPA–FWIx, and d = noPPA–noFWIx.

$$OR = \frac{a \times d}{b \times c} \qquad \text{[Eq.2.1]}$$

I used a partial Haldane Correction to address the issue of cells containing zero values leading to errors in the reported OR and to minimise the estimation bias of the OR. This involves adding a correction factor to all values in the contingency table where there are any zero values (Greenland *et al.* 2000). A correction factor of +2 can be used to minimise estimation bias of small sample sizes such as in this dataset (Table S2.2) (Agresti 1999). I applied a correction factor of +2 to all the values in the OR calculation where grid cells contained a zero value for (c) (i.e., all fire activity occurred during a PPA) to obtain a sensical value of the PPA–fire association. I similarly applied a correction factor of +2 where normal OR values were obtained (i.e., cells with no zero values) to allow comparability between these two scenarios. Grid cells that did not experience any fire between 2001–2021 returned no real OR value and are not suitable for exploring PPA–fire relationships. Therefore, no correction was added to these cells so they would be excluded from subsequent descriptive statistics. Where grid cells contained a zero value for (a) (i.e., no fire activity occurred during a PPA), the resulting OR value is zero, which is reflective of the lack of PPA–fire association, so no correction was added to these cells. I calculated the OR for each grid cell and month using counts of the daily timeseries of records as defined in Table 2.1. I presented summary statistics of the grid-cell level OR by region (and by country in the Supplementary Material) to reduce the sensitivity of the reported OR to individual grid cells. I also calculated the OR for the association between PPAs and extreme fire weather following the above approach. The PPA algorithm and all statistical analyses were carried out in R version 4.1.2 (R Core Team 2022), using packages igraph (Csardi and Nepusz 2006), Raster (Hijmans 2022a), Terra (Hijmans 2022b), and zyp (Bronaugh and Werner 2019).

2.3 RESULTS

2.3.1 CHARACTERISTICS OF EUROPEAN PPAS

I identified 514 PPA events between March–August 2001–2021 across Europe (an average of 24.5 events per year), and the median event duration was 10.2 days (Figure S2.2). July and August had the highest percentage of PPA days, which were centred over Scandinavia and the North Atlantic Ocean, respectively (Figure 2.2).

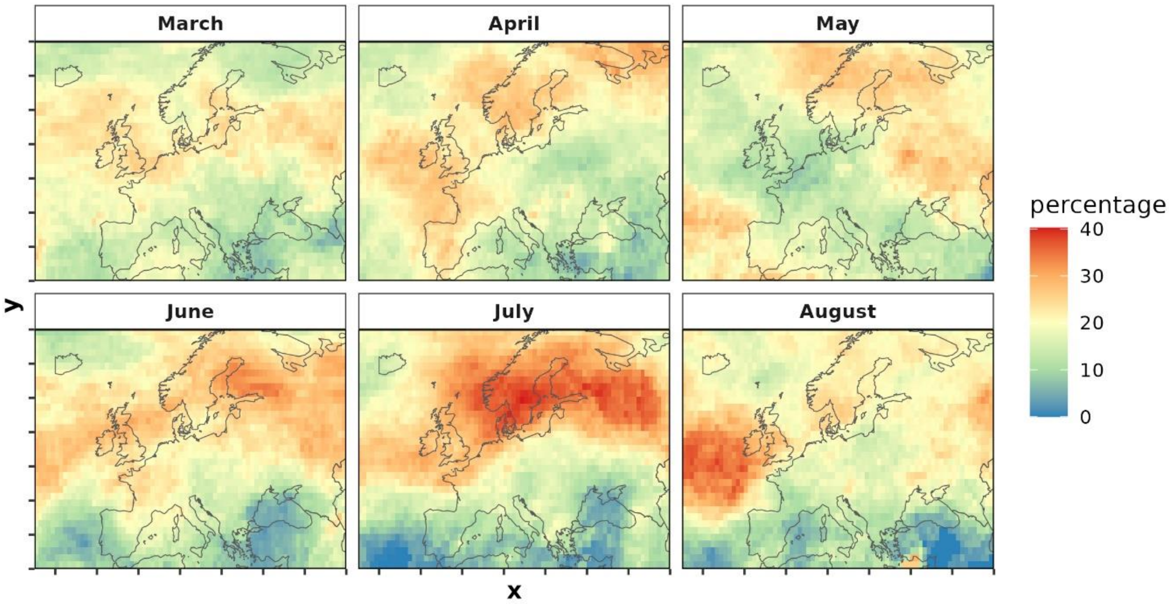

Figure 2.2 Average monthly percentage PPA days for each grid cell across the pan-European spatial domain of 30°N to 75°N and -50°E to 60°E, 2001–2021.

2.3.2 PPAS AND SURFACE FIRE WEATHER

Anomalies of surface air temperature (Temp) and VPD are greater for PPA days than non-PPA days, while wind speed anomalies (WS) are lower during PPAs. These relationships are consistent across Europe, though anomalies are greatest in central and northern Europe (Figure 2.3). The FWI, FFMC, and ISI are higher for PPA days but not to the same extent as the surface meteorological variables. DC and DMC anomalies are greater on PPA days for parts of central and Northern Europe but are lower for parts of Southern and Western Europe compared to non-PPA days. PPA–non-PPA differences were stronger during summer than spring months (Figure S2.3).

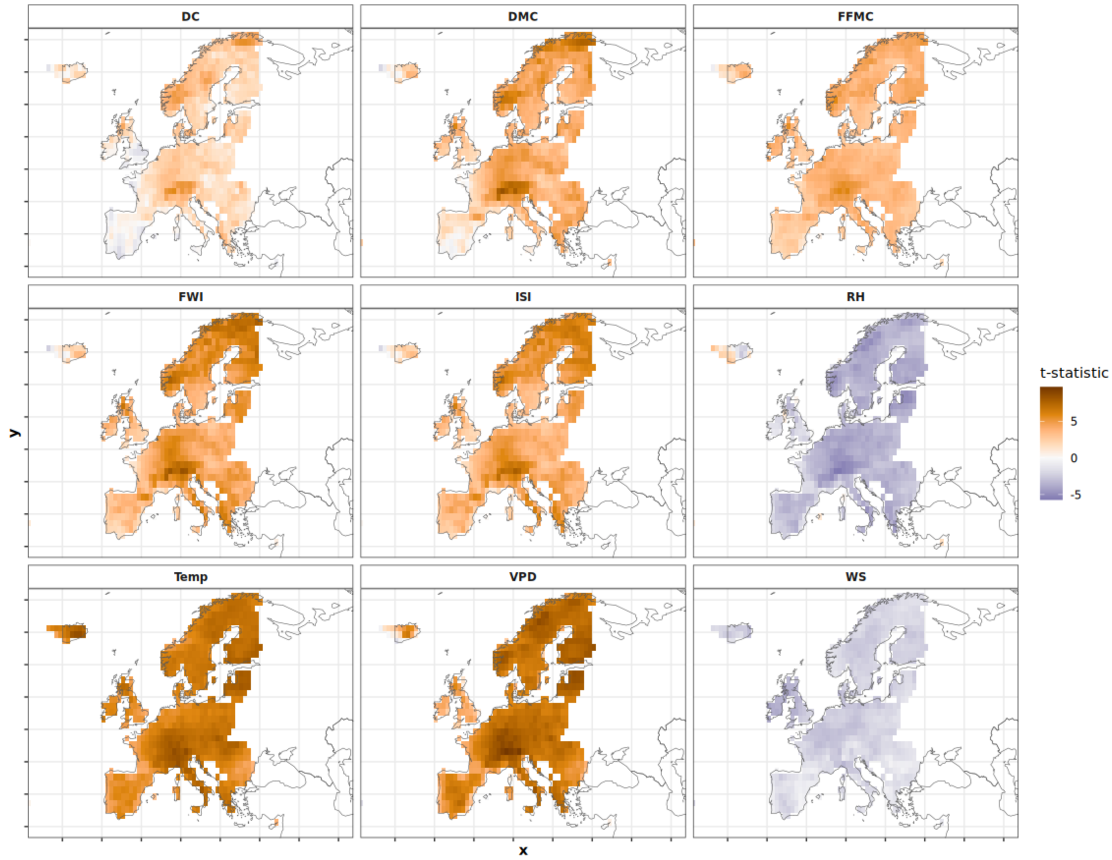

Figure 2.3 Average test statistic from monthly linear regression models comparing surface anomalies between PPA and non-PPA days. Positive values (orange) denote grid cells where surface anomalies are higher on PPA days than days where there was no PPA. Negative values (purple) denote grid cells where surface anomalies are lower on PPA days than non-PPA days.

Daily VPD and midday temperature anomalies increase with strengthening PPA, while midday relative humidity and accumulated precipitation decreases (Figure 2.4Figure 2.4). The peak/trough of surface anomalies coincide with peak PPA strength, except for precipitation, which reaches a low two days following maximum PPA strength. Temperature increases slightly ahead of increasing PPA strength, which is most pronounced for Southern Europe (Figures S5.4–S5.7). The CFWIS components have a shifted lag following peak PPA strength, which is consistent with the longer response times of the DMC and DC and continued drying within the soil following the peak of the event. Wind speeds are anomalously low during the maximum PPA strength and increase following the breakdown of the system, but there is a lag of several days for wind speeds to return to normal levels.

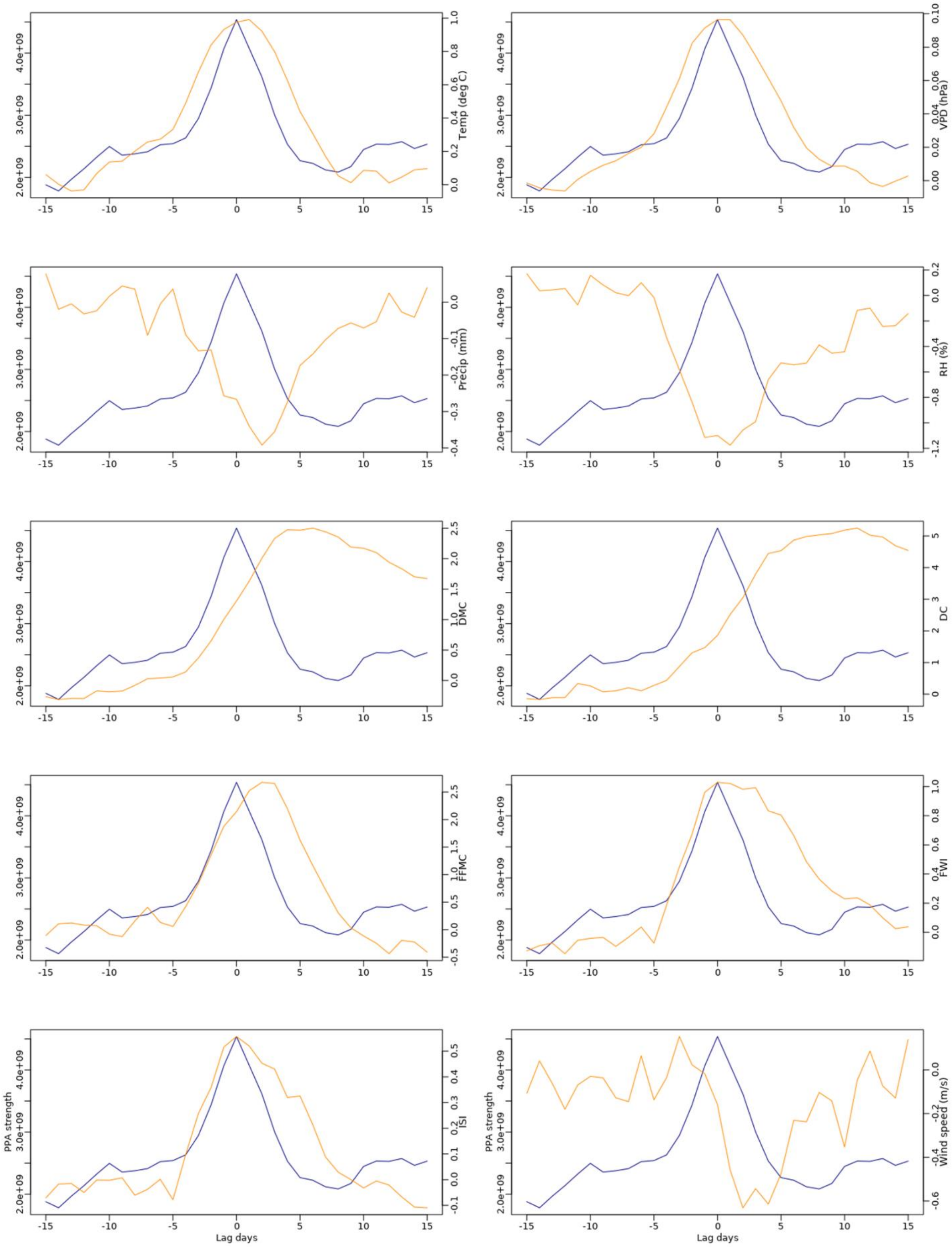

Figure 2.4 Lead-lag relationship between PPA strength and surface anomalies. Blue line = PPA strength with maximum strength on day 0. Orange line = average surface anomalies for the maximum PPA strength area 15 days either side of maximum PPA strength.

2.3.3 PPAS AND EXTREME FIRE WEATHER

The odds of the 95th percentile of FWI values being exceeded is an average of 4.3 times greater under PPA conditions. Extreme FWI values are most likely to coincide with PPA events for Northern (mean OR = 5.1) and Eastern Europe (mean OR = 4.3), followed by Western (mean OR = 3.9), and Southern Europe (mean OR = 3.5). There are very few records of extreme FWI values in March, hence the very high or low odds ratio values that are only comprised of a few grid cells (Figure 2.5). A more detailed breakdown of odds ratios by country and region can be found in Figure S2.8 and Table S2.3.

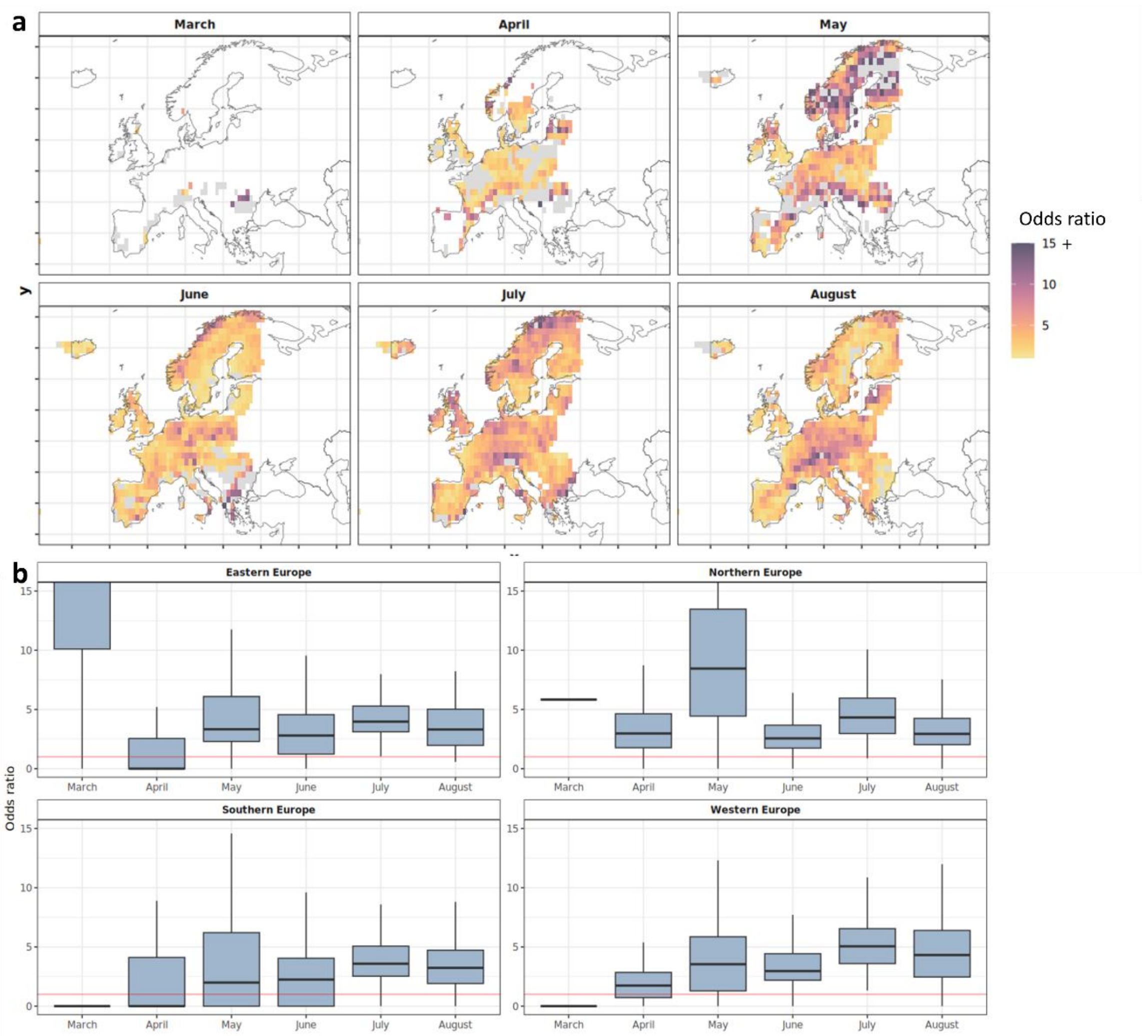

Figure 2.5 Odds ratio (OR) analysis showing the likelihood of a PPA occurring concurrently with extreme FWI (above the 95th percentile). OR were calculated monthly for each grid cell (a) and summarised by region (b). OR > 1 (non-grey colour ramp in (a) and above red line in (b)) indicate a higher likelihood of experiencing extreme FWI values concurrently with the presence of a PPA. Grey cells in (a) depict locations where extreme FWI values are less likely during PPAs, and white cells are locations with insufficient data to calculate an OR. The colour ramp in (a) is set to a maximum of 15, where OR > 15 are set to OR = 15 to allow for ease of interpretation.

2.3.4 PPAS AND WILDFIRE BURNED AREA

On average, the odds of a wildfire occurring concurrently with a PPA increases by a factor of 2.7 across the four regions of Europe between March and August. My findings are spatiotemporally variable, reflecting the differences in wildfire regimes across Europe. I therefore also look at monthly and regional associations between PPAs and wildfire (Figure

2.6). Regionally, wildfires are most likely to occur concurrently with PPAs for Southern Europe (mean OR = 3.3), followed by Eastern, Western (mean OR = 2.4 each), and Northern Europe (mean OR = 1.9). In contrast, the percentage of burned area associated with PPAs was highest for Northern (49%) and Western Europe (36%), followed closely by Eastern (34%), then Southern Europe (27%) (Figure S2.10). A more detailed breakdown of odds ratios and burned area associated with PPAs by region and country in addition to month is given in Figures S2.9–S2.11 and Table S2.4. Overall, burned area is highest 1–3 days following the presence of a PPA. For Northern and Western Europe, burned area is higher up to 5 days after the presence of a PPA (Figure S2.12).

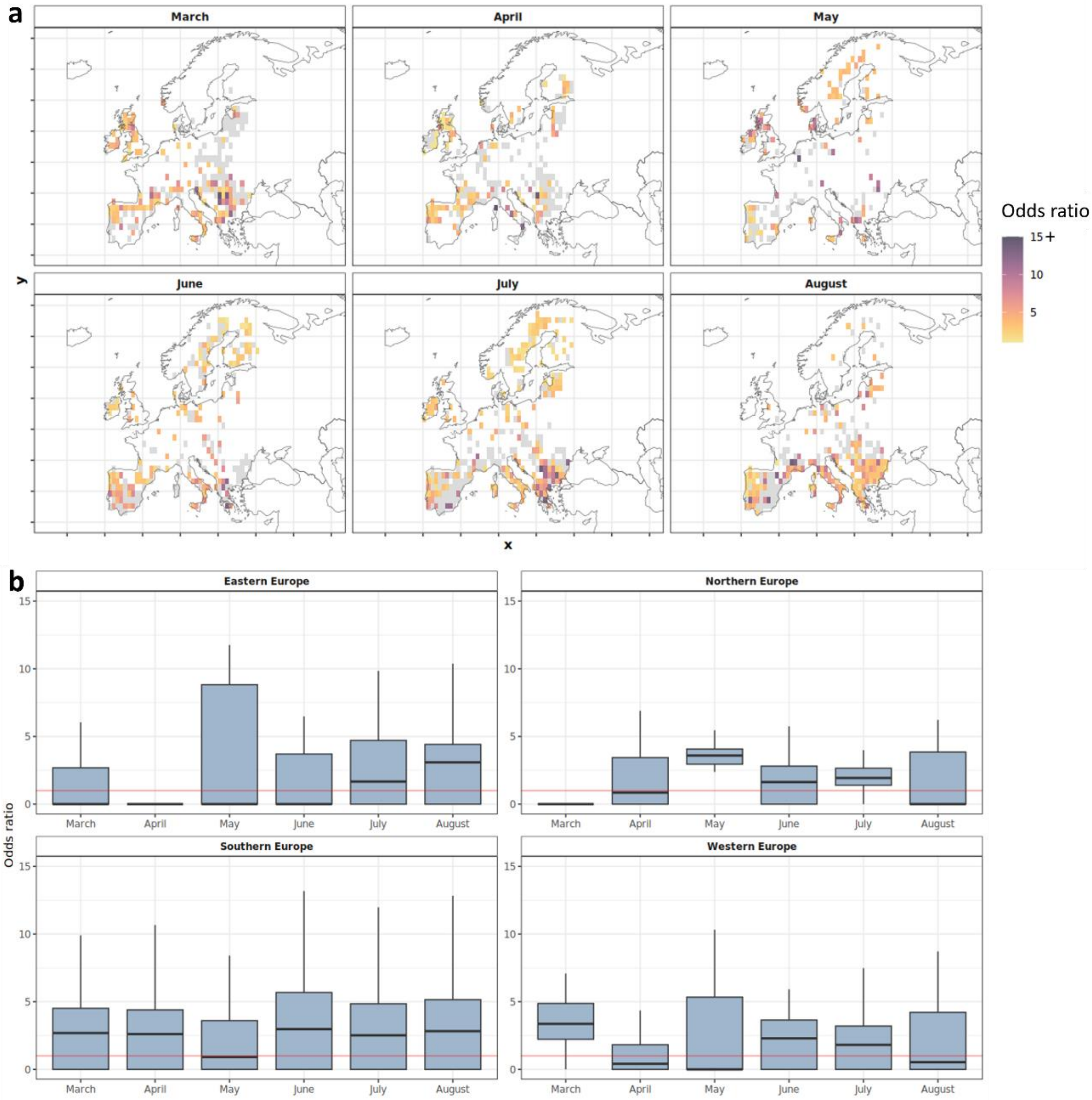

Figure 2.6 OR analysis showing the likelihood of burned area being recorded during or following (up to five days) PPA overlap. ORs were calculated monthly for each grid cell (a) and summarised by region (b). OR > 1 (non-grey colour ramp in (a) and above red line in (b)) indicates a higher likelihood of wildfires occurring during or following (up to five days) the presence of a PPA. Grey cells in (a) depict locations where wildfires are less likely during PPAs, and white cells are locations with insufficient data to calculate an OR. The colour ramp in (a) is set to a maximum of 15, where OR > 15 are set to OR = 15 to allow for ease of interpretation.

2.4 DISCUSSION

PPAs are significant drivers of surface fire weather and wildfire activity across Europe and their importance relative to other processes increases latitudinally from Southern to Northern Europe. PPAs have been associated with significant wildfire events experienced across Europe, including the June 2017 Portugal wildfires, the 2018 Saddleworth Moor wildfire in the UK, the July 2018 Sweden and Finland forest fires, and the August 2021 Greece wildfires. The July 2022 London wildfires, where UK temperatures exceeded 40 degrees Celsius for the first time were also associated with a PPA over much of the country.

2.4.1 PAN-EUROPEAN PPA CLIMATOLOGY

I have characterized a climatology of spring and summer PPAs across Europe. Different methods for quantifying atmospheric blocking make direct between-study comparisons difficult. However, the patterns of PPA persistence across Europe that I detected agree with previous research, including peak blocking frequency across Scandinavia (Tyrlis and Hoskins, 2008; Liu *et al.* 2018; Miller *et al.* 2020). I detected a higher frequency of PPAs across Europe than those found by Sharma *et al.* (2022) for western North America (although my minimum PPA size was lower, which is likely a contributing factor). Higher blocking frequency in Europe compared to elsewhere in the Northern Hemisphere by a factor of 3–4 has also been found in other research (Tyrlis and Hoskins, 2008; Rousi *et al.* 2022).

2.4.2 PPAS AND SURFACE FIRE WEATHER

Higher surface temperature, vapour pressure deficit, and CFWIS components (including extreme FWI values) are especially associated with PPAs for Northern and Eastern Europe, while PPAs appear to be less important in driving surface extremes for Southern Europe, particularly for the drought indicators (DC and DMC) and extreme FWI values. This suggests that PPAs are more important controls on surface fire weather in Northern Europe while other processes may be more important in driving extreme surface conditions in Southern Europe (Ruffault *et al.* 2020; Manning *et al.* 2023). This latitudinal gradient may also be related to the increased pattern variability at higher latitudes associated with the jet stream position and temperature gradient. My findings are consistent with previous research that has related blocking highs and heatwaves to surface fire weather in specific countries and regions of Europe (Hayasaka *et al.* 2019; Sousa *et al.* 2020), as well as research finding synoptic–surface associations were strongest at high latitudes .

Giannaros and Papavasileiou (2023) recently linked extreme fire weather (ISI > 95th percentile) to atmospheric blocking in Northern Europe. My results agree with these findings and extend them by demonstrating how PPAs drive enhanced surface wildfire activity and fire weather. While Giannaros and Papavasileiou (2023) demonstrated the role of subtropical ridges in driving extreme fire weather in Southern Europe, my results have shown this synoptic pattern was not coincident with the persistent anomalous Z500 geopotential heights that characterise PPAs.

2.4.3 PPAS AND WILDFIRE

I have quantified the pan-European importance of PPAs for wildfire occurrence and burned area, building on previous country level analyses that have linked anticyclonic blocking to significant wildfire seasons (Hayasaka *et al.* 2019; Drobyshev *et al.* 2021). The importance of PPAs for burned area increases across a latitudinal gradient from South to North, with nearly 50% of burned area in Northern Europe occurring under PPA events. The latitudinal increase in burned area under PPAs is consistent with Sharma *et al.* (2022). The likelihood of wildfires occurring during PPAs was highest overall for Southern Europe, though the percentage of burned area associated with these events was lowest. This is likely linked to the higher number of wildfires recorded in Southern Europe and highlights the additional importance of other factors driving large wildfires in Southern Europe.

While I have demonstrated the significance of PPAs for European wildfire, PPAs appear to be less important than that observed for Western North American wildfires. Sharma *et al.* (2022) found that wildfires larger than 500 ha were on average seven times more likely to occur during PPA conditions. Direct comparisons between North America and Europe are difficult to make due to the larger spatial thresholds used for PPA detection and minimum wildfire size, but these differences may be related to the larger wildland–urban interface and associated complexity of human-driven ignitions and overall smaller wildfires in Europe, and the dominance of boreal forest fuels for wildfire spread under PPA conditions in the North American mid-latitudes.

Burned area was largest up to three days following the presence of a PPA. This is likely due to a lag between the presence of the PPA, the time taken for the system to breakdown when smaller positive anomalies may still occur, and the associated drying of fuels that allows subsequent ignitions to take place. The extended peak in the moisture components (FFMC, DC, and DMC) of the CFWIS following peak PPA strength observed reflect this. Furthermore, surface wind speeds are likely to be greater at the edge of PPAs, facilitating the spread of wildfires through drier fuels and higher wind speeds (Drobyshev *et al.* 2021). The lead lag graphs show a reduction in wind speeds during peak PPA strength, followed by a delayed return to normal wind speeds. However, surface winds are not well resolved within reanalyses and include topographically forced winds, mixing of mid and surface wind levels, and fire generated downdrafts, making it difficult to elucidate the role of wind speed at the edge of PPAs and during event breakdown. Future research might consider narrowing in on the significance of edge effects on wind and wildfire burned area by looking at the vertical profile of wind through the atmosphere.

I have demonstrated the pan-European importance of PPAs for surface fire weather and wildfire activity, recognising my analyses are constrained by the number of fires detectable by MODIS. National data sets that include smaller wildfires may provide a more comprehensive understanding of synoptic–fire relationships for individual countries, but my aim here was to examine PPAs as drivers of wildfire across large regions of Europe and involving multiple countries concurrently. Furthermore, PPAs are part of a larger picture of atmospheric controls on wildfire activity that need to be understood, including the full range of synoptic drivers of wildfire and how they are influenced by larger teleconnections.

2.4.4 OTHER INFLUENCES ON WILDFIRE

While I have focused on the role of PPAs as drivers of wildfire, there are many other factors that are also important, especially fuels, but also local topography, human behaviour, policy, and fire suppression practices among others. Future research should especially consider how fuels modify fire–climate relationships. Land–atmosphere feedbacks may further amplify drought conditions and high surface temperatures through soil moisture deficits, vegetation desiccation, and snow melt and albedo reduction (Trigo *et al.* 2005; Miralles *et al.* 2019). Understanding the modulating influence of land–atmosphere feedbacks on PPA-related wildfires as well as the mechanistic linkages between blocking pattern breakdown and wildfire activity would help to develop a process-based understanding of the controls on wildfire for improving Earth System models.

2.4.5 IMPLICATIONS

My pan-European synthesis of PPA–fire associations demonstrate how PPAs can impact large regions across political borders simultaneously and for extended durations. My findings have implications for the following areas of research and operations:

(1) Suppression resource management

My findings have important implications for strategic planning of European resource allocation, for example through RescEU, and coordinating firefighting response to large, long duration events or high numbers of synchronous events. Medium range forecasting of potential PPA-driven wildfire periods may provide early warning for resource mobilisation where large wildfires are occurring under extended duration PPAs. Even at the local scale, advanced warning of expected high numbers of ignitions from PPA-related wildfires can help local resource allocation decisions. The London 2022 wildfires occurred concurrently with a PPA over the country, when 11 of the UK's 43 Fire and Rescue Services declared major incidents, including London Fire Brigade where resources were overwhelmed (London Fire Brigade 2023).

(2) Extended forecasting ability

The strong association between PPAs and extreme surface fire weather may help to extend forecasting using synoptic feature-based methods in wildfire occurrence prediction models (Pfahl and Wernli 2012; Ruffault *et al.* 2017). Papavasileiou and Giannaros (2023) recently demonstrated that the extreme fire weather conditions of the 2018 Mati wildfire in Greece could be well predicted seven days in advance using critical fire weather patterns in forecasts. The inclusion of synoptic weather patterns to develop early warning systems for dangerous fire weather conditions would enhance wildfire awareness and preparedness, with benefits for public communication of wildfire danger and informing policy and wildfire management. Across Europe, subsidence under PPAs associated with wildfires leads to poor surface air quality conditions. Smoke air pollution and health impacts from these events can reach densely populated regions of Europe, such as occurred in the 2021 PPA-related wildfires over Greece (Masoom *et al.* 2023). Advanced forecasting and awareness of PPA-driven air pollution events may aid early implementation of mitigation strategies, particularly for the densely populated regions of Eastern and Western Europe.

(3) Future PPA–fire risk

While I have established the role of PPAs in wildfire activity across Europe, there is uncertainty in how PPAs are expected to change in the future, which contributes to uncertainty in future fire risk (Shepherd 2014). Some research has demonstrated historical increases in blocking frequency and heatwaves over Europe (Russo *et al.* 2014; Horton *et al.* 2015; Rousi *et al.* 2022). Regarding historical trends in PPAs, Sharma *et al.* (2022) found a statistically significant expansion of PPAs (but no increase in number or magnitude) over western North America since 1979, driven primarily by warming in the lower atmosphere (thermodynamic changes) rather than dynamic atmospheric changes.

Projections of future fire weather have mainly examined changes in the FWI with anthropogenic warming, but this does not explicitly account for atmospheric circulation changes and feedbacks (Lehtonen *et al.* 2016; Perry *et al.* 2022). Climate change projections have suggested an increase in the frequency, duration, and intensity of extreme weather events like heatwaves and drought for Southern Europe (Giorgi and Lionello 2008). However, climate models typically underestimate the frequency of blocking events (Davini and D'Andrea 2020), and most predict future decreases in blocking frequency. Arctic Amplification (AA) thus far has favoured increased double jet stream formation, weakening westerlies, and formation of high pressure blocking cells in the mid-latitudes (Francis and Vavrus 2015; Coumou *et al.* 2018; Rousi *et al.* 2022). Previous research has linked summer-time weakening and northward movement of the polar jet stream to wildfire activity in North America (Jain and Flannigan 2021) and mid-latitude weather extremes (Trouet *et al.* 2018). How these patterns will change with future anthropogenic warning is uncertain, linked to the poor representation of dynamic atmospheric circulation in climate models (Coumou *et al.* 2018). Research predicting future fire weather and wildfire regimes should consider dynamic atmospheric circulation changes in addition to thermodynamic changes (Scholten *et al.* 2022).

(4) Compounding PPA–fire vulnerabilities for high latitude Europe

I observed a latitudinal increase in the percentage of area burned during PPAs. Extended periods of extreme surface fire weather associated with PPAs can lead to drought conditions through land–atmosphere feedbacks, and subsequent wildfires and carbon emissions can have critical ecological and climate consequences (Yu 2012; Chen *et al.* 2021; Meng and Gong 2022). Future PPA-driven wildfire burned area in the high latitudes will also be impacted by changing ignition patterns due to projected increases in summer lightning flashes. Chen *et al.* (2021) predicted for 1 °C of warming, summer lightning flash rates will increase by 40±19% over Arctic tundra and 23±6% over boreal forest in the circumpolar high-northern-latitudes. Climate change feedbacks may further amplify impacts from PPA-wildfires at high latitudes, through reduced snow cover and declines in permafrost, earlier snow melt, and exposure of carbon stores to smouldering combustion under wildfires (Meng and Gong 2022).

2.4.6 CONCLUSIONS

PPAs are important drivers of surface fire weather and wildfire activity, and my findings highlight the significance of these relationships at a pan-European scale. My key findings are:

(1) Extreme fire weather is 4.3 times more likely to occur during PPAs across Europe.

(2) Wildfires are 2.7 times more likely to occur concurrently with a PPA event across Europe.

(3) There is significant spatiotemporal variability in PPA–fire associations. The likelihood of PPA-concurrent wildfires is highest for Southern Europe (factor of 3.3), while the percentage of area burned under PPAs increases with latitude (up to 49% in Northern Europe).

(4) There is a lag between PPA presence and peak burned area associated with the role of PPAs in pre-drying fuels for subsequent ignition.

It is critical to understand the mechanisms driving PPA–fire relationships now, to understand how wildfire risk may change in the future. More broadly, my findings highlight opportunities for a more proactive approach to wildfire response at a pan-European scale, through extended forecasting within wildfire occurrence models for effective decision making during large, extended periods of elevated wildfire danger. Consideration of multi-scale controls on wildfire occurrence and behaviour through both synoptic and surface fire weather may provide a more holistic approach to anticipating and preparing for wildfire dangerous conditions.

3

3 LANDSCAPE CONTROLS ON FUEL MOISTURE VARIABILITY IN FIRE PRONE PEATLAND AND HEATHLAND LANDSCAPES

ABSTRACT

Background: Cross-landscape fuel moisture content is highly variable but not considered in existing wildfire danger assessments. Capturing fuel moisture complexity and its associated controls is critical for understanding wildfire behaviour and danger in emerging fire prone environments that are influenced by local heterogeneity. This is particularly true for temperate heathland and peatland landscapes that exhibit spatial differences in the vulnerability of their globally important carbon stores to wildfire. Here I quantified the range of variability in the live and dead fuel moisture of *Calluna vulgaris* across a temperate fire prone landscape through an intensive fuel moisture sampling campaign conducted in the North Yorkshire Moors, UK. I also evaluated the landscape (soil texture, canopy age, aspect, and slope) and micrometeorological (temperature, relative humidity, vapor pressure deficit, and windspeed) drivers of landscape fuel moisture variability for temperate heathlands and peatlands for the first time. **Results:** I observed high cross-landscape fuel moisture variation, which created spatial discontinuity in the availability of live fuels for wildfire spread (fuel moisture < 65%) and vulnerability of the organic layer to smouldering combustion (fuel moisture < 250%). This heterogeneity was most important in spring, which is also the peak wildfire season in these temperate ecosystems. Landscape and micrometeorological factors explained up to 72% of spatial fuel moisture variation and were season and fuel layer dependent. Landscape factors predominantly controlled spatial fuel moisture content beyond modifying local micrometeorology. Accounting for direct landscape–fuel moisture relationships could improve fuel moisture estimates, as existing estimates derived solely from micrometeorological observations will exclude the underlying influence of landscape characteristics. I hypothesise that differences in soil texture, canopy age, and aspect play important roles across the fuel layers examined, with the main differences in processes arising between live, dead, and surface/ground fuels. I also highlight the critical role of fuel phenology in assessing landscape fuel moisture variations in temperate environments. **Conclusions:** Understanding the mechanisms driving fuel moisture variability opens opportunities to develop locally robust fuel models for input into wildfire danger rating systems, adding versatility to wildfire danger assessments as a management tool.

3.1 INTRODUCTION

Temperate peatlands and heathlands contain globally important carbon stores that are becoming increasingly susceptible to wildfires under climate and land use change (Page and Baird 2016; Kirkland *et al.* 2023). Peatlands store 550 gigatons of organic soil carbon globally, and approximately 0.19–0.88 million km^2 of these peatlands are found in the temperate latitudes (30–50 degrees) (Batjes 1996; Yu 2012). Surface wildfires can lead to smouldering combustion of carbon-rich peatland soils (Kirkland *et al.* 2023). These fires are resource intensive to extinguish and can result in significant carbon emissions (Mickler 2021). Fuel moisture is a key component of fuel flammability, ignition probability, and subsequent wildfire behaviour (Matthews 2014; Scarff *et al.* 2021). As such, fuel moisture content is important for determining peatland and heathland wildfire danger—the combination of factors affecting the initiation, spread, and ease of control of a wildfire (Natural Resources Canada 2021).

Existing operational fire weather indices across northwest Europe (e.g., EFFIS: San-Miguel-Ayanz *et al.* 2012) use weather information to predict the danger of a successful ignition, drawing on regional assessments of fuel moisture (for example the Fine Fuel Moisture Code of the Canadian Fire Weather Index System (CFWIS)). However, fuel moisture content can be highly spatially variable at the landscape level (Nyman *et al.* 2015; Walsh *et al.* 2017). Regional estimates do not capture this spatial heterogeneity of fuel moisture and consequently may not reflect local conditions (Nyman *et al.* 2018; Matthews *et al.* 2019). Current risk assessments therefore do not account for fuel-driven within-landscape vulnerability to wildfires and their consequent ecological, biogeochemical, or socioeconomic impacts (Davies *et al.* 2016; Hokanson *et al.* 2016).

Studies that have captured the extent of fuel moisture variability at the landscape level using direct measurement techniques are rare and have not been conducted within temperate peatland and heathland landscapes. Previous research has utilised indirect measures of fuel moisture content such as soil and litter moisture sensors to quantify the moisture variability of fire prone forest litter layers (Nyman *et al.* 2015; Slijepcevic *et al.* 2018). However, in dwarf shrub *Calluna vulgaris* dominated temperate peatland and heathlands, both the dead and live vegetation are important for wildfire ignition and spread, with live fuels often comprising the largest component of the fuel load (Davies and Legg 2008, Davies and Legg 2010). The magnitude of fuel moisture variability at the landscape scale and the controls on that variability will therefore strongly differ from forest ecosystems (Dickman *et al.* 2023). Further, fuel moisture within the surface moss, litter, and organic soils is important for determining the potential for smouldering combustion and the associated fire severity (Grau-Andrés *et al.* 2018). Low organic soil moisture (< 250%) facilitates below-ground smouldering and consequent loss of carbon to the atmosphere (Lukenbach *et al.* 2015).

In addition to the quantification of cross-landscape fuel moisture variability, the landscape characteristics that control this variability have not yet been fully resolved. Average regional-scale fuel moisture is likely modulated by landscape scale variability in hydrology, meteorology, ecology, and plant physiology. Again, previous research into how landscape characteristics control fuel moisture content has primarily focused on forested fuels and landscapes. Four key landscape characteristics have emerged: soil properties, landscape position, topography/aspect, and vegetation structure (see references within Table 3.1). The extent to which these landscape characteristics are important for fuel moisture within temperate peatland and heathland fuels is unknown. The complexity of landscape ecological field studies has also meant that landscape characteristics can be confounded and difficult to isolate (e.g., all of the south facing sites contained all of the highest porosity soils, and the link between vegetation cover on equatorial versus polar facing slopes (Nyman *et al.* 2015; Slijepcevic *et al.* 2018).

Cross-landscape differences in fire behaviour and wildfire danger are particularly relevant to consider in emerging fire prone environments, where fire behaviour, including wildfire spread through live fuels and smouldering combustion of organic soils, can be influenced by small-scale heterogeneity in landscape characteristics. It is therefore important to understand fuel moisture dynamics at the landscape level to develop appropriate fuel models for inclusion in wildfire danger assessments in temperate ecosystems. To this end, I assess (1) what is the range of variability in the live and dead fuel moisture content of *Calluna vulgaris* across a temperate fire prone landscape? And (2) what are the relative contributions of landscape and micrometeorological drivers of fuel moisture variability at the landscape scale? In doing so, I provide critical understanding necessary to develop tailored fuel moisture models for input in wildfire danger rating systems, to support local scale fire management decisions.

3.2 METHODS

3.2.1 STUDY REGION

My study region was the North Yorkshire Moors National Park, United Kingdom (Figure 3.1). The dwarf shrub *Calluna vulgaris* is abundant in peatlands and heathlands that form large areas of fire prone landscapes across north-western Europe, including the United Kingdom (Gimingham *et al.* 1979; Glaves *et al.* 2020). Upland areas of the North Yorkshire Moors comprise extensively managed *Calluna vulgaris*-dominated peatland and wet heathland ecosystems (Simmons 1990). *Calluna* has been burned on rotation, creating a patchwork mosaic of homogenous *Calluna* plots of different ages across the landscape, allowing the role of vegetation structure and topography/aspect that have previously been confounded to be isolated (Nyman *et al.* 2015; Slijepcevic *et al.* 2018). The landscape also consists of a diversity of soil textures and associated geologies, slopes, aspect, and landscape positions, within the given regional moist, maritime climate. As such, the region provides an ideal location to examine the underlying controls on spatial fuel moisture variability in critical fire prone temperate landscapes.

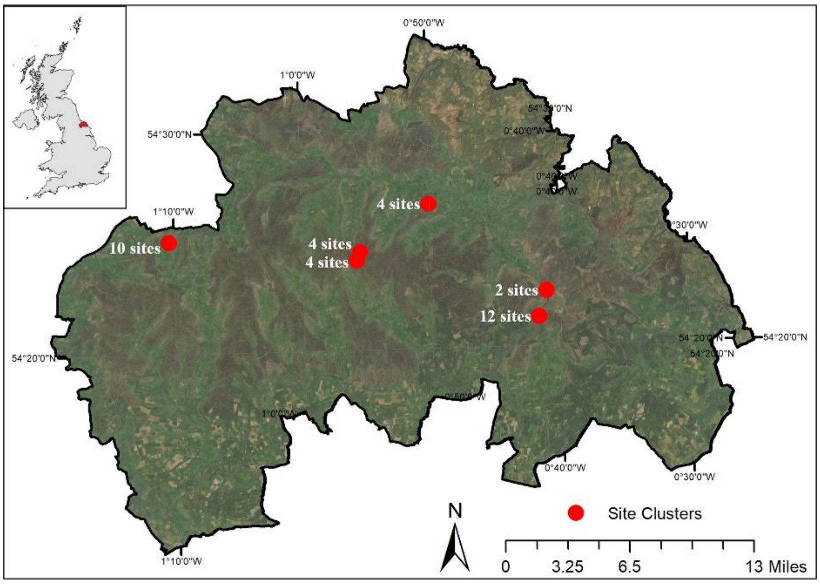

Figure 3.1 The North Yorkshire Moors National Park study region situated in northeast England. I established 36 measurement plots clustered in six key areas of the national park. Source: Esri, Maxar, Earthstar Geographics, and the GIS User Community. © Natural England copyright. Contains Ordnance Survey data © Crown copyright and database right 2022.

3.2.2 EXPERIMENTAL DESIGN AND SITE SELECTION

I selected 36 plots across the North Yorkshire Moors. The plot dimensions were approximately 20 x 20 m of homogenous *Calluna* as this was the size burned by land managers to create the patchwork mosaic of *Calluna* across the landscape. I decided on 36 plots as this allowed each plot to contain a unique combination of the four landscape factors hypothesised to be important for spatial fuel moisture variability based on previous research: soil texture, canopy age, aspect, and hillslope position (Figure 3.2; Table 3.1). I selected potential plots by overlaying the source maps from Table 3.1 to identify areas that contained all possible combinations of landscape factors. I then visited the areas to identify suitable plots with land managers. The criteria for the 36 plots were: (1) each plot must possess a unique combination of landscape factors, (2) plots must be sufficiently accessible to allow sampling to be carried out at all plots on the same day (using multiple samplers), and (3) plots must meet requirements of land managers (e.g., minimise disruption to nesting birds or land management activities). Fuel moisture sampling is intensive, so I selected plots that were sufficiently close to allow field campaigns to be conducted within a single day in accessible locations, while capturing the diversity of soils that tend to be spatially disparate.

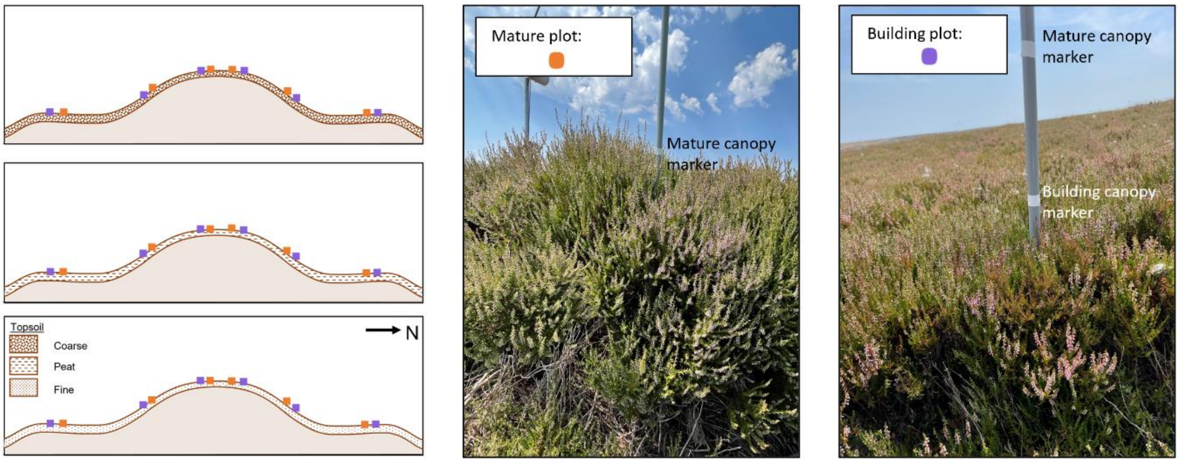

Figure 3.2 Conceptual figure of the 36 sample plots (coloured circles) comprising each possible combination of hypothesised landscape drivers: soil texture (coarse, peat, or fine); canopy age (building or mature); hillslope position (low, medium, or high) and aspect (north or south). I installed weather stations next to each pair of building and mature *Calluna* plots.

Table 3.1 The hypothesised landscape drivers of fuel moisture variability examined for plot selection. I classified landscape drivers using the provided sources and validated these with field assessments.

Driver	Classification (number of sites in each classification, n = 36 sites)	Source	Significance (hypothesised from previous research)
Soil texture	Coarse: Freely draining very acid sandy and loamy soils (12 sites) Fine: Slightly acid loamy and clayey soils with impeded drainage; slowly permeable seasonally wet acid loamy and clayey soils (12 sites) Peat: Blanket bog peat soils and slowly permeable wet very acid upland soils with a peaty surface (12 sites)	Soilscapes class numbers (Farewell *et al.* 2011)	Soil texture captures the soil hydraulic traits (e.g., soil depth, porosity, permeability, drainage flow paths, and water table depth) hypothesised to control water availability to dead fuels via capillary action and live fuels via water uptake by roots (Matthews 2014; Nyman *et al.* 2015).
Canopy age	Building: 5–10 years since last burn, 30 cm height (18 sites) Mature: 15–20 years since last burn, 60 cm height (18 sites)	Land managers' records and satellite imagery	Fuel age and height influence fuel moisture by creating differences in shading, fuel structure and plant hydraulic traits. Live fuel canopy cover and biomass have been shown to regulate the moisture content of underlying fuels (Nyman *et al.* 2018; Brown, Inbar, *et al.* 2022). But also within the same species, variability in biomass, age and the proportion of live-to-dead material influence the moisture content of live fuels themselves (Davies and Legg 2011; Brown, Hoylman, *et al.* 2022).
Hillslope position	Low: low plateau (12 sites) Medium: mid-slope (12 sites) High: high plateau (12 sites)	OS Terrain® 50 DTM OS data © Crown copyright and database right 2022	Hillslope position influences drainage flow paths across the landscape and thus the availability of water to live fuels (Tromp-van Meerveld and McDonnell 2006).
Aspect	North (18 sites) South (18 sites)	OS Terrain® 50 DTM OS data © Crown copyright and database right 2022	North and south aspects capture the range of variation in incoming solar radiation to dry out fuels. Topography and aspect influence fuel moisture through the formulation of complex microclimates that modify the meteorological controls on drying (humidity, temperature, windspeed) (Nyman *et al.* 2015, 2018; Brown, Hoylman, *et al.* 2022). Dead fine fuels are typically drier on equatorial than polar facing slopes (Nyman *et al.* 2015; Walsh *et al.* 2017; Slijepcevic *et al.* 2018) where spatial differences driven by variations in incoming solar radiation between polar and equatorial facing slopes are created.

I identified coarse, fine, and peaty textured soils using Soilscapes, a classification derived from the detailed National Soil Map for England and Wales (Farewell *et al.* 2011). I validated soil texture classifications with manual textural assessments of soil samples collected in the field (Thien 1979). I selected plots on north- and south-facing hillslopes using the OS Terrain® 50 DTM (Ordnance Survey 2019). In the North Yorkshire Moors, peatland and heathland land covers transition to grassland/agricultural land prior to reaching the topographic low, so hillslope position in these ecosystems is defined as: high, the plateau on the hilltop; mid, the hillslope below this plateau; and low, a plateau below a slope.

I examined the combined influence of fuel age and height between contrasting building and mature heather canopies. I used these terms to represent the two different classes of younger (shorter) and older (taller) heather life stages. Previous research has established the significance of *Calluna* biomass, proportion of live and dead fuel, and life stage for fuel moisture content and wildfire behaviour (Gimingham 1992; Davies and Legg 2011; Santana and Marrs 2014; Log 2020). Within the constraints of the landscape, I selected existing building and mature *Calluna* plots side by side to isolate canopy differences from my other landscape factors of interest. I distinguished age using time-since-last-burn records held by land managers. Mature canopy plots were last burned 15–20 years ago and had an average height of 60 cm and accumulated moss/litter layer depth of 5 cm. Building canopy plots were burned in the last 5–10 years and had an average height of 30 cm and accumulated moss/litter layer depth of 2.5 cm. This classification allowed me to (1) maximise differences between the two categories of interest, so the building canopy plots were distinctly different from the mature canopy plots, (2) ensure consistency across sites as all sites within each category have a similar age, height, structure, and management approach, and (3) ensure within-plot variation is low relative to between-plot variation.

3.2.3 DATA COLLECTION

Fuel moisture sampling - Wildfires generally occur across two fire seasons in northwestern temperate Europe, a primary peak season in spring and a secondary season in summer (Belcher *et al.* 2021; Cardíl *et al.* 2023). To capture the temporal variations in landscape controls on a phenological timescale I collected fuel moisture samples in hot, dry fire weather conditions across the spring and summer fire seasons (Figure S3.1). I collected three sets of samples across a 1-week drying period in April 2021, during the peak spring wildfire season, and two further sets in June and July 2021, respectively, during the secondary summer wildfire season. During each campaign, I collected samples within each of the 36 plots between 1100 and 1700, randomising the order of sampling as much as logistically possible.

Fuel moisture exhibits vertical variation from organic to canopy layer that is relevant for determining wildfire behaviour. For example, fires will often burn through the canopy of *Calluna* without involving litter and ground fuels. Therefore, in each plot I sampled seven fuel layers: *Calluna* live canopy, live stems (< 2 mm diameter), dead canopy, dead stems (< 2 mm diameter), surface moss (top 2 cm), litter (top 2 cm), and the organic layer beneath the *Calluna* (top 5 cm of organic material above mineral soil). I combined lower canopy material with live stems following a study by Davies and Legg (2011), in which a factor analysis grouped these two fuel layer together, separate from the upper canopy.

I collected samples following the sampling protocol of Little *et al.* (2023), modified from Norum and Miller (1984). I set out a 25-m transect through each plot and walked along it, collecting fuel clippings from ca. 10 different plants into one aluminium tin (250 ml) with a screw-fit lid sealed with masking tape. I collected the same amount of biomass from each plant along the transect, filling the 250 ml tin ¾ full. I selected plants haphazardly, as the aim was to ensure samples were representative of within-plot variability rather than individual plants. I collected *Calluna* canopy and stem material by clipping sprigs with stem diameter < 2 mm and separating the leafy canopy material from the woody lower stems. I collected the top 2 cm of surface moss and litter at 10 points along the transect, removing any highly decomposed material from the base of the layer. Finally, after exposing the material beneath the surface moss and litter, I extracted the top 5 cm of organic material at five points along the transect using a small corer.

I measured gravimetric fuel moisture content (mass of water per mass of dried sample, %, referred to throughout as fuel moisture content (Equation 3.1)) following the same protocol. Briefly, I weighed the tinned samples (wet weight) as soon as possible after collection, and within a maximum of 24 hours. I subsequently dried the samples for at least 48 h at 80 ˚C, consistent with previous *Calluna vulgaris* fuel moisture studies (e.g., Davies *et al.* 2010), and then reweighed the samples (dry weight).

$$\text{Fuel moisture content} = \frac{(\text{sample wet weight} - \text{sample dry weight})}{(\text{sample dry weight} - \text{container tare weight})} * 100 \qquad \text{[Eq.3.1]}$$

Micrometeorological variables - I recorded 1.25 m air temperature and relative humidity at 15-minute intervals at each pair of building and mature *Calluna* sites with HOBO U23-001A PRO V2 (Onset Computer Corporation, Bourne, MA) sensors housed within radiation shields. I installed Davis Vantage Pro wind anemometers (Davis Instruments) at 2 m on the north and south sides of the three main hillslopes at equivalent elevations to monitor wind speed and direction at 1-minute intervals.

3.2.4 DATA ANALYSIS

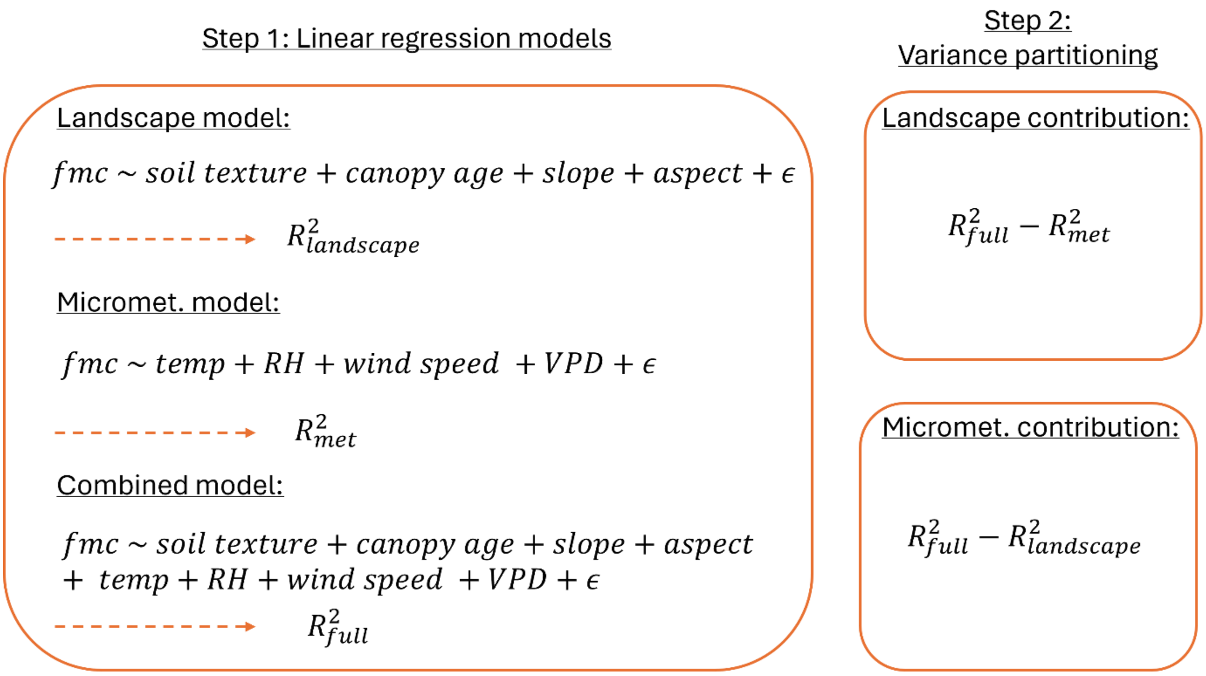

Figure 3.3 Conceptual diagram outlining the landscape, micrometeorological, and combined linear regression model equations (Step 1). The landscape model includes categorical soil texture, canopy age, slope, and aspect variables. The micrometeorological model includes 1.25 m air temperature (temp), relative humidity (RH), wind speed, and vapour pressure deficit (VPD) averaged 5-h before time-of-sampling. The combined model includes all landscape and micrometeorological factors. I used the R^2 values from the models to calculate the individual contribution of the landscape model and micrometeorological model to explaining fuel moisture variance (Step 2).

Each of the 36 sites represented a unique combination of the four landscape factors of interest. This experimental design allowed me to use linear regression models to assess the influence of landscape factors without confounding between my hypothesised drivers. I developed three linear regression models to assess the influence of landscape factors, micrometeorological factors, and the overall contribution of both groups of factors on fuel moisture variation (Figure 3.3). I ran these three models for each combination of fuel layer and sampling month to examine fuel layer and season dependent relationships (21 variations of each model).

The landscape model was defined by the hypothesised controls on landscape-scale fuel moisture variability, as identified from the literature—soil texture, canopy cover, hillslope position, and aspect. To define the micrometeorological model, I first selected parameters considered to be important for fire weather to investigate—temperature, relative humidity, wind speed, and vapour pressure deficit. I included vapour pressure deficit (calculated from air temperature and relative humidity measurements) based on recent demonstrations of its importance for live fuel moisture content (Griebel *et al.* 2023). I then evaluated different lag periods and parameters to derive the best relationship between the micrometeorological variables and fuel moisture, with micrometeorological variables averaged 5-h before time-of-sampling performing best (Table S3.1). I excluded uneven precipitation distribution as a significant control on spatial fuel moisture variability in this study, as I targeted the driest periods of the fire season and monitoring of precipitation using hand gauges at each pair of sites throughout the sampling period did not reveal any major between-site differences. I also considered relationships between fuel moisture content and the Canadian Fire Weather Index System (CFWIS) as this is the system currently used within the UK Met Office Fire Severity Index (MOFSI) to assess aspects of fire weather (Arnell *et al.* 2021). However, I excluded these from the main analyses due to their comparatively poorer performance (Figure S3.2).

I used variance partitioning to understand the relative importance of landscape or micrometeorological variables for fuel moisture content (Nakagawa and Schielzeth 2013). I calculated the variance explained (R^2) for the landscape (soil texture, canopy age, hillslope position, and aspect), micrometeorological (1.25 m air temperature, relative humidity, vapour pressure deficit, and wind speed averaged 5-h before time-of-sampling), and combined (both landscape and micrometeorological factors) statistical models. I calculated the independent contributions of landscape and micrometeorological models as $R^2_{full} - R^2_{met}$ and $R^2_{full} - R^2_{landscape}$, respectively. The shared variance explained was the difference between the total variance explained and the independent contributions of the two sub models.

I used weighted effect coding on individual regression models (21 variations of four landscape models) for each landscape factor to narrow in on the role of landscape drivers by producing model estimates as deviations from the sample mean (Sweeney and Ulveling 1972). I tested the assumptions of all of the linear models by producing Q-Q plots (for normality) and residual vs predicted plots (for heteroscedasticity) using the DHARMa R package (Hartig 2022). No significant deviations from the assumptions were seen in the majority of the 147 models (Figure S3.3). To test for spatial autocorrelation I calculated Moran's I using the lctools R package (Kalogirou 2020). No significant deviations from the assumptions were found for the majority of the models (Table S3.3–S3.5). I conducted all statistical analyses in R version 4.1.2 (R Core Team 2022), using packages cffdrs (Wang *et al.* 2017), plantecophys (Duursma 2015), and wec (Grotenhuis *et al.* 2016).

3.3 RESULTS

3.3.1 FUEL MOISTURE VARIABILITY

Fuel moisture content was highly spatially variable across the 36 plots in the North Yorkshire Moors. Observed fuel moisture variability was season- and fuel layer-dependent (Figure 3.4). Live *Calluna* fuel moisture content was lowest and least variable in spring. Live fuel moisture content varied by 54% (percentage points) for *Calluna* canopy between the driest and wettest site in spring, increasing to 97% by July. Previous research has developed fuel moisture thresholds for certain fuel layers that indicate the fuel moisture content below which a fire is likely to sustain ignition (vertical lines in Figure 3.4). Live fuel moisture content was found to vary across the 47–65% threshold for sustained fire ignition (Taylor *et al.* 2021), particularly in spring (Figure 3.4 dashed vertical lines on live canopy graph). Cross-landscape organic layer fuel moisture content varied across the 250% fuel moisture threshold for smouldering combustion (Lukenbach *et al.* 2015) during both spring and summer (Figure 3.4 vertical dashed line on organic layer graph). Dead *Calluna*, moss, litter, and organic layers were more variable in spring than summer. Surface moss and litter layer fuel moisture content spanned a range of 191% and 156%, respectively, between driest and wettest sites.

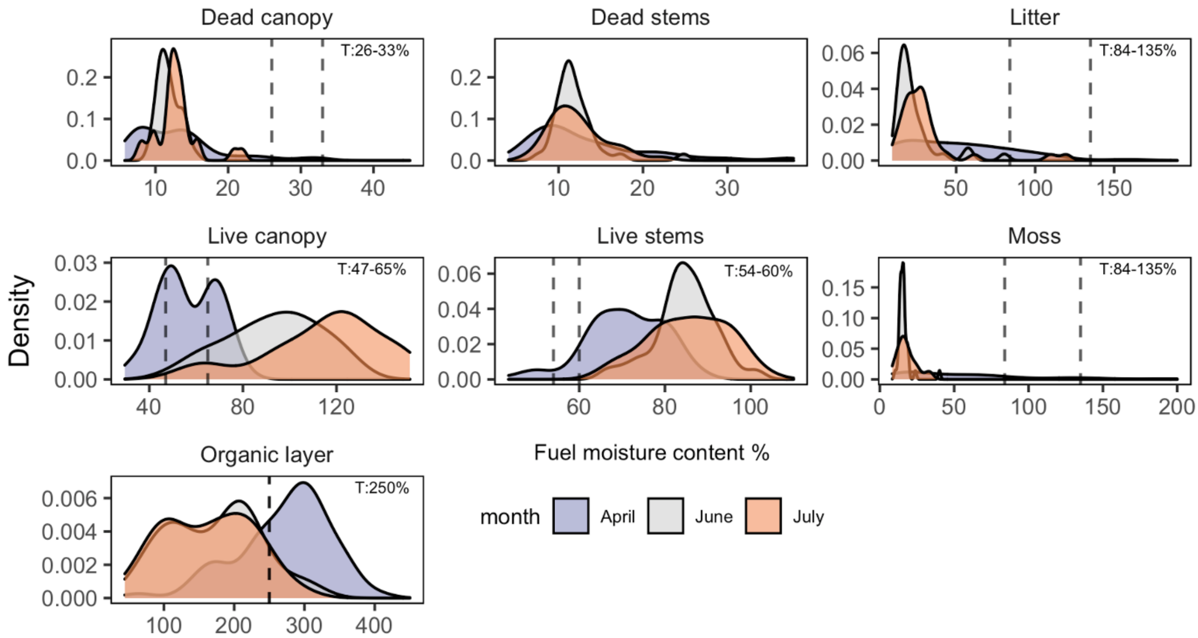

Figure 3.4 Density plots of fuel moisture distribution for *Calluna vulgaris* fuel layers across the 36 plots in the North Yorkshire Moors during hot, dry conditions April–July 2021 (number of samples for each fuel layer panel = ca. 180). Dashed vertical lines depict fuel moisture thresholds for sustained ignition within the different fuel layers based on previous research (Lukenbach *et al.* 2015; Taylor *et al.* 2021). One line = threshold; two lines = range of lower and upper threshold; no line = no conclusive threshold for this species.

3.3.2 LANDSCAPE AND MICROMETEOROLOGICAL DRIVERS OF FUEL MOISTURE VARIABILITY

Combined landscape and micrometeorological factors explain 16–72% of the total cross-landscape fuel moisture variability (Figure 3.5). Overall, the landscape models tend to outperform the micrometeorological models in explaining the spatial distribution of fuel moisture. However, the importance of landscape and micrometeorological factors show differences between fuel layers and seasons. The overlap between the landscape and micrometeorological models in Figure 3.5 shows the shared variance explained between the models. For live *Calluna* canopy fuel moisture, the shared variance exceeds the individual variance of each model, which suggests there is an interaction between landscape and micrometeorological factors. Landscape factors are consistently more important drivers of dead *Calluna* and litter layer fuel moisture. Total variance explained for dead *Calluna* is higher in summer (50–72%) than spring. Where landscape factors drive fuel moisture variability, the individual contribution of the landscape model largely outweighs the shared variance, indicating that landscape factors control fuel moisture variation beyond simply modifying local micrometeorology. The micrometeorological model only outperforms the landscape model for the moss layer in April (21%) and June (45%), the live canopy in April (47%), and the organic layer in July (22%). There is no clear difference in the importance of landscape and micrometeorological factors for organic layer fuel moisture variation outside of July.

Linear regression models quantified the deviation in fuel moisture percentage from the sample mean associated with specific landscape factors (Table S3.2). Soil texture exerts the greatest control on the spatial distribution of fuel moisture content for all layers except dead

Calluna. Live *Calluna* canopy material is up to 20% drier than average on fine-textured soils and up to 19% wetter than average on coarse textured soils, resulting in a 39% percentage point difference in fuel moisture estimates across the landscape. This magnitude of difference increases through summer. Live *Calluna* stems show a seasonal reversal in relationship with soil texture, where fuel moisture is highest (lowest) on fine soils in April (June and July). There are also some instances where relationships between landscape factors and fuel moisture switch backwards and forwards inconsistently across the sampling period (e.g., moss, litter, and organic layer relationships with soil texture). In July, organic layer fuel moisture is significantly (46.6%) lower than average on coarse soils.

Canopy age consistently controls fuel moisture variation across all fuel layers. Live *Calluna* canopy is up to 9% drier in mature *Calluna*, increasing in magnitude from spring to summer. Dead *Calluna* and organic layer fuels are driest in building *Calluna* (organic layer fuel moisture is 20–29% lower in summer). The influence of aspect varies between live *Calluna* and surface fuels. Live canopy fuel moisture content is up to 9% wetter on south slopes in summer. Surface fuels in contrast are driest on south slopes, except for June, where all fuel layers are wetter on south slopes than north slopes. The influence of slope position is least clear, though *Calluna* live stems and the organic layer are consistently driest at low hillslope positions. Conversely, *Calluna* live canopy is wettest at low hillslope positions.

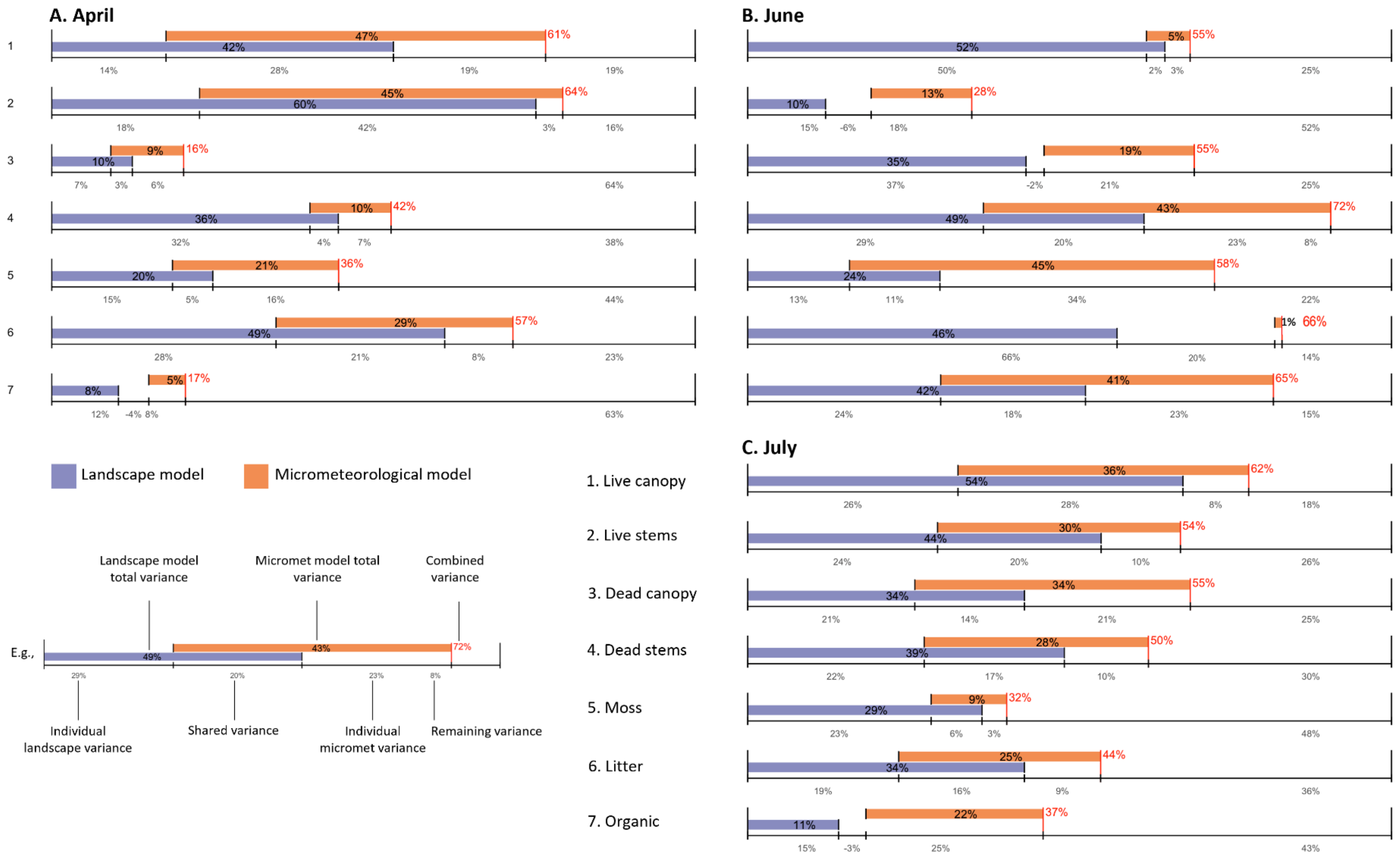

Figure 3.5 Spatial variation in fuel moisture that can be explained by the landscape and micrometeorological linear regression models. Variance partitioning for the (a) April, (b) June, and (c) July sample sets, showing the contribution of the overall linear regression model towards explaining fuel moisture variation (red) and the total variance explained by the landscape factors (purple) and micrometeorological factors (orange).

3.4 DISCUSSION

3.4.1 CROSS-LANDSCAPE FUEL MOISTURE IS HIGHLY VARIABLE

Plant phenology drives fuel moisture variability in live *Calluna.* Fuel moisture content is low in spring following winter dormancy, resulting in high load of fuel in an ignitable state. As temperatures increase and sap flow restarts in *Calluna*, a "green-up" is observed where new leaf and shoot growth increases fuel moisture content (Bannister 1964b; Davies *et al.* 2010). There is an important spatial dimension to this recognised temporal variability in fuel moisture. Live fuel moisture content was found to be most variable in summer, linked to observations of spatial variation in the timing of *Calluna* green-up across the landscape. However, it is the spatial variation in live fuel moisture in the peak wildfire season of spring in the UK (Belcher *et al.* 2021) that is especially important from a wildfire danger perspective. On the days sampled, live canopy fuel moisture content varied across the threshold for sustained ignition (47–65%) identified by Taylor *et al.* (2021). Due to landscape heterogeneity, live *Calluna* fuel moisture was below the threshold for contributing to wildfire spread in some locations and above it in others (Figure 3.4). Moreover, live *Calluna* can form a major component of the available fuel for wildfire spread and can behave independently akin to a mini-crown fire (Fernandes *et al.* 2000; Davies and Legg 2016). Similarly, fuel moisture in the organic layer was distributed above and below the 250% threshold for smouldering combustion (Lukenbach *et al.* 2015; Figure 3.4), indicating differential potential for higher severity wildfires due to smouldering combustion across the landscape.

3.4.2 LANDSCAPE FACTORS DRIVE FUEL MOISTURE VARIABILITY

Spatial variation in the distribution of fuel moisture creates a cross-landscape on/off thresholding of fuel availability. It is clear from my results that regional estimates of fuel moisture will not capture important local spatial variability driven by either landscape or micrometeorological factors. Overall, landscape factors were found to be more important drivers of fuel moisture variation than micrometeorological factors. There are a small number of instances where the shared variance outweighs the individual contributions of each model, suggesting there may be some form of interaction between landscape and micrometeorological factors, such as the landscape factors modifying micrometeorology. However, for the most part, landscape factors control fuel moisture content beyond simply modifying micrometeorology. This is a key insight towards improving the accuracy of fuel moisture estimates by accounting for landscape–fuel moisture relationships directly, as estimates derived solely from micrometeorological observations will exclude the underlying influence of landscape controls. Fire weather index systems that are based on weather parameters alone will have limited ability to provide fire managers with accurate predictions in these ecosystems.

I hypothesise that soil texture differences are important controls on fuel moisture variability. I observed higher live canopy fuel moisture content on coarse textured soils than fine textured soils and blanket peat, with the magnitude of difference increasing through summer, which is consistent with my field observations of *Calluna* green-up occurring earlier over coarse soils. Fine textured soil and blanket peat more effectively retain water, but this water is not necessarily available for plants to uptake (Easton and Bock 2016). Moreover, it may be that the North Yorkshire Moors did not experience a sufficiently moisture-limited state during field sampling to observe the expected impact of soil drainage properties on live fuel moisture. These results likely reflect the complexity of soil–fuel moisture relationships beyond simply water availability and are hypothesised to be related to both plant adaptive and soil hydraulic traits.

Ecophysiological research has demonstrated the importance of soil and plant hydraulic traits in regulating live fuel moisture content (Scarff *et al.* 2021; Brown *et al.* 2022a; Nolan *et al.* 2022; Rao *et al.* 2022; Ruffault *et al.* 2022). This may provide a useful framework to simulate the moisture of temperate fuels like *Calluna*, building on pioneering physiological (Bannister 1964a; 1964b) and more recent live fuel moisture modelling (Davies and Legg 2008). Ecophysiological traits governing fuel moisture variability have been explored temporally for *Calluna* (Davies and Legg 2008; Davies *et al.* 2010) and between different species (Brown *et al.* 2022a; Rao *et al.* 2022); however, the ecophysiological controls on the spatial distribution of within-species fuel moisture as quantified here have not yet been unravelled. Collaboration between wildfire scientists and plant physiologists remains (cf. Davies and Legg 2008, Dickman *et al.* 2023) highly important for discerning the cross-landscape controls on live fuel moisture and therefore wildfire danger in temperate fire prone landscapes.

I observed a fuel layer-dependent relationship between canopy age and fuel moisture content. Live fuel moisture content was found to be lower in mature *Calluna* plant canopies and is linked to the greater proportion of old growth and lower proportion of new growth when compared to younger *Calluna plants*. Conversely, in the dead fuel components of the canopy and in the and organic layer, fuel moisture contents were found to be lower in the building stage of *Calluna*. These findings suggest that the *Calluna* canopy (that is elevated above the ground) acts in a similar manner to that of the overstory in forested fuels, that form a boundary between the atmosphere and underlying surface fuels (Walsh *et al.* 2017; Nyman *et al.* 2018; Brown, Inbar, *et al.* 2022). Contrary to previous studies, aspect and slope were found to play a smaller role in influencing cross-landscape fuel moisture variation. However, this could be due to the absence of sufficiently steep slopes in the study region such that I did not observe large differences between sites. On steeper gradients and in more complex environments, I would expect these factors to be more important. I was able to separate the correlation between denser vegetation cover on polar aspects that likely amplified the 'aspect effect' in previous research (Slijepcevic *et al.* 2018). Therefore, it is not particularly surprising that I observed a smaller influence of aspect when isolated from other landscape factors.

While the role of phenology in the temporal variability of live *Calluna* fuel moisture has been well documented (Davies and Legg 2008), it is clear that there is also an important phenological component to the spatial distribution of live fuel moisture variability. I have demonstrated that the direction of landscape–fuel moisture relationships can switch between spring and summer, highlighting the importance of accounting for plant phenology in wildfire danger assessments in temperate environments. Understanding how landscape and micrometeorological factors modulate cross-landscape differences in the timing of green-up may aid the development of live fuel moisture models for assessing wildfire danger and behaviour.

I hypothesise that cross-landscape fuel moisture variability is associated with specific landscape controls through careful experimental design, literature-based model selection, and interpretation based on my scientific understanding of landscape processes. However, I acknowledge that inherent variability within natural landscapes means there may be unknown spatial controls not accounted for that may impact my findings. In particular, plots tended to be clustered around soil textures as soil properties are spatially disparate by nature. Future research could narrow in on specific landscape controls of interest like soil texture to validate my hypotheses. These sorts of experimental studies are critical for advancing our understanding of landscape processes and disturbances and provide valuable insights despite the spatial complexity (Davies and Gray 2015).

3.4.3 IMPLICATIONS

Landscape fuel moisture variability can create spatial discontinuity in the availability of fuel that is in the correct state for ignition (surface fuels) and wildfire spread (live fuels), including potential for spot-fires in extreme conditions, and vulnerability of the organic layer to smouldering (Finney *et al.* 2021). Spatial heterogeneity in fuel moisture can therefore influence how a fire will propagate across the landscape. For example, the percolation threshold describes the point at which a fire will spread continuously throughout the landscape irrespective of landscape connectivity (Gardner *et al.* 1987). Knowing the magnitude of fuel moisture variability may allow for spatial pattern analyses of the role of fuel moisture in landscape connectivity, as well as targeting fire prevention in areas where this threshold for continuous fire spread may be breached (Rahimi and Salman Mahini 2018; Duane *et al.* 2021). Fuel moisture models should therefore have high spatial fidelity to capture cross-landscape fuel moisture variation and dynamics, which can then be integrated into fire behaviour modelling systems (Dickman *et al.* 2023).

Tailored fuel moisture models of *Calluna* dominated landscapes that sit within systems that predict fire behaviour during incidents may aid wildfire event decision making for fire managers by informing resource deployment (particularly where locations may be vulnerable to smouldering) and identifying suppression opportunities. I suggest that knowing the specific landscape characteristics of an area of interest, a look-up tool could be applied to adjust fuel moisture estimates to local conditions by land managers or fire and rescue services. For example, controlled burns in the UK are typically small scale where accurate estimates of local fuel moisture variability may help to identify the best burn locations if seeking to reduce the risk of out-of-control fires or failed ignitions for land managers. Beyond this, the availability of digital landscape information (e.g., elevation models and soil maps) opens opportunities to enhance spatial resolution of regional fuel moisture estimates to better reflect local conditions. Such downscaling has previously been used to account for the effect of topography on net radiation and aridity (Nyman *et al.* 2014) and has subsequently been developed to downscale regional weather observations for wildfire management (Nyman *et al.* 2015; Walsh *et al.* 2017). The recently developed Australian Fire Danger Rating System is the first to forecast wildfire danger at an improved spatial resolution of 1.5 x 1.5 km (Matthews *et al.* 2019), highlighting recent recognition of the need for operational wildfire danger forecasts at the local scale.

3.4.4 CONCLUSIONS

I have quantified the magnitude of cross-landscape fuel moisture variability and the extent to which this is driven by landscape scale and micrometeorological factors in temperate peatlands and heathlands, finding:

1. Within landscape scale variations in fuel moisture content creates spatial discontinuity in the availability of live fuels for wildfire spread and vulnerability of the organic layer to high severity smouldering.

2. Within landscape scale fuel moisture variation is controlled by both landscape and micrometeorological factors, though landscape factors show greater overall performance (beyond modifying local micrometeorology).
3. Accounting for within landscape–fuel moisture relationships directly will improve the accuracy of fuel moisture estimates because estimates derived solely from micrometeorological observations will exclude the underlying influence of landscape scale controls.
4. Differences in soil texture, shrub canopy age, and slope aspect are hypothesised to be important within landscape scale controls.
5. Phenology is capable of switching within landscape scale fuel moisture variability between spring and summer.

My work thus sets the scene for a new avenue of landscape-scale wildfire danger research to support regional-scale predictions, recognising that wildfire danger ratings and fire behaviour models may require different levels of detail for the different functions they perform.

4

4 CROSS-LANDSCAPE FUEL MOISTURE DIFFERENCES IMPACT SIMULATED FIRE BEHAVIOUR

ABSTRACT

Predicting fire behaviour is an ongoing challenge in temperate peatland and heathlands, where live fuels can form the dominant fuel load for wildfire spread. Wildfire behaviour can be affected by spatial heterogeneity in landscape characteristics, including fuel moisture content, which is highly spatially variable. Cross-landscape variability in simulated fire behaviour is particularly relevant to consider when fire behaviour crosses thresholds for the safe use of suppression tools and tactics. Therefore, there is a need to understand how cross-landscape fuel moisture variability impacts simulated fire behaviour within existing temperate shrub fuel models. Here I examine the impact of fuel moisture content variation on simulated fire behaviour across a temperate peatland/heathland landscape. I collected field measurements of the *Calluna vulgaris* shrub fuel moisture content from 36 sites across the landscape and used these to define the fuel moisture inputs within existing shrubland fuel models to simulate fire behaviour in the BehavePlus fire behaviour modelling system. Simulated rates of spread varied with fuel moisture content; average mean variance

of 23–80% from the landscape average rate of spread. The driest sites had simulated rates of spread up to 135% above the landscape average and the wettest sites up to 86% below average. The temperate shrub fuel model selected dramatically impacted simulated fire behaviour, with the SH6 model simulating rates of spread 5-fold higher than the SH3 model. The choice of live fuel layer was also important, highlighting the need to validate existing fuel models and tailor models where needed to capture live fuel moisture dynamics. Furthermore, the underlying relationships within fire spread models that determine the importance of live fuel loads may require adjusting to better capture the importance of live fuel moisture to develop accurate predictions of fire behaviour in temperate peatland and heathlands.

4.1 INTRODUCTION

Fire is integral to many ecosystems. Wildfires are a natural component of the landscape and there is a long history of human use of fire to manage landscapes (McLauchlan *et al.* 2020). Global climate and land use changes are promoting increased interaction between humans and changing wildfire behaviour (Shuman *et al.* 2022). One facet of this is the increasing wildfire risk in regions that have traditionally been considered to be less vulnerable to extreme wildfires, such as the temperate peatlands and heathlands of Northwestern Europe (Belcher *et al.* 2021). These ecosystems contain globally critical carbon stores that are vulnerable to smouldering combustion during severe wildfires. Alignment of fuel and weather conditions conducive to wildfires in temperate peatlands and heathlands promote increased wildfire activity and their associated ecological consequences (Kirkland *et al.* 2023). Moreover, the seasonal window for conducting burning to meet management objectives is decreasing alongside changing policy and viewpoints on the use of fire to manage landscapes (Minsavage-davis 2022; Pandey *et al.* 2023). Accurate fire behaviour predictions are therefore critical for safe and effective land and wildfire management decision making. Understanding spatial variability in wildfire behaviour is important for determining how wildfire risk may change across a landscape. This has implications for determining suppression tactics and resource requirements within wildfire response operations, as well for determining suitable locations for burning to meet land management objectives while minimising the risk of out of control fires or failed ignitions (Minsavage-davis 2022).

4.1.1 MODELLING FIRE BEHAVIOUR

Fire behaviour models use simplified inputs of fuel, weather, and topography to assess potential fire behaviour, including rate of spread (ROS), flame length, and fire line intensity (Section 1.2). Rothermel's surface fire spread model is a fundamental model used to predict fire behaviour within surface fuels (Rothermel 1972). BehavePlus is a fire behaviour modelling system that provides a user interface to Rothermel's model (among others). BehavePlus is widely used to predict fire behaviour for different scenarios across fire management, prescribed fire planning, and research applications (Andrews 2014). It provides point-based fire behaviour metrics that can also be integrated with systems like FlamMap and FARSITE to model fire behaviour in space (Finney 1998, 2006). Wildfire Analyst operationalised fire spread models for real-time wildfire risk forecasting, wildfire spread predictions, wildland fire behaviour analysis, and risk mitigation planning in many regions, including temperate ecosystems such as The Netherlands (Monedero *et al.* 2019; Cardil *et al.* 2021). BehavePlus has previously been used to predict surface fire behaviour in *Calluna* (Davies *et al.* 2009) and was recently used by (Minsavage-davis 2022) to evaluate ROS models in heathlands.

4.1.2 TEMPERATE PEATLAND AND HEATHLAND FUEL MODELS

Fuel models are used to describe fuel availability in fire behaviour models and exist for a range of fuel types, including shrubland fuels (Scott and Burgan 2005). These are designed for non-specific vegetation types and rely on user selection. The choice of fuel model is important in determining the proportion of live to dead fuels and therefore sensitivity to fuel moisture changes. Dead fuel moisture content is the water content of dead vegetation and is important for the initial ignition of fuels. Because dead fuels respond mainly to changing weather conditions, there are simple models that can be used for predicting dead fuel moisture content. For example, the Fosberg model uses temperature and relative humidity measurements to predict 1-h fine fuel moisture, making adjustments for time of year, slope, aspect, and shading (Fosberg *et al.* 1971). Live fuel moisture content, the water content of living vegetation, is different as it can regulate drying through ecohydrological and plant physiological controls (Dickman *et al*. 2023).

In the dwarf shrub *Calluna vulgaris* that dominates peatland and heathland landscapes, both dead and live fuel moisture are important for wildfire behaviour (Davies *et al.* 2009, 2010). Despite increasing wildfire risk associated with climate and land use change, predicting fire behaviour continues to be challenging within these environments (Cardíl *et al.* 2023). Previous research has observed intense fire behaviour in temperate shrublands during fire weather conditions that are considered to be low risk in forested landscapes (Davies *et al.* 2019; Pepin and Wotton 2020). A major aspect of this is whether existing fuel models are able to incorporate the role of live fuel moisture content that can drive spring-time wildfires in peatlands and heathlands (Jolly and Johnson 2018). This is an ongoing challenge for temperate landscapes even within traditionally fire prone countries (e.g., Canada (Pepin and Wotton 2020)) in addition to emerging fire prone temperate regions like northwestern Europe (Cardíl *et al.* 2023). We need to understand fuel moisture dynamics to constrain functioning fuel models for key fuel types in temperate peatlands and heathlands.

Some previous research has focused on the role of live fuel moisture content of the dwarf shrub Calluna vulgaris on flammability, fire ignition, and ROS (e.g., Davies and Legg 2008, 2011; Santana and Marrs 2014; Log 2020). Davies *et al.* (2009) observed ROS in experimental fires in the Scottish uplands and developed empirical ROS models and later fire line intensity and flame length for *Calluna*-dominated heathlands (Davies *et al.* 2019). Cardíl *et al.* (2023) used Visible Infrared Imaging Radiometer Suite (VIIRS) remotely sensed hotspots to derive the ROS for wildfires across northwestern Europe. Understanding the response of fire behaviour models to the range of live fuel moisture conditions across a landscape is critical in addressing scenarios where models may underestimate fire behaviour. Phenologically-driven declines in live fuel moisture at the end of winter and into spring are particularly important drivers of wildfire risk in *Calluna*-dominated landscapes that are critical to capture in fire behaviour predictions (Davies *et al.* 2010; Log *et al.* 2017).

4.1.3 IMPACT OF FUEL MOISTURE SPATIAL COMPLEXITY ON FIRE BEHAVIOUR

Fuel loadings and fuel moisture are represented by single values within fuel models yet are highly spatially variable in reality (Jolly 2007; Chapter 3). Recent research demonstrated that cross-landscape fuel moisture differences in a temperate peatland/heathland created spatial discontinuity in the availability of fuel for sustained ignition of live fuels and potential for smouldering combustion in organic soils (Chapter 3; Little *et al.* (2024)). However, the influence of cross-landscape fuel moisture differences, particularly live fuel moisture, on simulated fire behaviour is still largely unknown.

Fire behaviour within emerging fire prone environments like the temperate peatlands and heathlands of northwestern Europe can be affected by fine-scale heterogeneity in landscape and fuel characteristics. Some previous research has examined the sensitivity of fire behaviour models using hypothetical live fuel moisture scenarios (Jolly 2007; Minsavage-davis 2022). Jolly (2007) systematically varied live fuel moisture content across existing standard fuel models, finding high sensitivities to live fuel moisture depending on the fuel model used. Minsavage-Davis and Davies (2022) evaluated different ROS models against observed ROS from experimental burns in *Calluna* heathlands. They found that various implementations of the Rothermel surface spread model could adequately predict ROS observed in *Calluna* heathlands. Both studies reported a lack of sensitivity in existing fire behaviour models to live fuel moisture content (Jolly 2007; Minsavage-davis 2022). However, there are no previous studies that have evaluated fire behaviour predictions using a cross-landscape range of direct live and dead fuel moisture content measurements. These field-based fuel measurement campaigns are needed to develop robust fuel models for temperate fuel types that inform fire behaviour predictions.

4.1.4 RESEARCH QUESTIONS

This chapter examines the impact of cross-landscape fuel moisture variation on simulated rate of spread across a temperate peatland and heathland landscape utilising direct fuel moisture content measurements in BehavePlus. I address the following specific research questions: (1) To what extent does landscape-scale fuel moisture variability impact simulated fire behaviour? (2) How is cross-landscape simulated fire behaviour influenced by existing fuel models used for temperate shrubby fuels? (3) Does cross-landscape simulated fire behaviour change when different live and dead *Calluna* fuel layers are used? (4) Can existing operational dead fuel moisture models adequately capture cross-landscape predicted fire behaviour?

4.2 METHODS

4.2.1 STUDY REGION

I measured cross-landscape variability in the fuel moisture content of *Calluna vulgaris* within the North Yorkshire Moors National Park, United Kingdom (Figure 4.1), which provides an ideal example to assess the impact of measured fuel moisture content on cross-landscape simulated fire behaviour. The North Yorkshire Moors is representative of the temperate peatland and heathland landscapes present across northwestern Europe that are dominated by the dwarf shrub *Calluna vulgaris* (Glaves *et al.* 2020).

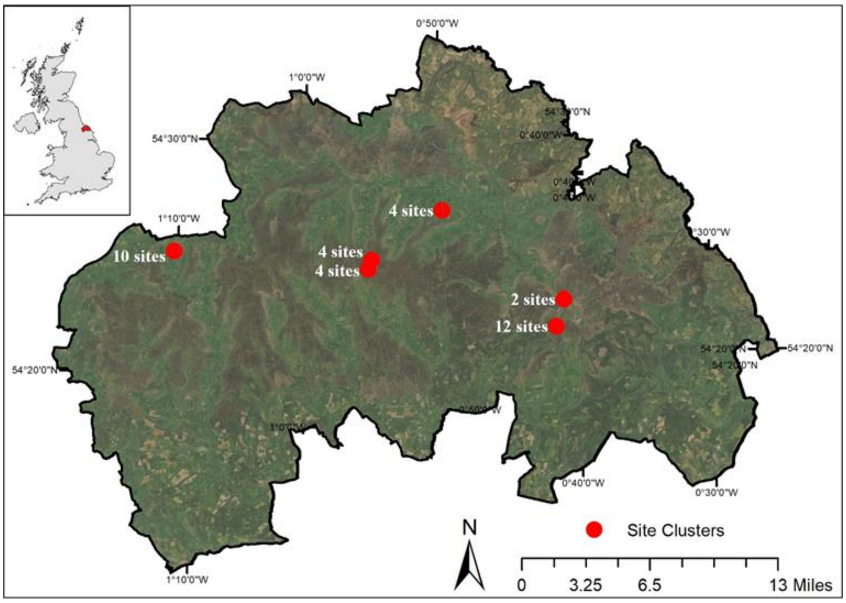

Figure 4.1 Study region of the North Yorkshire Moors, UK reproduced from Little *et al.* (2024). Live and dead Calluna fuel samples were collected from a total of 36 sites across the landscape on five days in spring and summer 2021. Source: Esri, Maxar, Earthstar Geographics, and the GIS User Community. © Natural England copyright. Contains Ordnance Survey data © Crown copyright and database right 2022.

4.2.2 SAMPLING DESIGN

I established 36 plots of 20 x 20 m homogenous *Calluna* across the landscape, with each plot comprising a unique combination of soil textures, slope positions, aspects, and canopy ages that make up the diversity of the North Yorkshire Moors (Chapter 3; Little *et al.* (2024)). I distinguished canopy age using time-since-last-burn records from land managers. Building canopy plots were burned in the last 5-10 years and averaged 30 cm height with an accumulated moss/litter layer depth of 2.5 cm. Mature canopy plots were burned 15-20 years ago and averaged 60 cm height with an accumulated moss/litter layer depth of 5 cm.

4.2.3 FIELD MEASUREMENTS

I collected fuel samples during hot, dry fire weather conditions between 1100 and 1700, randomising the order of plots visited as much as logistically possible (see Chapter 3 for full details). Briefly, I collected three sets of samples during a 1-week period of drying in April, and two further sets in June and July to capture the peak spring and summer wildfire seasons of 2021. I sampled seven fuel layers in each plot to capture the vertical variation in fuel moisture: *Calluna* live canopy, live stems (< 2 mm diameter), dead canopy, dead stems (< 2 mm diameter), surface moss (top 2 cm), litter (top 2 cm), and the organic layer beneath the *Calluna* (top 5 cm of organic material above mineral soil). Of these seven fuel layers, BehavePlus only uses the live and dead fine fuel moisture inputs to model fire behaviour, so only the live and dead *Calluna* canopy and stem fuel layers are described further in this manuscript. I collected sprigs of live and dead *Calluna* following the protocol of Little *et al.* (2023). Briefly, ca. 10 sprigs with stem diameter < 2 mm were collected from different plants along a 25-m transect, to ensure fuel samples were representative of the entire plot area. I separated the leafy canopy material from the woody lower stems into separate 250 ml aluminium tins filled 3/4 full. I measured gravimetric fuel moisture content (mass of water per mass of dried sample, %, Equation 4.1) by recording the wet weight of tinned samples, drying the samples for at least 48 h at 80 ˚ C, and reweighing the dried samples.

$$\text{Fuel moisture content} = \frac{(\text{sample wet weight} - \text{sample dry weight})}{(\text{sample dry weight} - \text{container tare weight})} * 100 \qquad [\text{Eq. } 4.1]$$

The 36 plots were spread across the landscape in pairs of building and mature canopy *Calluna*. At each pair of plots, I housed HOBO U23-001A PRO V2 (Onset Computer

Corporation, Bourne, MA) sensors in radiation shields to monitor 1.25 m air temperature and relative humidity at 15-minute intervals.

4.2.4 FUEL MODELS

I used Scott and Burgan's (2005) SH3 and SH6 shrub fuel models, which are currently the most representative of *Calluna*. The SH3 and SH6 models have both been used in temperate peatlands and heathlands: the SH3 fuel model in Northern Ireland and SH6 in the Netherlands (Stoof *et al.* 2020) and Nova Scotia, Canada (Pepin and Wotton 2020). I used the dead and live input fuel moisture categories, which describe the fine (< 2mm diameter) live and dead shrub fuel moisture contents. The SH3 fuel model describes a moderate fuel load with a high live (6.2 t/ac) compared to fine dead (0.45 t/ac) fuel load and fuel height of 2.4 ft. The SH6 fuel model describes dense shrublands where there is a higher fine dead fuel load (2.90 t/ac) compared to fine live fuels (1.40 t/ac) and fuel height of 2 ft.

I used different combinations of measured live and dead *Calluna* fuel moisture content as the fuel moisture inputs in simulations to explore the response of the models to fuel moisture content (Table 4.1). In addition to using the canopy and stem fuel moisture inputs individually in simulations, I also used the plot-average combined fuel moisture content (the average of the canopy and stem fuel moisture contents for the plot). I calculated the landscape average fuel moisture content as the average of all the plot-average combined fuel moisture contents.

I also calculated dead fuel moisture content using the Fosberg model that uses site relative humidity and temperature measurements at time of sampling for one case study each in spring (23/04/2021) and summer (22/07/2021). The Fosberg model is used to estimate fine dead fuel moisture content from relative humidity and temperature measurements and can be adjusted for canopy shading, elevation, aspect, slope, and season (Fosberg *et al.* 1971). The model has been incorporated into operational tools because of its simplicity and accessible data inputs, including look-up tables for predicting dead fine fuel moisture content and probability of ignition that are used within the National Wildfire Coordinating Group Incident Response Pocket Guide (NWCG 2022) and fire weather instruments, such as the Kestrel Fire Weather Meters (Kestrel Instruments, Boothwyn, PA). The Fosberg model was also integrated into Rothermel's surface fire spread model in the USA and associated fire prediction modelling systems (NWCG 2023).

4.2.5 FIRE BEHAVIOUR SIMULATIONS

I used the Rothermel surface ROS model in BehavePlus to simulate surface ROS at each of the 36 plots across the landscape on each of the five sampling dates, using the plot measured fuel moisture contents as fuel moisture inputs. I ran a series of different fuel simulations for each sampling date to address each of the research questions (Table 4.2). I kept all factors except fuel moisture constant, using 10 km/h midflame wind speed and 10% slope steepness to isolate the influence of fuel moisture content on ROS conditions. This scenario represented a moderate wind speed and slope that could reasonably occur within the landscape without impacting the simulated fire behaviour by using high wind speeds and slopes. I used the SH3 model as the default fuel model as it best represented the proportion of live to dead fuel load in the North Yorkshire Moors.

Existing fire behaviour models used operationally generally use a single live and dead fuel moisture content estimate to represent the average fuel moisture content for the region. I therefore calculated the landscape-average simulated fire behaviour as a null model to compare to the variability in simulated fire behaviour using the range of observed fuel moisture contents (Table 4.2, simulation 1). This simulation used the landscape average live and dead fuel moisture content inputs to produce a single average simulated ROS for the landscape. The main simulation of cross-landscape ROS variability uses the plot average canopy and stem fuel moisture content as the fuel moisture inputs to characterise the extent of landscape fuel moisture variability and its influence on simulated ROS (Table 4.2, simulation 2). I repeated the main simulation using the SH6 fuel model for comparison (Table 4.2, simulation 3). To assess the differences in simulated ROS using different fuel layer inputs, I ran the model using plot live canopy fuel moisture inputs while keeping dead fuel moisture constant as the landscape average dead fuel moisture content. I repeated this simulation for live stem fuel moisture and then plot average combined live fuel moisture (Table 4.2, simulation 4). This simulation setup was reversed, varying dead canopy, dead stem, and plot average dead fuel moisture content while keeping live fuel moisture constant as the landscape average (Table 4.2, simulation 5). Finally, I simulated ROS for the Fosberg modelled dead fuel moisture contents (Table 4.2, simulation 6).

Table 4.1 Summary table of the main fuel moisture combinations used as inputs for predicting rate of spread (ROS) and referred to throughout the text. Fuel moisture and consequent ROS scenarios are named by the fuel layer of the fuel moisture content that is varying in the ROS predictions.

Fuel moisture / ROS scenario name	Fuel moisture description	ROS dead fuel moisture input	ROS live fuel moisture input
Live canopy	Observed live canopy FMC	Average dead	Live canopy
Live stems	Observed live stem FMC	Average dead	Live stems
Live combined	Plot average of observed live canopy and live stem FMC	Average dead	Live combined
Average live	Landscape average of live combined FMC across all sites	Average dead	Average live
Dead canopy	Observed dead canopy FMC	Dead canopy	Average live
Dead stems	Observed dead stem FMC	Dead stems	Average live
Dead combined	Plot average of observed dead canopy and live stem FMC	Dead combined	Average live
Average dead	Landscape average of dead combined FMC across all sites	Average dead	Average live
Fosberg dead unshaded	Predicted dead FMC from the unshaded Fosberg model using observed temperature and relative humidity measurements at time of sampling	Fosberg dead unshaded	Average live
Fosberg dead shaded	Predicted dead FMC from the shaded Fosberg model using observed temperature and relative humidity measurements at time of sampling	Fosberg dead shaded	Average live

Table 4.2 Behave Plus model inputs used to address each of my research questions. Total number of unique runs = 1589 (simulation 6.A is a repeat of 5.A so does not contribute to the overall number of unique runs).

Simulation description	Fuel model	Dead fuel moisture content input	Live fuel moisture content input	Number of runs
1: What is the predicted RoS for the landscape using only average fmc?	SH3	Overall average dead for each date (5)	Overall average live for each date (5)	5
2: How variable is simulated RoS across a landscape?	SH3	Dead combined fmc per site (36) and date (5)	Live combined fmc per site (36) and date (5)	180
3: How is predicted RoS impacted by the fuel model selected?	SH6	Dead combined fmc per site (36) and date (5)	Live combined fmc per site (36) and date (5)	180
4: What live *Calluna* fuel layers are important to collect?	SH3	Overall average dead fmc for each date (5)	A. Live combined fmc per site (36) and date (5) B. Live canopy fmc per site (36) and date (5) C. Live stem fmc per site (36) and date (5)	540
5: What dead *Calluna* layers are important to collect?	SH3	A. Dead combined fmc per site (36) and date (5) B. Dead canopy fmc per site (36) and date (5) C. Dead stem fmc per site (36) and date (5)	Overall average live fmc for each date (5)	540
6: Do existing operational tools perform just as well?	SH3	A. Dead combined fmc per site (36) and date (2) B. Fosberg dead unshaded predicted fmc for each site (36) and date (2) C. Fosberg dead shaded predicted fmc for each site (36) and date (2)	Overall average live fmc for each date (2)	144

4.2.6 STATISTICAL ANALYSES

For each site, I calculated the percentage difference in the simulated ROS (Table 4.2, simulation 2) from the overall average ROS (Table 4.2, simulation 1) for each date. This metric was used to show how much simulated fire behaviour varied across the landscape (rather than using absolute values that vary day to day). I tested for statistically significant differences between the predicted ROS values calculated using canopy, stem, and combined fuel moisture content for both live and dead *Calluna* for each date (Table 4.2, simulation 4 and 5). I performed ANOVA tests and checked the assumptions of normality of residuals visually and homogeneity of variance using a Levene's test. Some of the fuel layers and dates violated the assumption of variance homogeneity, so I opted to use Kruskal Wallis tests for all fuel layers and dates for consistency. The results from the ANOVA and Kruskal Wallis tests were the same for all fuel layers and dates except for the live fuels on April 15, 2021, where the Kruskal Wallis test revealed significant differences while the ANOVA did not. I performed pairwise Wilcoxon tests where Kruskal Wallis tests were significant to determine which fuel layers were different. I followed the same approach to compare predicted rates of spread between the observed and Fosberg modelled fuel moisture inputs (Table 4.2, simulation 6). I used Spearman correlations to compare fuel moisture predictions using the Fosberg model with observed dead fuel moisture content. I conducted all statistical analyses in R version 4.0.3 (R Core Team 2022), using packages stats (inbuilt), car (Fox and Weisberg 2019), and Hmisc (Harrell Jr 2022) .

4.3 RESULTS

Cross-landscape fuel moisture differences resulted in a 23–80% mean variation from average ROS predicted using single fuel moisture inputs (Figure 4.2; Table 4.3). The driest sites predicted rates of spread up to 135% above the landscape average. The range of variation from average ROS between the driest and wettest sites was between 46% and 160%. Predicted ROS variance and absolute ROS was highest in spring (Figure S4.1).

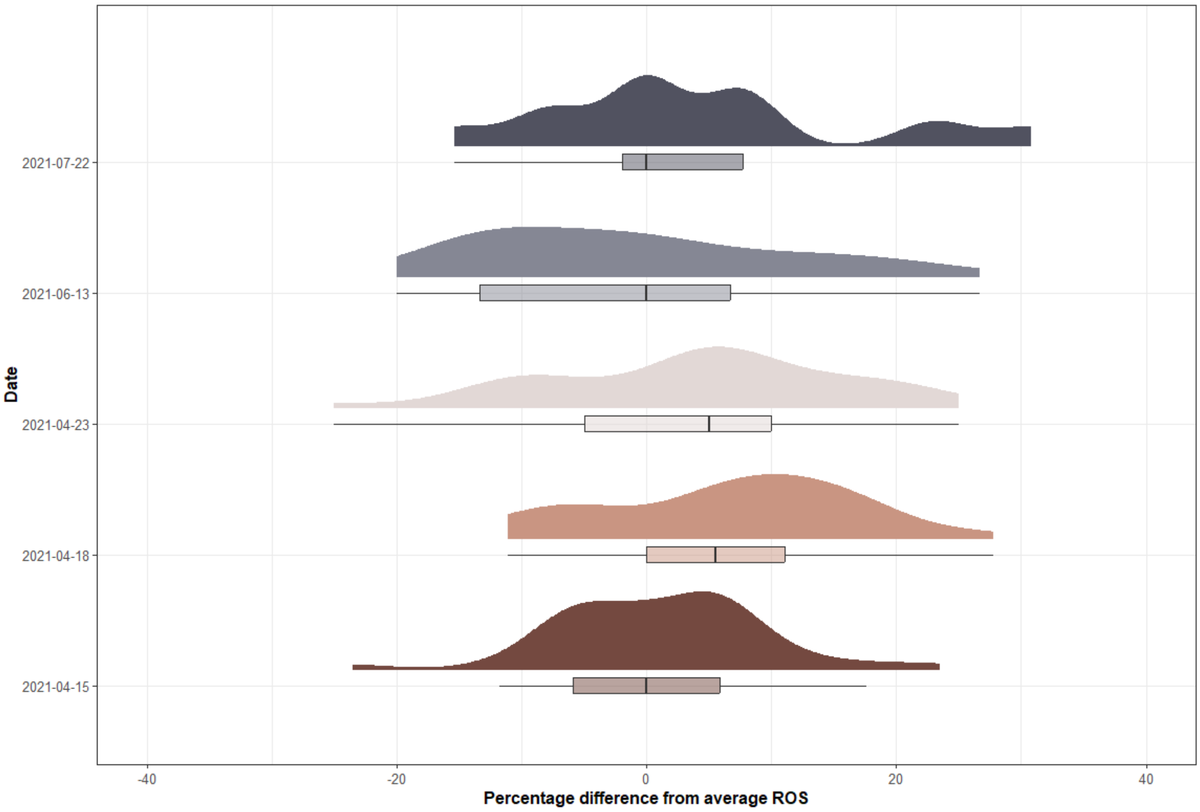

Figure 4.2 Box- and half violin-plots showing percentage variation from average rate of spread (ROS) across a landscape for each of the five days of fuel moisture measurements, i.e., the percentage difference between simulations one and two). Each value in the distribution represents a site (n = 36).

Table 4.3 Cross-landscape rate of spread (ROS) variation due to fuel moisture differences. Absolute (m/min) and percentage variation from average ROS, where average ROS is predicted from landscape averaged fuel moisture content under both the SH3 and SH6 fuel models (Table 4.2, simulation 1).

Date	Fuel model	Max ROS (m/min)	Min ROS (m/min)	Average ROS (m/min)	Max variation from average	Min variation from average	Mean variation from average
15/04/21	SH3	2.1	1.3	1.7	23.5	-23.5	23.5
18/04/21	SH3	2.3	0.9	1.9	27.8	-50.0	38.9
23/04/21	SH3	4.7	1.5	2.2	135.0	-25.0	80
13/06/21	SH3	1.9	1.2	1.5	26.7	-20.0	23.3
22/07/21	SH3	1.7	1.1	1.4	30.8	-15.4	23.1
15/04/21	SH6	12.3	7.2	10.4	57.7	-7.7	32.7
18/04/21	SH6	10.5	6.5	8.4	22.1	-24.4	23.3
23/04/21	SH6	15.1	1.6	11.4	31.3	-86.1	58.7
13/06/21	SH6	10.9	6.9	8.7	2.8	-34.9	18.9
22/07/21	SH6	10.1	6.2	8.0	3.1	-36.7	19.9

Simulated absolute ROS is significantly higher when the SH6 fuel model is used compared to the SH3 fuel model (Figure 4.3). Average ROS is more than five-fold higher overall when the SH6 fuel model is used to simulate ROS using the same fuel moisture content inputs. However, the mean ROS variance is comparable between the SH3 and SH6 simulations.

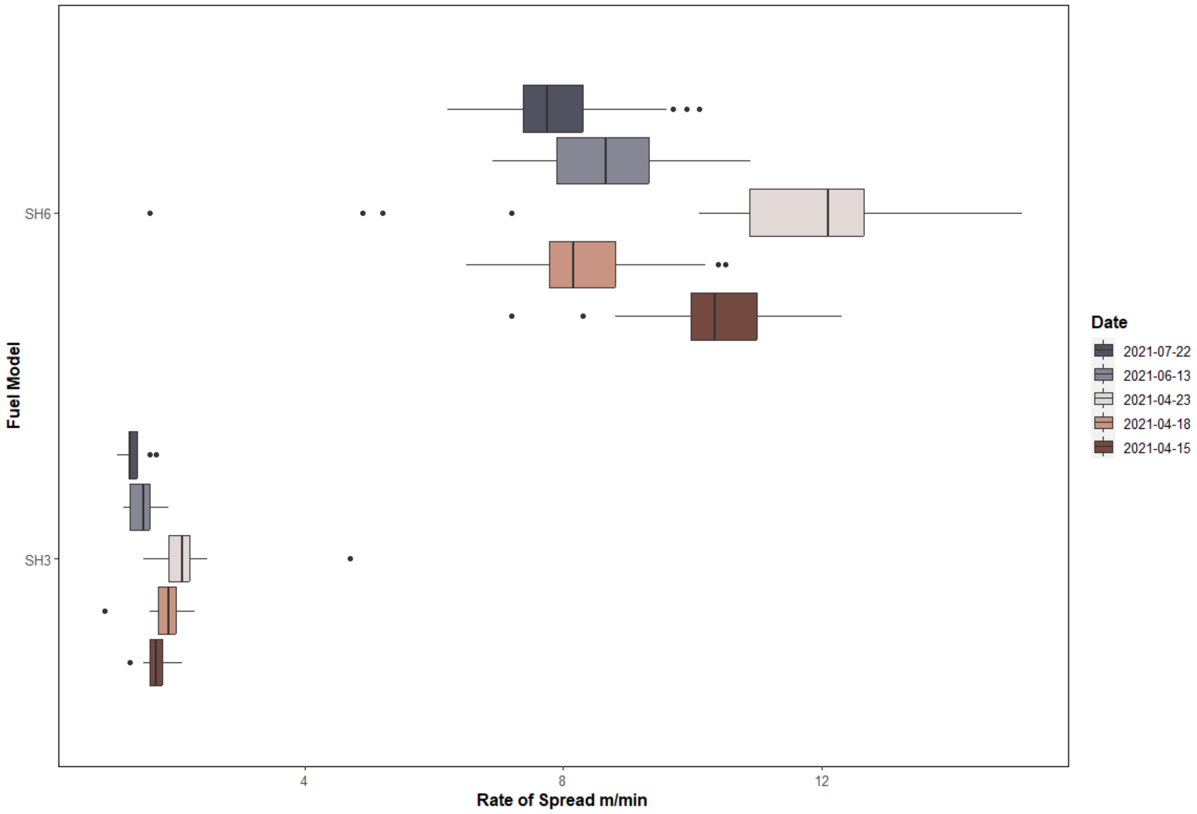

Figure 4.3 Boxplots of cross-landscape predicted rate of spread (ROS) from observed fuel moisture variability between the SH3 and SH6 fuel models.

There were no statistically significant differences in predicted ROS when using dead canopy, dead stem, or combined fuel moisture contents (Tables S4.1–S4.2). All live fuel moisture combinations led to significantly different ROS predictions, except for the June 13 field measurements (Table S4.2). Cross-landscape ROS predictions were more variable when live canopy *Calluna* fuel moisture values were used, leading to higher predicted rates of spread in spring and lower in summer (Figure 4.4).

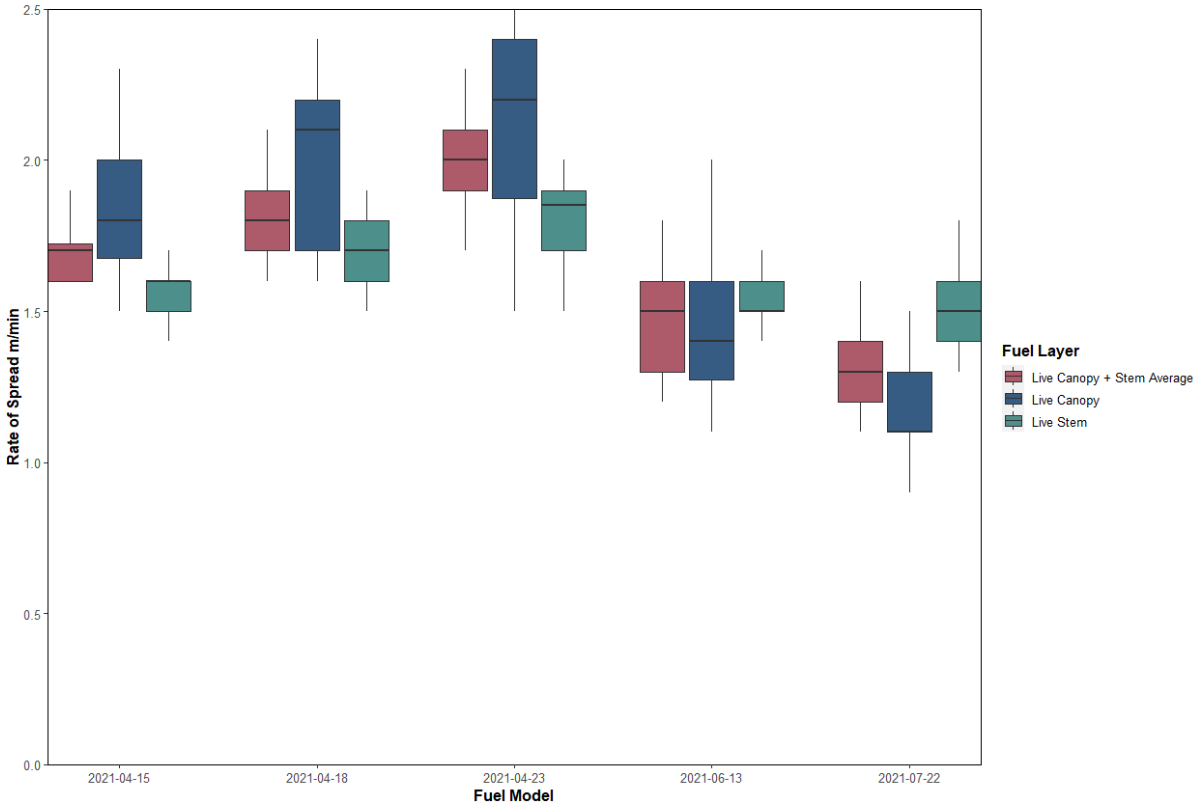

Figure 4.4 Boxplots of cross-landscape predicted rate of spread (ROS) calculated for each of the live fuel layers (using landscape-averaged 1-h fine fuel moisture).

The Fosberg model predicted lower dead fuel moisture content using temperature and relative humidity measurements than the observed values (Figure 4.5a). The predictions using the shaded position Fosberg model were closer to observed dead fuel moisture despite the plots technically being unshaded. Predicted shaded (correlation coefficient = 0.48) and unshaded (0.46) fuel moisture content was, however, significantly positively correlated with observed fuel moisture for July 22. These differences did not translate to significantly different ROS predictions between the Fosberg shaded and observed combined dead fuel moisture simulations, but predicted ROS was significantly higher for the Fosberg dead unshaded simulations (Tables S4.2–S4.3). Predicted ROS was higher in spring than summer (Figure 4.5b).

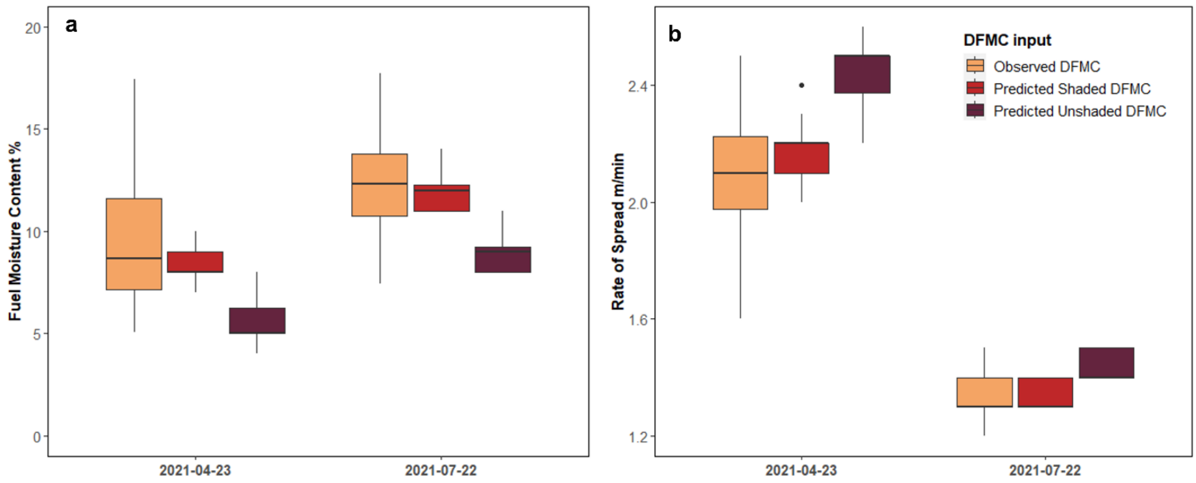

Figure 4.5 Boxplots showing variation between observed and predicted dead fuel moisture content using the Fosberg model (left) and consequent variation in predicted rates of spread (right) for a spring (April 23) and summer (July 22) example.

4.4 DISCUSSION

My research highlights the importance of including cross-landscape fuel moisture content differences in fire behaviour prediction models. This means it is also key that we collect fuel moisture content data and understand how its variability is controlled by landscape features. By comparing a null model with uniform fuel moisture content values to models that realistically represent the variability in fuel moisture across a landscape, my results show that the predicted fire behaviour differs significantly when incorporating natural variability in fuel moisture.

4.4.1 LANDSCAPE FUEL MOISTURE VARIABILITY IMPACTS SIMULATED FIRE BEHAVIOUR

Cross-landscape fuel moisture differences impacted predicted ROS by 23–80% on average, compared to predictions based on a single fuel moisture estimate for the entire landscape (Table 4.3). The significance of this magnitude of variation is context specific. On the days I collected fuel samples, the absolute ROS predicted was low and cross-landscape variation would not likely cause concern. However, during drier conditions, this may be useful information to fire managers, particularly where fire behaviour crosses thresholds for the safe use of suppression tools and tactics. Similarly, points on the landscape where ROS is slower may provide FRS with opportunities to focus suppression activities or create fire breaks.

This study contributes to existing model sensitivity studies as it utilises the measured magnitude of fuel moisture variation across a landscape on the same day and thus represents the range of differences in fire behaviour that could be expected in such a landscape. Fuel moisture content was more variable in my field campaigns than the observed fuel moisture ranges in previous experimental burns (Davies *et al.* 2009). Absolute ROS tended to be lower than previous research has observed from experimental burns. This is likely due to the set moderate slope and wind speed parameters used in my simulations compared to observed fire data (Minsavage-davis 2022).

4.4.2 SIMULATED FIRE BEHAVIOUR IS IMPACTED BY CHOICE OF FUEL LAYER AND FUEL MODEL

Absolute ROS was significantly higher when the SH6 fuel family was used in place of the SH3. There are a range of fuel models that are used for temperate shrubby fuels (Scott and Burgan

2005), and I demonstrate that the choice of fuel model can dramatically affect predictions. Fine dead fuel load in the SH6 fuel model (2.9 t/ac) was six times higher than that of the SH3 fuel model (0.45 t/ac). I selected the SH3 model for the main simulations as my field measurements were collected in a high live fuel load landscape; however, under future climate change the proportion of live to dead fuel may change, and it is not unrealistic to think the higher dead fuel load SH6 fuel model may become more representative. A number of studies using climate projections point to future increased fire risk in the UK and Northwest Europe due to increases in fire weather (Arnell *et al.* 2021; Perry *et al.* 2022). Moreover, the SH3 model contained a 3 t/ac 10-hour dead fuel load (representing 6.35 mm to 25.4 mm diameter dead fuels), which is unrealistic within many *Calluna*-dominated peatland and heathlands. As such, ROS is likely underpredicted in my simulations. In reality, a scenario somewhere between the SH3 and SH6 models would be most appropriate and highlights the importance of tailoring fuel models for robust predictions of fire behaviour.

Previous research has demonstrated fuel moisture differences between the different fuel layers of *Calluna* (i.e., canopy and stem fuel moisture differs for both live and dead *Calluna*) (Davies *et al.* 2010; Davies and Legg 2011). Predicted rates of spread were not significantly different when either dead canopy, dead stem or a combined average was used. For simplicity, either material could be used from a fire behaviour modelling perspective. Predicted rates of spread were more variable for live *Calluna* canopy than stems or combined and predicted higher rates of spread in spring and lower in summer. Fire behaviour has proven challenging to model in temperate peatland and heathland fuels like *Calluna* where live fuel can form the dominant fuel load for fire spread during spring (Belcher *et al.* 2021). Moreover, previous experimental research found a strong relationship between *Calluna* canopy fuel moisture and variation in observed fire behaviour (Davies *et al.* 2009). In lieu of customised fuel models that specifically account for phenology, using *Calluna* canopy live fuel moisture for fire behaviour model inputs would help capture the role of phenology in influencing wildfire behaviour. Previous research has described fire behaviour in *Calluna* as akin to mini crown fires as sustained spread can occur through the canopy without consumption of the surface material (Fernandes *et al.* 2000; Davies *et al.* 2016). As such, capturing *Calluna* canopy fuel moisture variation may provide the most realistic fire behaviour scenarios. These findings suggest that the underlying relationships that apportion the importance of dead and live fuel loads within the Rothermel family of fire spread models may need to be adjusted to better account for the importance of live fuel moisture in these fuel types.

Direct fuel moisture measurements are generally too time consuming to collect to be utilised in a wildfire response fire behaviour modelling capacity. In these scenarios we need to rely on modelled fuel moisture. The Fosberg model uses relative humidity and temperature to predict fine dead fuel moisture content. The ability to use a look-up table to generate quick predictions of fire behaviour is incredibly beneficial for response decision-making needs. These forms of fuel moisture models, like the Fosberg model, likely need to be customised for shrub fuel types that may not fully cure in the way grasses or litter do. Field-based measurements of fuel moisture in shrub fuels would allow for a correction factor to adapt existing models to temperate shrub ecosystems.

The Fosberg model was unable to capture the range of variability in fuel moisture content because factors beyond these meteorological controls also influence fuel moisture. While the unshaded model predicted lower fuel moisture contents and consequently higher ROS, the shaded model fuel moisture content was closer aligned to the observed dead fuel moisture despite a lack of shading effect in the traditional sense. The shaded Fosberg model simulated ROS that were not significantly different to those simulated using observed fuel moisture content (Figure 4.5). This suggests that the density of *Calluna* canopy may shade understory fuels and make shaded fuel moisture predictions more appropriate to use, adding further weight to the narrative of *Calluna* behaving akin to a mini forest canopy.

4.4.3 FIRE BEHAVIOUR MODELS ARE INSENSITIVE TO CROSS-LANDSCAPE LIVE FUEL MOISTURE CONTENT

There is a broader issue of whether fire behaviour models are sufficiently sensitive to fuel moisture changes. Little *et al.* (2024) found fuel moisture was highly spatially variable; however, the resulting variability in predicted ROS was much smaller. This is a reflection of the sensitivity of the Rothermel model to live fuel moisture. Previous experimental research has suggested that ROS is likely more sensitive to live fuel moisture changes than existing models predict, and this sensitivity increases with fuel aridity (Jolly 2007; Nolan *et al.* 2016; Pimont *et al.* 2019). This creates high risk scenarios in temperate regions where ROS may be underpredicted when live fuels are dry, such as at the end of winter and early spring when both managed burning and the main wildfire season are taking place in the UK's peatland and heathland landscapes (Davies *et al.* 2010). There is a need to constrain the role of fuel moisture, particularly live fuel moisture, within models to develop accurate predictions of fire behaviour in temperate environments (Dickman *et al.* 2023). One such avenue to achieve this would be to develop live fuel moisture models that capture plant phenological and physiological processes and constrain the sensitivity of fire behaviour models to live fuel moisture of temperate fuels.

4.4.4 IMPLICATIONS FOR FIRE MANAGEMENT

In emerging fire prone environments like the temperate peatlands and heathlands of northwestern Europe, spatial heterogeneity in fire behaviour as a result of landscape characteristics is relevant to consider. Cross-landscape fire behaviour is important for fire management decision making, particularly where this variability may require changes in suppression tools and tactics employed or provide opportunities for suppression. Capturing cross-landscape fire behaviour variation would allow strategic decision-making for conducting burns to safely and effectively achieve management outcomes. Existing fire behaviour prediction tools based on a single regional average fuel moisture input could underpredict fire behaviour and create dangerous situations for those suppressing wildfires or increase the risk of escaped managed burns. Likewise, overpredictions could limit opportunities for managed burning and increase suppression costs associated with wildfire event turnouts.

As the risk from wildfires in these environments increases, availability of tools like BehavePlus to inform decision-making become increasingly important. These tools require user decisions such as choice of fuel model and fuel layer inputs, which can significantly impact predictions. Minsavage-Davis and Davies (2022) suggested fire behaviour modelling systems using Rothermel's surface fire spread model can be applied within *Calluna* heathlands but implored caution in interpreting predictions. While spatial variation in dead fuel moisture between *Calluna* fuel layers is not likely to impact predicted rates of spread, care should be taken in defining live fuel moisture inputs and emphasis should be put on capturing *Calluna* canopy fuel moisture. My findings highlight the need to validate existing fuel models or develop tailored models that capture live fuel moisture dynamics and fuel loads in temperate shrub fuels.

5

5 ACCOUNTING FOR AMONG-SAMPLER VARIABILITY IMPROVES CONFIDENCE IN FUEL MOISTURE CONTENT FIELD MEASUREMENTS

ABSTRACT

Background: Direct fuel moisture content measurements are critical for characterising spatiotemporal variations in fuel flammability and for informing wildfire danger assessments. However, among-sampler variability (systematic differences in measurements between samplers) likely contributes to fuel moisture measurement variability in most field campaigns. **Aims:** I assessed the magnitude of among-sampler variability in plot-scale *Calluna vulgaris* fuel moisture measurements. **Methods:** Seventeen individuals collected samples from six fuel layers hourly from 10:00–18:00. I developed mixed effects models to estimate the among-sampler variability. **Key results:** Fuel moisture measurements were highly variable between individuals sampling within the same plot, fuel layer, and time of day. The importance of among-sampler variability in explaining total measured fuel moisture variance was fuel layer dependent. Among-sampler variability explained the greatest amount of measurement variation in litter (58%) and moss (45%) and was more important for live

(19%) than dead (4%) *Calluna*. **Conclusions:** Both consideration of samplers within the experimental design and incorporation of sampler metadata during statistical analysis will improve understanding of spatiotemporal fuel moisture dynamics obtained from field-based studies. **Implications:** Accounting for among-sampler variability in fuel moisture campaigns opens opportunities to utilise sampling teams and citizen science research to examine fuel moisture dynamics over large spatiotemporal scales.

5.1 INTRODUCTION

Fuel moisture is a primary determinant of fuel flammability, ignition, and rate of spread; therefore, being able to accurately determine fuel moisture content is integral to predicting wildfire danger and behaviour (Scarff *et al.* 2021; Ellis *et al.* 2022; Dickman *et al.* 2023). Field-based sampling of fuels provides the only direct measure of fuel moisture content. However, fuel moisture contents vary both rapidly in time through the day in response to humidity fluctuations (Matthews 2014) and over long time periods in response to seasonal and interannual weather patterns (Pivovaroff *et al.* 2019; Brown, Hoylman, *et al.* 2022). Fuel moisture contents also likely vary over a range of spatial scales (plot – landscape – regional) in response to diverse ecohydrological and climatological controls (Nyman *et al.* 2018; Nolan, Foster, *et al.* 2022). Intensive large-scale and long-term sampling campaigns with a large number of people are necessary to adequately sample this complex spatiotemporal variability in fuel moisture contents, particularly to sample spatial variability in fuel moistures across extensive research areas during short periods of consistent fire weather conditions (Matthews *et al.* 2010).

In these large fuel moisture measurement campaigns, there are two key sources of variability in the sampling process: (a) random sampling error, where different plants or parts of the plant from the appropriate layer are selected, and (b) sampler error, for example where a sampler consistently has a different interpretation of a fuel layer. Because the error associated with (a) is random, it can be averaged out through repetition. However, (b) is systematic and likely becomes a relevant source of measurement error. I define this as 'among-sampler variability' within the text (systematic differences in fuel moisture content measurements between samplers; Figure 5.1).

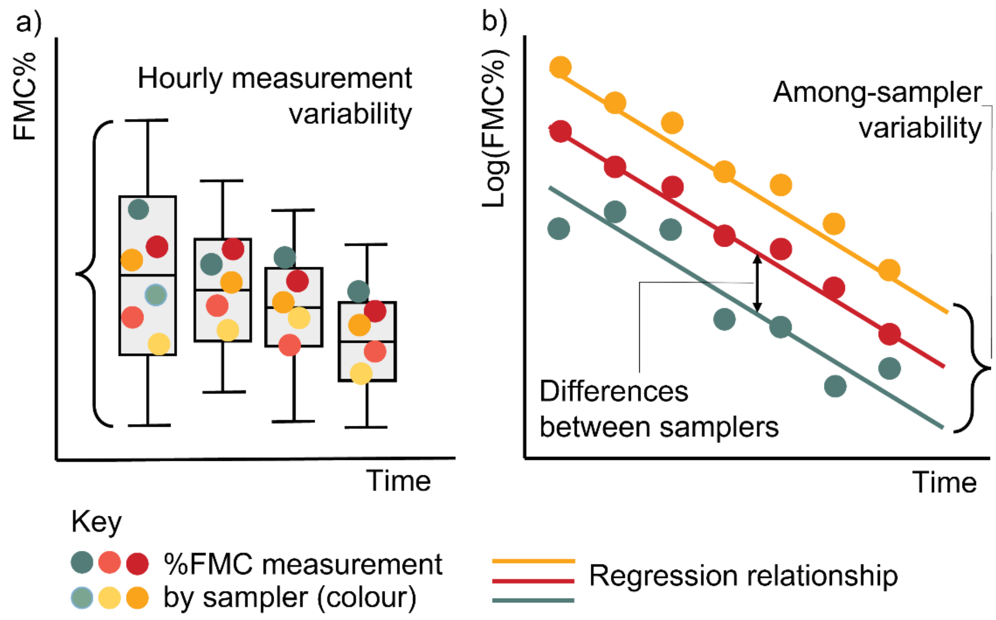

Figure 5.1 Schematic diagram outlining definitions of variability. a) 'Hourly measurement variability' is the variation in the moisture content measurement of a given fuel layer in each hour. This results from both among sampler variability and random sampling error in the plot. b) 'Among-sampler variability' is variability due to systematic differences between samplers that occur across repeated measurements during the day.

Where direct measurements are not feasible, various models have been developed to indirectly estimate fuel moisture, particularly across long time periods (e.g., Cawson *et al.* 2020; Miller *et al.* 2022). While we routinely quantify sources of uncertainty associated with fuel moisture models (Lai *et al.* 2022), field-based fuel moisture measurement errors are rarely considered explicitly. To improve fuel moisture experimental designs and analyses it is important to be able to extract among-sampler variability from other sources of fuel moisture measurement variability. In doing so, we improve our scientific understanding of fuel moisture contents and our ability to accurately simulate its values for fire management.

5.1.1 *CITIZEN SCIENCE FOR FUEL MOISTURE MONITORING*

Citizen science is a powerful approach for collecting large quantities of environmental data and is critical for understanding processes operating across large spatiotemporal scales

(Devictor *et al.* 2010; Isaac *et al.* 2014). Among-sampler variability is inherent in field studies involving multiple individuals, as people naturally carry out tasks differently, and can arise through different levels of experience, motivation, and different interpretations of protocols. The importance of among-sampler variability has been reported in previous environmental citizen science projects, particularly for studies monitoring species presence-absence and quantifying flora percentage cover (e.g., Morrison 2016 and references therein; Sicacha-Parada *et al.* 2021; Nolan, Gilbert, *et al.* 2022). Some sources and impacts of among-sampler variability can be lessened through careful experimental design (e.g., developing effective training protocols, recruiting individuals with similar levels of prior experience). However, among-sampler variability cannot be completely eliminated, and this error is incorporated into the resulting measurements (Bird *et al.* 2014; August *et al.* 2020).

Accounting for among-sampler variability allows us to optimise citizen science opportunities to understand fuel moisture dynamics at broad spatiotemporal scales that cannot be captured by traditional, controlled field experiments (Dickinson *et al.* 2010; Arazy and Malkinson 2021). This is important for developing robust fuel models and is especially important in environments where cross-scale fuel moisture dynamics are not fully understood. Considering potential among-sampler variability prior to conducting large-scale fuel moisture campaigns can allow for targeted collection times, locations, and sampler metadata to isolate spatiotemporal fuel moisture dynamics.

5.1.2 RESEARCH QUESTIONS

I conducted an intensive sampling campaign to determine the magnitude of among-sampler variability in measured fuel moisture at the plot scale within a *Calluna vulgaris* dominated temperate fire prone landscape. My findings are widely applicable for estimating among-sampler variability in fuel moisture measurements and enabling a confidence range to be applied to estimates used in a practical setting. Accounting for among-sampler variability also opens opportunities for large-scale fuel moisture monitoring campaigns using citizen science, which are necessary for understanding fuel moisture dynamics at regional and national scales.

5.2 METHODS

5.2.1 STUDY SITE

The field campaign was completed by an undergraduate geography field class (n = 17) in the Lickey Hills Country Park, Birmingham, England (52.3723˚N, 2.0045˚W). The site was selected as it is representative of the type of heathland landscapes that are found throughout temperate fire prone environments (Glaves *et al.* 2020). Two *Calluna*-dominated plots were selected, and samplers were evenly split across the two plots to minimise overall destruction of *Calluna* in one location. The two plots were both ca. 300 m^2 situated on hillslopes on the same shallow, acidic, peaty soils (Soilscapes, Farewell *et al.* 2011) ca. 1000 m apart. Plots were dominated by *Calluna vulgaris* and interspersed with *Vaccinium myrtillus* (common bilberry) and *Pteridium aquilinum* (bracken).

5.2.2 FUEL MOISTURE SAMPLING CAMPAIGN

Students sampled six *Calluna* fuel layers each hour (**Error! Reference source not found.**). T hese layers were: live canopy; live stems; dead canopy; dead stems; surface moss (*Kindbergia praelonga* dominant species); and surface litter. Each sampler collected one set of samples every hour between 1000 and 1800, resulting in nine sets of samples per sampler and a total of 918 samples overall. None of the samplers had monitored fuel moisture before, and all samplers received the same protocol (Supplementary Material; Figure S5.1) adapted from (Norum and Miller 1984). I provided a briefing prior to beginning sampling and advice during the first hour of sampling to ensure correct species identification and sample size for laboratory analysis. Each sampler was instructed to haphazardly collect fuel clippings from each fuel layer across the entire plot area (ca. 10 different plants) in accordance with Norum and Miller (1984). The undergraduate students stored clippings in an aluminium tin with a screw-fit lid sealed with masking tape. I calculated gravimetric fuel moisture content (mass of water per mass of dried sample, %) following Norum and Miller (1984). I weighed the tinned samples (wet weight) as soon as possible the morning after collection. I then dried the samples for at least 48 h at 80 ˚C and reweighed them (dry weight). All fuel moisture contents are presented throughout as percentages; mass of water as a percentage of the mass of the dried sample (%).

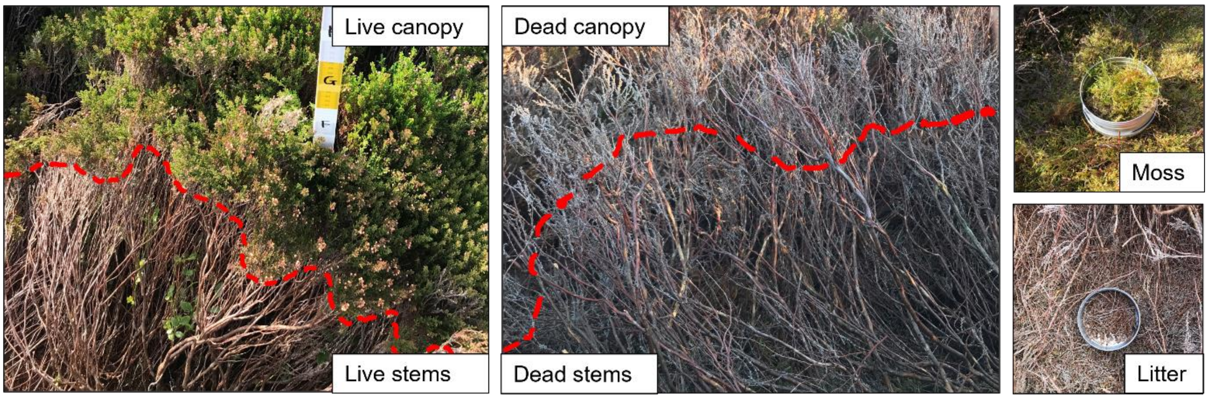

Figure 5.2 Visual depiction of the six different fuel layers sampled by the students each hour through the sampling period. Red line depicts the boundary between the canopy above and the stems below (Photo credit: Kerryn Little).

5.2.3 DATA ANALYSIS

I used mixed effects models with time as a fixed effect and sampler identity as a random effect. By including sampler as a random effect, this allowed me to estimate the among-sampler variability (Figure 5.2), where the actual identity of the sampler is not important. The standard deviation of the random effect can be interpreted as the among-sampler variability once fixed effects (in this case time of day) have been accounted for. I also calculated the coefficient of variation (standard deviation of the random effect divided by the mean fuel moisture content (FMC%) for a given layer) to facilitate comparability across fuel layers of different fuel moisture content ranges.

Finally, I calculated the model marginal R^2 (variation explained by the fixed effects) and conditional R^2 (variation explained by both fixed and random effects) (Nakagawa and Schielzeth 2013). The difference represents the amount of variation explained by among-sampler variability, and therefore gives an understanding of how important accounting for among-sampler variability is for a given layer. I conducted all statistical analyses in R version 4.1.2 (R Core Team 2022) using packages lme4 (Bates *et al.* 2015) and MuMIn (Bartoń 2022).

5.3 RESULTS

5.3.1 FUEL MOISTURE MEASUREMENT VARIABILITY

High fuel moisture content measurement variability was observed across all fuel layers (Figure 5.3). Individuals sampling within the same plot at the same time obtained different fuel moisture content measurements up to a maximum range of 320% (moss), 249% (litter), 76% (live canopy), 72% (dead canopy), 68% (dead stems), and 39% (live stems). Most fuel layers had a right-skewed distribution of measured fuel moisture content, with a high upper quartile, upper extreme and high fuel moisture outliers. Live *Calluna* had more of an even distribution of above and below median measured fuel moisture content. Measured live and dead *Calluna* fuel moisture content was highest at 10:00 and generally decreased throughout the day before starting to increase again at the end of the sampling period. This diurnal pattern was not evident in the wettest fuel layers (Figure S5.2).

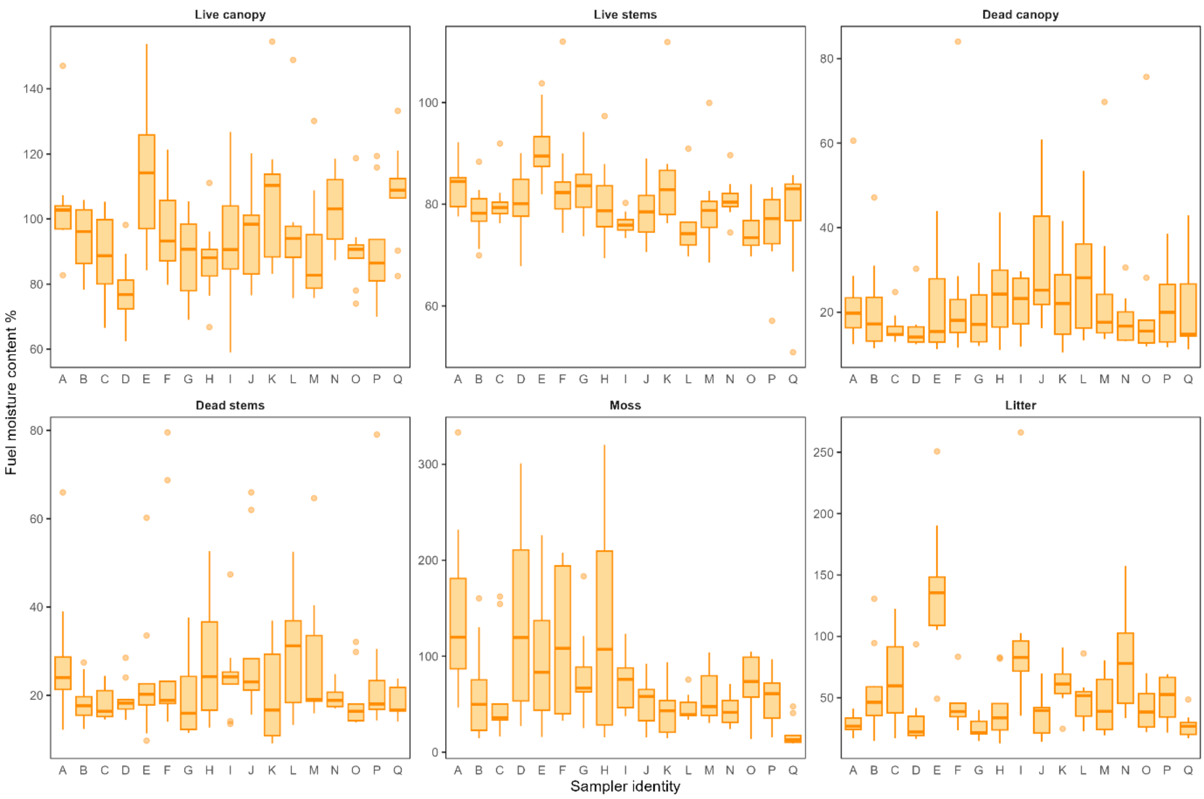

Figure 5.3 Measurement variability in fuel moisture content measurements collected by each sampler from 10:00 to 18:00 by fuel layer. Each y-axis is scaled independently to clearly visualise within-fuel layer measurement variability.

5.3.2 *AMONG-SAMPLER VARIABILITY IN FUEL MOISTURE CONTENT*

Among-sampler variation, measured as the standard deviation of the random effect, ranged from 1.25 (dead canopy layer) to 32.13 (moss layer). Because each layer has a very different mean value for FMC%, I also present the coefficient of variation which allows me to provide relative estimates of among-sampler variation. These range from 0.04 (live stems and dead canopy) to 0.56 (litter layer). In general, among-sampler variation is larger in the wetter layers (moss and litter) (Table 5.1). The amount of variance explained by the random effects (conditional R^2 – marginal R^2) can provide us with information about how important it is to take account of the among-sampler variability. This was greater than the amount of variation explained by the fixed effects for all layers except dead canopy, suggesting it is crucial to account for among-sampler variability in such studies. It should be noted, however, that the R^2 values are sensitive to the sample size and study specifics. Time of sampling explained up to 14% (live canopy layer) of the variability in the data.

Table 5.1 Summary statistics from the mixed effects model of diurnal fuel moisture measurement variability with sampler as a random effect. Values represent fuel moisture contents as percentages; mass of water as a percentage of the mass of the dried sample (%).

Fuel layer	SD of the random effect (raw among-sampler variability in FMC%)	Coefficient of variation (relative among-sampler variability in FMC%)	Estimate of time of day (standard error)	Marginal R^2	Conditional R^2	Difference
Live canopy	7.48	0.07	-2.45 (0.44)	0.14	0.32	0.18
Live stems	3.51	0.04	-0.47 (0.22)	0.02	0.21	0.19
Dead canopy	1.25	0.04	-1.59 (0.38)	0.10	0.11	0.01
Dead stems	2.63	0.10	-0.53 (0.40)	0.01	0.05	0.04
Moss	32.13	0.40	-0.64 (1.79)	< 0.01	0.45	0.45
Litter	27.37	0.56	1.19 (0.95)	<0.01	0.58	0.58

5.4 DISCUSSION

5.4.1 QUANTIFYING AMONG-SAMPLER VARIABILITY IN FUEL MOISTURE ESTIMATES

Seventeen samplers collecting fuel moisture samples at the same time within the same site measured very different fuel moisture contents. With the exception of dead canopy material, among-sampler variability was more important than time-of-day in explaining the total measured fuel moisture variation of each fuel layer at the plot scale. Significant attention is given to diurnal variability in fuel moisture content in rapidly drying fine fuels (e.g. Slijepcevic *et al.* 2013; Bilgili *et al.* 2019; Zhang and Sun 2020). However, I have shown that among-sampler variability can exceed diurnal drying patterns and should also be considered in fuel moisture dynamics studies.

Among-sampler variability explained the greatest amount of variation in litter fuel moisture, followed by moss and live *Calluna* stems and canopy. Importantly, it is not exclusively the highest absolute values of fuel moisture that are associated with large among-sampler variability. I hypothesise that some fuel layers are harder to sample and require more subjective decision-making by the sampler. Even with protocols and training, any such subjective decision-making and variation in sampling effort will produce among-sampler variability in fuel layers. For instance, samplers must identify the top 2 cm of moss and litter material, remove any attached decomposing material, and ensure fuel sample separation where litter material is interspersed in patches of moss. Subjectivity in clipping live *Calluna* can also incorporate additional among-sample variability due to the length of sprigs collected, where samplers choose to separate the live canopy from the live stems, and even correctly identifying live from dead *Calluna*. A lack of confidence in the latter could lead to subconscious targeting of the greenest live material and missing the brown live material that is harder to identify.

At the other end of the scale, among-sampler variability was low in dead *Calluna* but the coefficient of variation was higher than expected for such a low among-sampler variability. This is likely attributable to outliers resulting from the misidentification of live *Calluna* as dead. Where dead fuel is correctly identified, this material is considered easy to collect following the sampling protocol and among-sampler variability is low. Among-sampler variability in this case is mainly a concern where brown *Calluna* is incorrectly identified as dead. Where dead fuel moisture is the most important variable, among-sampler variability may be less important to account for than time-of-day and illogical values from misidentifications can be filtered out of the dataset.

There may also be variability within individual samplers through time. For instance, sampler accuracy may increase with experience gained or decrease due to fatigue as the day goes on. These changes may be intertwined with diurnal fluctuations in fuel moisture variability, as was the case in this study, and so are unable to be disentangled. However, temporal changes in individual sampler variability should be considered during sampling campaign design to minimise this influence (e.g., allow time for instructions, practice, and feedback before beginning and consider the required length of sampling campaigns to manage fatigue and comfort of samplers).

5.4.2 CONSIDERING AMONG-SAMPLER VARIABILITY IN SURVEY DESIGN

Carefully considered sampling protocols can minimise sources of among-sampler variability prior to field collection (Dickinson *et al.* 2010; Morrison 2016). I aimed to reduce sampling effort variability by having a clear protocol for where, when, and how samples should be collected. I also controlled for among-sampler differences by recruiting volunteers from the same cohort with no prior fuel moisture sampling experience and provided them with the same level of training. Where sources of variability cannot be minimised through sampling protocols, statistical tools can sometimes be used to account for among-sampler variability from other sources of error (Bird *et al.* 2014; August *et al.* 2020). Statistical models such as mixed effects models (Aagaard *et al.* 2018) and machine learning tools like boosted regression trees (Cox *et al.* 2012), random forests, and artificial neural networks (Fink and Hochachka 2012) have been used in citizen science ecological studies to account for this variability. However, statistical tools can only be utilised when it is possible to isolate sampler identity from other covariates. Where sampler identity is not known or is confounded with other variables such as geographic location or time, the underlying controls on fuel moisture variability cannot be disentangled.

Larger fuel moisture sampling campaigns that aim to quantify the spatiotemporal variability in fuel moisture content will likely require greater flexibility in where and when samples are collected and who is recruited to collect samples. In these situations, the collection of sampler metadata (e.g., sampler experience, training received, and profession (e.g., heathland land managers may have greater familiarity and confidence in identifying fuel layers than others)) could also be collected to further quantify among-sampler variability (Kelling *et al.* 2015). Fuel moisture samples should have a sampler identifier to relate metadata metrics to fuel moisture content. Sampler metadata can be used to control sampling designs to prevent confounding with covariates, filter databases for analyses, and include metrics in models to isolate fuel moisture measurements from sources of sampler variability (August *et al.* 2020).

5.4.3 IMPLICATIONS

Among-sampler variability can lead to high variability in fuel moisture content measurements within the same plot, fuel layer, and time of day. With this knowledge, it is possible to give a range of confidence in fuel moisture estimates associated with among-sampler variability that will be more accurate than a single value. Accounting for among-sampler variability opens opportunities to maximise the potential of citizen science research to characterise fuels and understand regional fuel dynamics beyond the capability of most traditional field experiments. For instance, capturing fuel load and fuel flammability are also essential to develop fuel models that are representative of the range of regional ecosystems they are being developed for. Fuel height and fuel samples could be collected by citizen scientists for research developing wider aspects of fuel and fire behaviour models. Furthermore, community hubs of citizen scientists could implement long-term fuel moisture monitoring campaigns to assess local wildfire danger, thereby creating wildfire-aware community networks within rural–urban interfaces and promoting risk reduction strategies.

6

6 RESEARCH SYNTHESIS AND FUTURE DIRECTIONS

6.1 INTRODUCTION

The research in this thesis was motivated by the need for a more flexible approach to wildfire danger research that captures the underlying scientific controls and addresses the diversity of decision-making needs, particularly in understudied emerging fire prone regions. This thesis aimed to assess the multi-scale controls on components of wildfire danger. To meet this aim, Chapter 2 examined the association between Persistent Positive Anomalies (PPAs), surface fire weather, and wildfire activity at a pan-European level. Chapter 3 assessed the range of variability in the live and dead fuel moisture content of *Calluna vulgaris* across a temperate fire prone landscape and examined the landscape and micrometeorological drivers of landscape-scale fuel moisture variability through an intensive, direct fuel moisture measurement campaign. Chapter 4 then examined the impact of this cross-landscape fuel moisture variability on simulated fire behaviour using BehavePlus. Finally, Chapter 5 examined the extent of among-sampler variability in measured fuel moisture at the plot scale that is an inherent part of broad-scale field campaigns involving multiple samplers through a direct fuel moisture measurement campaign involving seventeen samplers.

Collectively, the research in this thesis is novel in that: (1) it is not confined by what existing models and systems are capable of. It seeks to understand the real-world processes influencing wildfire danger and how new scientific understanding can inform decision making tools to meet diverse user needs. (2) Similarly, this thesis is not confined to conventional schools of knowledge. It is transdisciplinary in its consideration of wildfire danger across geographical spheres, from synoptic climatology using large, gridded data sets to landscape ecology using experimental field campaigns. The structure of this thesis reflects the holistic approach that is essential for integrated wildfire management. (3) The research focuses on an understudied region for wildfire research, where wildfire risk is increasing but there are significant gaps in our understanding of the processes driving wildfire danger and functional tools to develop wildfire prevention strategies. (4) This thesis includes intensive direct fuel moisture measurement campaigns that are rare but essential for understanding fuel moisture dynamics. Chapter 6 synthesises the key findings of this thesis, highlights any limitations and implications, and outlines areas of future research.

6.2 SYNTHESIS OF KEY FINDINGS

This section synthesises advances in our scientific understanding of multi-scale processes influencing components of wildfire danger.

6.2.1 SYNOPTIC SCALE

Using a pan-European analysis of PPA–fire interactions, I demonstrated the underlying processes driving surface fire weather and wildfire activity associated with PPAs in Europe, a region with complex human–fire interactions (Chapter 2). My research has found that Europe-wide, extreme fire weather and wildfires are more likely to occur under PPA conditions, associated with the role of PPAs in pre-drying surface fuels. I also found a latitudinal increase in the percentage of burned area attributable to PPA conditions, which is consistent with PPA–fire associations found in Western North America (Sharma *et al.* 2022) and previous research finding synoptic–surface weather associations are strongest at high latitudes (Pfahl and Wernli, 2012; Rousi *et al.* 2022; Wehrli *et al.* 2022). Understanding the mechanisms driving PPA–fire associations is essential to be able to develop early warning systems of dangerous wildfire conditions and consider how these processes might change and consequently impact wildfire risk under climate change.

6.2.2 LANDSCAPE SCALE

I measured the extent and drivers of spatial variability in the fuel moisture content of *Calluna vulgaris* across a temperate peatland/heathland landscape for the first time. Cross-landscape fuel moisture variability led to on/off thresholding of live fuel availability for wildfire spread and vulnerability of the organic layer to smouldering combustion (Chapter 3). The observed extent of cross-landscape fuel moisture differences significantly impacted simulated rates of spread (Chapter 4). These findings demonstrate that existing regional estimates of fuel moisture and fire weather may under or overpredict local wildfire danger and behaviour.

This is partly due to the importance of fine-scale heterogeneity for fire in temperate emerging fire prone regions. This thesis contributes towards understanding live fuel moisture dynamics and spring-time fires, which have been identified as a major challenge in temperate peatland/heathland landscapes. Existing models of fire behaviour are insensitive to observed live fuel moisture variation and are strongly impacted by the choice of temperate fuel type. Chapters 3 and 4 highlight the creation of high-risk scenarios at the end of winter and early spring in temperate peatland and heathlands, where fire behaviour may be underpredicted when live fuels are at their driest. The underlying relationships that determine the importance of dead and live fuel loads within fire spread models may need to be adjusted to better capture the importance of live fuel moisture in temperate fuel types.

While phenology is recognised as an important control on temporal fuel moisture variability, this research has demonstrated that there is also an important spatial dimension to phenology as a landscape control. My results suggest that the *Calluna* canopy acts in a similar manner to the overstory in forested fuels that form a boundary between the atmosphere and underlying surface fuels (Chapter 3). This is consistent with previous descriptions of the behaviour of wildfire spread through *Calluna* canopy akin to a mini-crown fire (Fernandes *et al.* 2000; Davies and Legg 2016). The results of Chapters 3 and 4 point to the potential benefits of utilising *Calluna* canopy fuel moisture to capture cross-landscape variations within fire behaviour models and wildfire danger estimates in lieu of fully functioning fuel types.

I found that landscape factors are more important drivers of spatial fuel moisture variation than micrometeorological factors in temperate peatland / heathland landscapes (Chapter 3). This is a key insight into the need to account for landscape–fuel moisture relationships directly as exiting fuel moisture estimates derived solely from micrometeorological observations will exclude the underlying influence of landscape controls. These findings contribute new knowledge in understanding the processes driving spatial fuel moisture variability, especially for non-forested environments where fuel moisture dynamics are understudied. Such studies are essential for developing tailored temperate fuel models that capture the complexity of fuel moisture dynamics.

6.2.3 PLOT SCALE

Large-scale direct fuel moisture measurement campaigns are essential for understanding fuel dynamics as evidenced by Chapters 3 and 4 of this thesis. Plot-scale fuel moisture variability is also incorporated in these fuel measurement campaigns, including fine-scale diversity in ecological, geomorphological, and hydrological controls and variability associated with the sampling campaign design. Chapter 5 found that among-sampler variability is a relevant source of measurement error in field measurement campaigns, particularly for surface fuels and live fuels that require subjective decision-making by the sampler. Such field measurement errors are rarely quantified, and in doing so, I presented specific experimental and sampling design considerations that could be used to minimise among-sampler variability and highlighted the importance of collecting sampler metadata to isolate fuel moisture dynamics of interest. My findings provide important guidelines for maximising the benefits of citizen science research and broad-scale field campaigns that are essential for scaling-up field campaigns to understand spatiotemporal fuel dynamics.

6.2.4 MULTI-SCALE FRAMEWORK FOR UNDERSTANDING WILDFIRE DANGER

Traditionally, wildfire danger is considered at broad spatial scales using surface fire weather and fuel moisture estimates. Developments in the availability of data products and increasing complexity of wildfire management needs have led to increasing recognition of the need for greater flexibility in wildfire danger assessments. However, the underlying processes that control components of wildfire danger across spatial scales have not yet been fully resolved.

The research presented in this thesis demonstrates how a multi-scale approach to considering wildfire danger can better capture the underlying processes influencing fire weather and fuel moisture and can be used to develop models that better reflect real-world processes.

Disentangling the synoptic drivers of surface fire weather improves our understanding of fire–climate relationships and provides insights towards forecasting fire weather beyond current surface forecast capabilities (Chapter 2). However, only considering regional fire weather and fuel moisture dynamics masks the landscape level processes that drive local wildfire danger and are essential to understand (Chapters 3 and 4). In order to fully understand spatiotemporal fuel and fire dynamics, it is essential to scale-up field-based fuel measurement campaigns. Accounting for among-sampler variability that is inherent in these campaigns is therefore critical for isolating environmental processes from measurement error (Chapter 5). A multi-scale approach to understanding wildfire danger allows for a more holistic understanding of the different processes that impact wildfire danger.

6.3 IMPLICATIONS

The results of this thesis have clear implications for the following areas of wildfire research and management across spatiotemporal scales:

1. Wildfire preparedness
2. Fire and land management decision-making needs
3. Potential of citizen science in wildfire research

6.3.1 WILDFIRE PREPAREDNESS

A multi-scale approach to wildfire danger would allow for the inclusion of synoptic controls within fire occurrence systems to develop the medium range forecasting potential for dangerous fire weather conditions. Advanced warning of extended, extensive periods of elevated wildfire danger that may impact large regions and overwhelm fire suppression resources would help to inform early wildfire awareness and preparedness and policy and management decisions like early mobilisation and resource sharing across regions. Given the association between PPA events and poor surface air quality during wildfires, early warning systems would help communicate wildfire dangerous conditions to the public and potential air pollution events. At the landscape level, identification of areas vulnerable to wildfire spread or smouldering can allow for targeted fuel reduction.

6.3.2 FIRE AND LAND MANAGEMENT DECISION-MAKING NEEDS

The findings of this research have implications for decision-making at many levels, from local land managers and fire rescue services to national and international scales. (1) Forecasting of extended and extensive events can help to inform resource allocation and decision making to avoid resources becoming overwhelmed, e.g., coordination of cross-region or international resource exchange. (2) Downscaling of regional fuel moisture estimates to capture local fuel moisture variability and consequent wildfire behaviour and danger could help inform local fire management decision making, as well as identifying where suppression tools and tactics may need to be adjusted or highlighting suppression opportunities. From a fuel management perspective, capturing cross-landscape fire behaviour variability would aid decision-making for conducting fuel management activities to safely and effectively achieve management outcomes. The multi-scale approach to understanding wildfire danger in this thesis recognises the multi-facetted nature of decision-making needs and that management tools may require different levels of detail for the different functions they perform.

6.3.3 POTENTIAL OF CITIZEN SCIENCE

By considering among-sampler variability in measurements within experimental designs and statistical analyses, the benefits of citizen science can be optimised to understand processes operating at broad spatiotemporal scales that cannot be captured by traditional, controlled field experiments (Dickinson *et al.* 2010; Arazy and Malkinson 2021). These findings are relevant for the wider wildfire research community to answer essential questions beyond fuel moisture, including collecting fuel load and flammability data to develop tailored fuel models. Beyond implications for our scientific understanding of spatiotemporal processes, the inclusion of citizen science research offers opportunities to develop long-term monitoring campaigns within community hubs of citizen scientists. This involvement would help to create wildfire-aware community networks within rural–urban interfaces, improving wildfire danger communication and agency over risk reduction and wildfire preparedness strategies.

6.4 METHODOLOGIES AND LIMITATIONS

I used a variety of techniques in examining the multi-scale drivers of wildfire danger. I used large-scale gridded climate data and remotely sensed burned area products to examine the association between PPAs and surface fire weather and wildfires (Chapter 2). I used a novel PPA detection algorithm that is robust to weaker summer pressure gradients for the first time at a pan-European level to detect PPAs and related these to surface conditions via statistical analyses across four geographically contiguous regions. The use of remotely-sensed burned area information was beneficial for examining extensive events that cross political borders as it ensured consistency through the use of a single database and collection method. However, this creates a bias in the omission of small fires (< 30 ha) that cannot be remotely sensed and may impact PPA–fire associations in some regions. Furthermore, the sparsity of records for some regions of Europe meant that I aggregated burned area across a 1x1 degree grid cell rather than considering individual burned area perimeters. Given the focus on synoptic-scale controls and the need to understand processes at a pan-European level this was appropriate; however, this may have removed some of the within-grid spatial complexity that may be insightful for unravelling PPA–fire relationships.

Chapters 3, 4, and 5 utilised intensive direct fuel moisture measurement campaigns. The field campaign conducted to collect data for Chapters 3 and 4 represented the first study to measure the extent of fuel moisture variability across a peatland and heathland landscape. Of the limited landscape-scale fuel moisture research, most were conducted using fuel moisture proxies within forested landscapes and experienced limitations relating to the confounding of landscape variables. I selected sampling sites to represent each possible combination of hypothesised landscape controls to prevent confounding between predictor variables. The field campaign conducted in Chapter 5 is the first attempt to characterise among-sampler variability within fuel and fire research. Both field campaigns conducted during this thesis advanced our understanding of fuel moisture dynamics in a landscape and region where the processes driving wildfire danger and behaviour are not well understood and are not captured in existing models.

Most ecological field-based research is affected by the inherent complexity of natural landscapes. I employed careful experimental design, literature-based model selection, and interpretation of results based on scientific understanding; however, I acknowledge that inherent variability in the environment means there may be unknown spatial controls that are unaccounted for and may impact the results of this thesis. I have highlighted this where relevant within the thesis and hypothesised specific landscape controls that should be further explored. The experimental studies conducted in this thesis are absolutely critical for advancing our understanding of landscape processes and disturbances and provide valuable insights despite spatial complexity. Such field studies should not be discouraged, but it is important to understand and mitigate limitations where possible during experimental design and analysis as well as report any limitations.

6.5 FUTURE RESEARCH

Wildfire danger is controlled by complex, interacting processes, and there are many opportunities to build on the findings of this thesis to better capture the mechanisms driving wildfire danger across spatiotemporal scales. Global climate and land use change will continue to impact wildfire danger, providing further impetus for resolving the processes driving wildfire danger for inclusion in practical applications. I identified three key priorities for future research:

1. Development of robust temperate fuel models
2. Unravelling how complex interactions across scales impact wildfire danger
3. Understanding the impact of future climate change on wildfire danger

6.5.1 DEVELOPMENT OF ROBUST TEMPERATE FUEL MODELS

This thesis has demonstrated the need to develop tailored fuel models for temperate fuels that capture the complexity of live fuel moisture dynamics. Further research might (1) unravel the mechanisms driving landscape–fuel moisture relationships (e.g., narrowing in on the role of soil texture), (2) scale-up field studies to understand whether these processes hold across the range of fuels and landscapes in temperate regions, and (3) revise the representation of live fuels in fire behaviour models. Plant physiology may hold the key to unravelling the controls on live fuel moisture content. Transdisciplinary collaboration would aid understanding of live fuel dynamics using the existing expertise of plant physiologists.

6.5.2 UNRAVELLING HOW COMPLEX INTERACTIONS ACROSS SCALES IMPACT WILDFIRE DANGER

Two-way interactions between different scales of processes impacting wildfire danger components are important for disentangling the underlying controls on wildfire danger. For example, this thesis examined the association between PPAs and surface fire weather. Future research might: (1) narrow in on the edge effects of PPAs and how their breakdown and interaction with other atmospheric circulation patterns influences surface fire weather and wildfire activity; (2) examine how PPA–fire interactions are influenced by larger teleconnections operating at longer time scales for producing seasonal forecasts, i.e., the North Atlantic Oscillation (NAO) and Arctic Amplification (AA); (3) understand the full range of synoptic controls on surface fire weather when PPAs are not the dominant circulation pattern; and (4) narrow in on land–atmosphere feedbacks that may create positive feedbacks in extreme fire weather and wildfire activity associated with PPAs, e.g., early permafrost melt. This research has demonstrated how processes driving wildfire danger operate at different spatiotemporal scales. There is a need to unravel the multi-scale interactions between processes the ultimately drive wildfire danger as well as develop appropriate methods to scale-up and downscale these controls.

6.5.3 UNDERSTANDING THE IMPACT OF FUTURE CLIMATE CHANGE ON WILDFIRE DANGER

There is uncertainty in how the processes controlling wildfire danger are likely to change under future climate scenarios. In fact, due to the brevity of wildfire records in temperate regions, historical trends in wildfire activity and associated controls are limited. Further research should examine how synoptic–fire relationships and landscape–fuel moisture controls are likely to be impacted by climate change as these will have implications for understanding future wildfire risk. For example, atmospheric dynamic changes in synoptic processes could substantially impact future wildfire risk but are not well represented in climate projections, and threshold tipping points in the ecohydrological and plant physiological controls on live fuel moisture are not well defined.

6.6 CONCLUSIONS

The research presented in this PhD thesis improves our understanding of the multi-scale drivers of wildfire danger, recognising the need for a flexible approach to assessing wildfire danger that captures the underlying scientific controls and addresses the diversity of decision-making needs. Such a holistic approach to understanding wildfire danger has implications for developing functional assessment tools for fire and land management decision-making needs that are lacking but urgently needed in emerging fire prone regions.

7 REFERENCES

Aagaard K, Lyons JE, Thogmartin WE (2018) Accounting for Surveyor Effort in Large-Scale Monitoring Programs. *Journal of Fish and Wildlife Management* **9**, 459–466. doi:10.3996/022018-JFWM-012.

Abatzoglou JT, Juang CS, Williams AP, Kolden CA, Westerling AL (2021) Increasing Synchronous Fire Danger in Forests of the Western United States. *Geophysical Research Letters* **48**, e2020GL091377. doi:10.1029/2020GL091377.

Agresti A (1999) On Logit Confidence Intervals for the Odds Ratio with Small Samples. *Biometrics* **55**, 597–602. doi:10.1111/j.0006-341X.1999.00597.x.

Andrews PL (2014) Current status and future needs of the BehavePlus Fire Modeling System. *International Journal of Wildland Fire* **23**, 21. doi:10.1071/WF12167.

Arazy O, Malkinson D (2021) A Framework of Observer-Based Biases in Citizen Science Biodiversity Monitoring: Semi-Structuring Unstructured Biodiversity Monitoring Protocols. *Frontiers in Ecology and Evolution* **9**,. https://www.frontiersin.org/articles/10.3389/fevo.2021.693602.

Arnell NW, Freeman A, Gazzard R (2021) The effect of climate change on indicators of fire danger in the UK. *Environmental Research Letters* **16**, 044027. doi:10.1088/1748-9326/abd9f2.

August T, Fox R, Roy DB, Pocock MJO (2020) Data-derived metrics describing the behaviour of field-based citizen scientists provide insights for project design and modelling bias. *Scientific Reports* **10**, 11009. doi:10.1038/s41598-020-67658-3.

Bannister P (1964a) The Water Relations of Certain Heath Plants with Reference to their Ecological Amplitude: III. Experimental Studies: General Conclusions. *The Journal of Ecology* **52**, 499. doi:10.2307/2257846.

Bannister P (1964b) Stomatal Responses of Heath Plants to Water Deficits. *Journal of Ecology* **52**, 151–158. doi:10.2307/2257789.

Barnes C, Boulanger Y, Keeping T, Gachon P, Gillett N, Haas O, Wang X, Roberge F, Kew S, Heinrich D, Singh R, Vahlberg M, Van Aalst M, Otto F, Kimutai J, Boucher J, Kasoar M, Zachariah M, Krikken F (2023) Climate change more than doubled the likelihood of extreme fire weather conditions in Eastern Canada. Imperial College London, doi:10.25561/105981.

Barnes EA, Slingo J, Woollings T (2012) A methodology for the comparison of blocking climatologies across indices, models and climate scenarios. *Climate Dynamics* **38**, 2467–2481. doi:10.1007/s00382-011-1243-6.

Barry RG, Carleton A M (2001) 'Synoptic and Dynamic Climatology.' (Routledge: London) https://books.google.com/books/about/Synoptic_and_Dynamic_Climatology.html?id=fHF7I6XVuC0C.

Bartoń K (2022) MuMIn: Multi-Model Inference. https://CRAN.R-project.org/package=MuMIn.

Bates D, Mächler M, Bolker B, Walker S (2015) Fitting Linear Mixed-Effects Models Using lme4. *Journal of Statistical Software* **67**, 1–48. doi:10.18637/jss.v067.i01.

Batjes NH (1996) Total carbon and nitrogen in the soils of the world. *European Journal of Soil Science* **47**, 151–163. doi:10.1111/ejss.12115.

Belcher CM, Brown I, Clay GD, Doerr SH, Elliott A, Gazzard R, Kettridge N, Morison J, Perry M, Smith TEL (2021) UK Wildfires and their Climate Challenges.

Bilgili E, Coskuner KA, Usta Y, Saglam B, Kucuk O, Berber T, Goltas M (2019) Diurnal surface fuel moisture prediction model for Calabrian pine stands in Turkey. *IForest* **12**, 262–271. doi:10.3832/ifor2870-012.

Bird TJ, Bates AE, Lefcheck JS, Hill NA, Thomson RJ, Edgar GJ, Stuart-Smith RD, Wotherspoon S, Krkosek M, Stuart-Smith JF, Pecl GT, Barrett N, Frusher S (2014) Statistical solutions for error and bias in global citizen science datasets. *Biological Conservation* **173**, 144–154. doi:10.1016/j.biocon.2013.07.037.

Blackport R, Screen JA (2020) Weakened evidence for mid-latitude impacts of Arctic warming. *Nature Climate Change* **10**, 1065–1066. doi:10.1038/s41558-020-00954-y.

Bloem S, Cullen AC, Mearns LO, Abatzoglou JT (2022) The Role of International Resource Sharing Arrangements in Managing Fire in the Face of Climate Change. *Fire* **5**, 88. doi:10.3390/fire5040088.

Boschetti L, Roy DP, Giglio L, Huang H, Zubkova M, Humber ML (2019) Global validation of the collection 6 MODIS burned area product. *Remote Sensing of Environment* **235**, 111490. doi:10.1016/j.rse.2019.111490.

Bronaugh D, Werner A (2019) 'zyp: Zhang + Yue-Pilon Trends Package.' https://CRAN.R-project.org/package=zyp.

Brown TP, Hoylman ZH, Conrad E, Holden Z, Jencso K, Jolly WM (2022) Decoupling between soil moisture and biomass drives seasonal variations in live fuel moisture across co-occurring plant functional types. *Fire Ecology* **18**, 14. doi:10.1186/s42408-022-00136-5.

Brown TP, Inbar A, Duff TJ, Lane PNJ, Sheridan GJ (2022) The sensitivity of fuel moisture to forest structure effects on microclimate. *Agricultural and Forest Meteorology* **316**, 108857. doi:10.1016/j.agrformet.2022.108857.

Cardil A, Monedero S, Schag G, de-Miguel S, Tapia M, Stoof CR, Silva CA, Mohan M, Cardil A, Ramirez J (2021) Fire behavior modeling for operational decision-making. *Current Opinion in Environmental Science and Health* **23**, 100291. doi:10.1016/j.coesh.2021.100291.

Cardíl A, Tapia VM, Monedero S, Quiñones T, Little K, Stoof CR, Ramirez J, de-Miguel S (2023) Characterizing the rate of spread of large wildfires in emerging fire environments of northwestern Europe using Visible Infrared Imaging Radiometer Suite active fire data. *Natural Hazards and Earth System Sciences* **23**, 361–373. doi:10.5194/nhess-23-361-2023.

Cawson JG, Nyman P, Schunk C, Sheridan GJ, Duff TJ, Gibos K, Bovill WD, Conedera M, Pezzatti GB, Menzel A (2020) Estimation of surface dead fine fuel moisture using automated fuel moisture sticks across a range of forests worldwide. *International Journal of Wildland Fire*. doi:10.1071/WF19061.

Chen Y, Romps DM, Seeley JT, Veraverbeke S, Riley WJ, Mekonnen ZA, Randerson JT (2021) Future increases in Arctic lightning and fire risk for permafrost carbon. *Nature Climate Change* **11**, 404–410. doi:10.1038/s41558-021-01011-y.

Coumou D, Di Capua G, Vavrus S, Wang L, Wang S (2018) The influence of Arctic amplification on mid-latitude summer circulation. *Nature Communications* **9**, 2959. doi:10.1038/s41467-018-05256-8.

Cox TE, Philippoff J, Baumgartner E, Smith CM (2012) Expert variability provides perspective on the strengths and weaknesses of citizen-driven intertidal monitoring program. *Ecological Applications* **22**, 1201–1212. doi:10.1890/11-1614.1.

Csardi G, Nepusz T (2006) The igraph software package for complex network research. *InterJournal* **Complex Systems**, 1695.

Davies GM, Domènech R, Gray A, Johnson PCD (2016) Vegetation structure and fire weather influence variation in burn severity and fuel consumption during peatland wildfires. *Biogeosciences* **13**, 389–398. doi:10.5194/bg-13-389-2016.

Davies GM, Gray A (2015) Don’t let spurious accusations of pseudoreplication limit our ability to learn from natural experiments (and other messy kinds of ecological monitoring). *Ecology and Evolution* **5**, 5295–5304. doi:10.1002/ece3.1782.

Davies GM, Legg CJ (2008) Developing a live fuel moisture model for moorland fire danger rating. *WIT Transactions on Ecology and the Environment* **119**, 225–236. doi:10.2495/FIVA080231.

Davies GM, Legg CJ (2011) Fuel Moisture Thresholds in the Flammability of Calluna vulgaris. *Fire Technology* **47**, 421–436. doi:10.1007/s10694-010-0162-0.

Davies GM, Legg CJ (2016) Regional variation in fire weather controls the reported occurrence of Scottish wildfires. *PeerJ* **4**, 25. doi:10.7717/peerj.2649.

Davies GM, Legg CJ, O'Hara R, MacDonald AJ, Smith AA (2010) Winter desiccation and rapid changes in the live fuel moisture content of Calluna vulgaris. *Plant Ecology and Diversity* **3**, 289–299. doi:10.1080/17550874.2010.544335.

Davies GM, Legg CJ, Smith AA, MacDonald A (2019) Development and participatory evaluation of fireline intensity and flame property models for managed burns on Calluna-dominated heathlands. *Fire Ecology* **15**,. doi:10.1186/s42408-019-0046-8.

Davies GM, Legg CJ, Smith AA, McDonald AJ (2009) Rate of Spread of Fires in Calluna vulgaris-Dominated Moorlands. *British Ecological Society* **46**, 1054–1063. doi:10.1111/j. 1365-2664.2009.01681.x.

Davini P, D'Andrea F (2020) From CMIP3 to CMIP6: Northern Hemisphere Atmospheric Blocking Simulation in Present and Future Climate. *Journal of Climate* **33**, 10021–10038. doi:10.1175/JCLI-D-19-0862.1.

Devictor V, Whittaker RJ, Beltrame C (2010) Beyond scarcity: citizen science programmes as useful tools for conservation biogeography. *Diversity and Distributions* **16**, 354–362. doi:10.1111/j.1472-4642.2009.00615.x.

Dickinson JL, Zuckerberg B, Bonter DN (2010) Citizen Science as an Ecological Research Tool: Challenges and Benefits. *Annual Review of Ecology, Evolution, and Systematics* **41**, 149–172.

Dickman LT, Jonko AK, Linn RR, Altintas I, Atchley AL, Bär A, Collins AD, Dupuy J-L, Gallagher MR, Hiers JK, Hoffman CM, Hood SM, Hurteau MD, Jolly WM, Josephson A, Loudermilk EL, Ma W, Michaletz ST, Nolan RH, O'Brien JJ, Parsons RA, Partelli-Feltrin R, Pimont F, Resco de Dios V, Restaino J, Robbins ZJ, Sartor KA, Schultz-Fellenz E, Serbin SP, Sevanto S, Shuman JK, Sieg CH, Skowronski NS, Weise DR, Wright M, Xu C, Yebra M, Younes N (2023) Integrating plant physiology into simulation of fire behavior and effects. *New Phytologist* **238**, 952–970. doi:10.1111/nph.18770.

Dijkstra J, Durrant T, San-Miguel-Ayanz J, Veraverbeke S (2022) Anthropogenic and Lightning Fire Incidence and Burned Area in Europe. *Land* **11**, 651. doi:10.3390/land11050651.

Dole RM, Gordon ND (1983) Persistent Anomalies of the Extratropical Northern Hemisphere Wintertime Circulation: Geographical Distribution and Regional Persistence Characteristics. *Monthly Weather Review* **111**, 1567–1586. doi:10.1175/1520-0493(1983)111<1567:PAOTEN>2.0.CO;2.

Drobyshev I, Ryzhkova N, Eden J, Kitenberga M, Pinto G, Lindberg H, Krikken F, Yermokhin M, Bergeron Y, Kryshen A (2021) Trends and patterns in annually burned forest areas and fire weather across the European boreal zone in the 20th and early 21st centuries.

Agricultural and Forest Meteorology **306**, 108467. doi:10.1016/j.agrformet.2021.108467.

Duane A, Miranda MD, Brotons L (2021) Forest connectivity percolation thresholds for fire spread under different weather conditions. *Forest Ecology and Management* **498**, 119558. doi:10.1016/j.foreco.2021.119558.

Duursma RA (2015) Plantecophys - An R Package for Analysing and Modelling Leaf Gas Exchange Data. *PLoS ONE* **10**, e0143346. doi:10.1371/journal.pone.0143346.

Easton ZM, Bock E (2016) Soil and Soil Water Relationships. *VCE Publication* **BSE-194P**, 9.

EFFIS (2023) EFFIS - Welcome to EFFIS. https://effis.jrc.ec.europa.eu/.

Elliott RD, Smith TB (1949) A STUDY OF THE EFFECTS OF LARGE BLOCKING HIGHS ON THE GENERAL CIRCULATION IN THE NORTHERN-HEMISPHERE WESTERLIES. *Journal of the Atmospheric Sciences* **6**, 68–85. doi:10.1175/1520-0469(1949)006<0068:ASOTEO>2.0.CO;2.

Ellis TM, Bowman DMJS, Jain P, Flannigan MD, Williamson GJ (2022) Global increase in wildfire risk due to climate-driven declines in fuel moisture. *Global Change Biology* **28**, 1544–1559. doi:10.1111/gcb.16006.

Farewell TS, Truckell IG, Keay CA, Hallett SH (2011) The derivation and application of Soilscapes: soil and environmental datasets from the National Soil Resources Institute, Cranfield University. https://www.cranfield.ac.uk/themes/environment-and-agrifood/landis/soilscapes#.

Fernandes PM (2019) Variation in the canadian fire weather index thresholds for increasingly larger fires in Portugal. *Forests* **10**,. doi:10.3390/f10100838.

Fernandes PM, Catchpole WR, Rego FC (2000) Shrubland Fire Behaviour Modelling with Microplot Data. *Canadian Journal of Forest Research* **30**, 889–899.

Fernandez-Anez N, Krasovskiy A, Müller M, Vacik H, Baetens J, Hukić E, Kapovic Solomun M, Atanassova I, Glushkova M, Bogunović I, Fajković H, Djuma H, Boustras G, Adámek M, Devetter M, Hrabalikova M, Huska D, Martínez Barroso P, Vaverková MD, Zumr D, Jõgiste K, Metslaid M, Koster K, Köster E, Pumpanen J, Ribeiro-Kumara C, Di Prima S, Pastor A, Rumpel C, Seeger M, Daliakopoulos I, Daskalakou E, Koutroulis A, Papadopoulou MP, Stampoulidis K, Xanthopoulos G, Aszalós R, Balázs D, Kertész M, Valkó O, Finger DC, Thorsteinsson T, Till J, Bajocco S, Gelsomino A, Amodio AM, Novara A, Salvati L, Telesca L, Ursino N, Jansons A, Kitenberga M, Stivrins N, Brazaitis G, Marozas V, Cojocaru O, Gumeniuc I, Sfecla V, Imeson A, Veraverbeke S, Mikalsen RF, Koda E, Osinski P, Castro ACM, Nunes JP, Oom D, Vieira D, Rusu T, Bojović S, Djordjevic D, Popovic Z, Protic M, Sakan S, Glasa J, Kacikova D, Lichner L, Majlingova A, Vido J, Ferk M, Tičar J, Zorn M, Zupanc V, Hinojosa MB, Knicker H, Lucas-Borja ME, Pausas J, Prat-Guitart N, Ubeda X, Vilar L, Destouni G, Ghajarnia N, Kalantari Z, Seifollahi-Aghmiuni S, Dindaroglu T, Yakupoglu T, Smith T, Doerr S, Cerda A (2021) Current Wildland Fire Patterns and Challenges in Europe: A Synthesis of National Perspectives. *Air, Soil and Water Research* **14**, 11786221211028184. doi:10.1177/11786221211028185.

Fink D, Hochachka WM (2012) Citizen Science. 'Public Participation in Environmental Research'. (Eds JL Dickinson, R Bonney) pp. 125–138. (Cornell University Press) doi:10.7591/9780801463952-015.

Finney MA (1998) FARSITE: Fire Area Simulator-model development and evaluation. *Res Pap RMRS-RP-4, Revised 2004 Ogden, UT: US Department of Agriculture, Forest Service, Rocky Mountain Research Station 47 p* **4**,. doi:10.2737/RMRS-RP-4.

Finney MA (2006) An Overview of FlamMap Fire Modeling Capabilities. *In: Andrews, Patricia L; Butler, Bret W, Comps 2006 Fuels Management-How to Measure Success: Conference Proceedings 28-30 March 2006; Portland, OR Proceedings RMRS-P-41 Fort Collins, CO: US Department of Agriculture, Forest Service, Rocky Mountain Research Station p 213-220* **041**,. https://www.fs.usda.gov/research/treesearch/25948.

Finney MA, McAllister SS, Grumstrup TP, Forthofer JM (2021) 'Wildland Fire Behaviour.' (CSIRO Publishing) doi:10.1071/9781486309092.

Fosberg MA, Deeming JE, Forest RM, Range Experiment Station (Fort Collins Colo) (1971) 'Derivation of the 1- and 10-hour Timelag Fuel Moisture Calculations for Fire-danger Rating.' (Rocky Mountain Forest and Range Experiment Station, Forest Service, U.S. Department of Agriculture) https://books.google.no/books?id=li3DwgEACAAJ.

Fox J, Weisberg S (2019) An R Companion to Applied Regression. https://socialsciences.mcmaster.ca/jfox/Books/Companion/.

Francis JA, Vavrus SJ (2015) Evidence for a wavier jet stream in response to rapid Arctic warming. *Environmental Research Letters* **10**, 014005. doi:10.1088/1748-9326/10/1/014005.

Galizia LF, Barbero R, Rodrigues M, Ruffault J, Pimont F, Curt T (2023) Global Warming Reshapes European Pyroregions. *Earth's Future* **11**, e2022EF003182. doi:10.1029/2022EF003182.

Gardner RH, Milne BT, Turnei MG, O'Neill RV (1987) Neutral models for the analysis of broad-scale landscape pattern. *Landscape Ecology* **1**, 19–28. doi:10.1007/BF02275262.

Gazzard R, McMorrow J, Aylen J (2016) Wildfire policy and management in England: an evolving response from Fire and Rescue Services, forestry and cross-sector groups. *Philosophical Transactions of the Royal Society of London Series B, Biological Sciences* **371**, 20150341. doi:10.1098/rstb.2015.0341.

Giannaros TM, Papavasileiou G (2023) Changes in European fire weather extremes and related atmospheric drivers. *Agricultural and Forest Meteorology* **342**, 109749. doi:10.1016/j.agrformet.2023.109749.

Gimingham CH (1992) 'The Lowland Heathland Management Handbook.' (English Nature) https://books.google.ca/books?id=jGZRPQAACAAJ.

Gimingham CH, Chapman SB, Webb NR (1979) European Heathlands. 'Heathlands and related shrublands'. (Ed RL Specht) Ecosystems of the world. pp. 365–413. (Elsevier: Amsterdam ; New York : New York)

Giorgi F, Lionello P (2008) Climate change projections for the Mediterranean region. *Global and Planetary Change* **63**, 90–104. doi:10.1016/j.gloplacha.2007.09.005.

Glaves DJ, Crowle AJ, Bruemmer C, Lenaghan SA (2020) The causes and prevention of wildfire on heathlands and peatlands in England (NEER014). (Peterborough)

Grau-Andrés R, Davies GM, Gray A, Scott EM, Waldron S (2018) Fire severity is more sensitive to low fuel moisture content on Calluna heathlands than on peat bogs. *Science of the Total Environment* **616–617**, 1261–1269. doi:10.1016/j.scitotenv.2017.10.192.

Greenland S, Schwartzbaum JA, Finkle WD (2000) Problems due to Small Samples and Sparse Data in Conditional Logistic Regression Analysis. *American Journal of Epidemiology* **151**, 531–539. doi:10.1093/oxfordjournals.aje.a010240.

Griebel A, Boer MM, Blackman C, Choat B, Ellsworth DS, Madden P, Medlyn B, Resco de Dios V, Wujeska-Klause A, Yebra M, Younes Cardenas N, Nolan RH (2023) Specific leaf area and vapour pressure deficit control live fuel moisture content. *Functional Ecology* **37**, 719–731. doi:10.1111/1365-2435.14271.

Grotenhuis MT, Pelzer B, Eisinga R, Nieuwenhuis R, SChmidt-Catran A, Konig R (2016) When size matters: advantages of weighted effect coding in observational studies. *International Journal of Public Health* 1–5.

Hall JV, Argueta F, Giglio L (2021) Validation of MCD64A1 and FireCCI51 cropland burned area mapping in Ukraine. *International Journal of Applied Earth Observation and Geoinformation* **102**, 102443. doi:10.1016/j.jag.2021.102443.

Harrell Jr FE (2022) Hmisc: Harrell Miscellaneous. https://CRAN.R-project.org/package=Hmisc.

Hartig F (2022) DHARMa: Residual Diagnostics for Hierarchical (Multi-Level / Mixed) Regression Models. https://CRAN.R-project.org/package=DHARMa.

Hayasaka H, Yamazaki K, Naito D (2019) Weather conditions and warm air masses during active fire-periods in boreal forests. *Polar Science* **22**, 100472. doi:10.1016/j.polar.2019.07.002.

Hersbach H, Bell B, Berrisford P, Hirahara S, Horányi A, Muñoz-Sabater J, Nicolas J, Peubey C, Radu R, Schepers D, Simmons A, Soci C, Abdalla S, Abellan X, Balsamo G, Bechtold P, Biavati G, Bidlot J, Bonavita M, De Chiara G, Dahlgren P, Dee D, Diamantakis M, Dragani R, Flemming J, Forbes R, Fuentes M, Geer A, Haimberger L, Healy S, Hogan RJ, Hólm E, Janisková M, Keeley S, Laloyaux P, Lopez P, Lupu C, Radnoti G, de Rosnay P, Rozum I, Vamborg F, Villaume S, Thépaut J-N (2020) The ERA5 global reanalysis. *Quarterly Journal of the Royal Meteorological Society* **146**, 1999–2049. doi:10.1002/qj.3803.

Hijmans RJ (2022a) 'raster: Geographic Data Analysis and Modeling.' https://CRAN.R-project.org/package=raster.

Hijmans RJ (2022b) 'terra: Spatial Data Analysis.' https://CRAN.R-project.org/package=terra.

Hohenegger C, Schär C (2007) Atmospheric Predictability at Synoptic Versus Cloud-Resolving Scales. *Bulletin of the American Meteorological Society* **88**, 1783–1793.

Hokanson KJ, Lukenbach MC, Devito KJ, Kettridge N, Petrone RM, Waddington JM (2016) Groundwater connectivity controls peat burn severity in the boreal plains. *Ecohydrology* **9**, 574–584. doi:10.1002/eco.1657.

Horton DE, Johnson NC, Singh D, Swain DL, Rajaratnam B, Diffenbaugh NS (2015) Contribution of changes in atmospheric circulation patterns to extreme temperature trends. *Nature* **522**, 465–469. doi:10.1038/nature14550.

ICF (2014) Evaluation of Civil Protection Mechanism—Case Study Report—Forest Fires in Europe. European Commission, (Brussels, Belgium)

Isaac NJB, van Strien AJ, August TA, de Zeeuw MP, Roy DB (2014) Statistics for citizen science: extracting signals of change from noisy ecological data. *Methods in Ecology and Evolution* **5**, 1052–1060. doi:10.1111/2041-210X.12254.

Jain P, Castellanos-Acuna D, Coogan SCP, Abatzoglou JT, Flannigan MD (2022) Observed increases in extreme fire weather driven by atmospheric humidity and temperature. *Nature Climate Change* **12**, 63–70. doi:10.1038/s41558-021-01224-1.

Jain P, Flannigan M (2021) The Relationship between the Polar Jet Stream and Extreme Wildfire Events in North America. *Journal of Climate* **34**, 6247–6265. doi:10.1175/JCLI-D-20-0863.1.

Jolly WM (2007) Sensitivity of a surface fire spread model and associated fire behaviour fuel models to changes in live fuel moisture. *International Journal of Wildland Fire* **16**, 503–509. doi:10.1071/WF06077.

Jolly W, Johnson D (2018) Pyro-Ecophysiology: Shifting the Paradigm of Live Wildland Fuel Research. *Fire* **1**, 5pp. doi:10.3390/fire1010008.

de Jong MC, Wooster MJ, Kitchen K, Manley C, Gazzard R, McCall FF (2016) Calibration and evaluation of the Canadian Forest Fire Weather Index (FWI) System for improved wildland fire danger rating in the United Kingdom. *Natural Hazards and Earth System Sciences* **16**, 1217–1237. doi:10.5194/nhess-16-1217-2016.

Kalogirou S (2020) lctools: Local Correlation, Spatial Inequalities, Geographically Weighted Regression and Other Tools. https://CRAN.R-project.org/package=lctools.

Kelling S, Fink D, La Sorte FA, Johnston A, Bruns NE, Hochachka WM (2015) Taking a 'Big Data' approach to data quality in a citizen science project. *Ambio* **44**, 601–611. doi:10.1007/s13280-015-0710-4.

Kirkland M, Atkinson PW, Pearce-Higgins JW, de Jong MC, Dowling TPF, Grummo D, Critchley M, Ashton-Butt A (2023) Landscape fires disproportionally affect high conservation value temperate peatlands, meadows, and deciduous forests, but only under low moisture conditions. *Science of The Total Environment* **884**, 163849. doi:10.1016/j.scitotenv.2023.163849.

Konovalov IB, Beekmann M, Kuznetsova IN, Yurova A, Zvyagintsev AM (2011) Atmospheric impacts of the 2010 Russian wildfires: integrating modelling and measurements of an extreme air pollution episode in the Moscow region. *Atmospheric Chemistry and Physics* **11**, 10031–10056. doi:10.5194/acp-11-10031-2011.

Lai G, Quan X, Yebra M, He B (2022) Model-driven estimation of closed and open shrublands live fuel moisture content. *GIScience & Remote Sensing* **59**, 1837–1856. doi:10.1080/15481603.2022.2139404.

Lehtonen I, Venäläinen A, Kämäräinen M, Peltola H, Gregow H (2016) Risk of large-scale fires in boreal forests of Finland under changing climate. *Natural Hazards and Earth System Sciences* **16**, 239–253. doi:10.5194/nhess-16-239-2016.

Little K, Graham LJ, Flannigan M, Belcher CM, Kettridge N (2024) Landscape controls on fuel moisture variability in fire-prone heathland and peatland landscapes. *Fire Ecology* **20**, 14. doi:10.1186/s42408-024-00248-0.

Little K, Graham LJ, Kettridge N (2023) Accounting for among-sampler variability improves confidence in fuel moisture content field measurements. *International Journal of Wildland Fire*. doi:10.1071/WF23078.

Liu P, Zhu Y, Zhang Q, Gottschalck J, Zhang M, Melhauser C, Li W, Guan H, Zhou X, Hou D, Peña M, Wu G, Liu Y, Zhou L, He B, Hu W, Sukhdeo R (2018) Climatology of tracked persistent maxima of 500-hPa geopotential height. *Climate Dynamics* **51**, 701–717. doi:10.1007/s00382-017-3950-0.

Log T (2020) Modeling Drying of Degenerated Calluna vulgaris for Wildfire and Prescribed Burning Risk Assessment. *Forests* **11**, 759. doi:10.3390/f11070759.

Log T, Thuestad G, Velle LG, Khattri SK, Kleppe G (2017) Unmanaged heathland – A fire risk in subzero temperatures? *Fire Safety Journal* **90**, 62–71. doi:10.1016/j.firesaf.2017.04.017.

London Fire Brigade (2023) Major Incident Review Extreme Weather Period 2022.

Lukenbach MC, Hokanson KJ, Moore PA, Devito KJ, Kettridge N, Thompson DK, Wotton BM, Petrone RM, Waddington JM (2015) Hydrological controls on deep burning in a northern forested peatland. *Hydrological Processes* **29**, 4114–4124. doi:10.1002/hyp.10440.

Manning C, Widmann M, Maraun D, Van Loon AF, Bevacqua E (2023) Large spread in the representation of compound long-duration dry and hot spells over Europe in CMIP5. *Weather and Climate Dynamics* **4**, 309–329. doi:10.5194/wcd-4-309-2023.

Masoom A, Fountoulakis I, Kazadzis S, Raptis I-P, Kampouri A, Psiloglou BE, Kouklaki D, Papachristopoulou K, Marinou E, Solomos S, Gialitaki A, Founda D, Salamalikis V, Kaskaoutis D, Kouremeti N, Mihalopoulos N, Amiridis V, Kazantzidis A, Papayannis A, Zerefos CS, Eleftheratos K (2023) Investigation of the effects of the Greek extreme wildfires of August 2021 on air quality and spectral solar irradiance. *Atmospheric Chemistry and Physics* **23**, 8487–8514. doi:10.5194/acp-23-8487-2023.

Matthews S (2014) Dead fuel moisture research: 1991-2012. *International Journal of Wildland Fire* **23**, 78–92. doi:10.1071/WF13005.

Matthews S, Gould J, McCaw L (2010) Simple models for predicting dead fuel moisture in eucalyptus forests. *International Journal of Wildland Fire* **19**, 459–467. doi:10.1071/WF09005.

Matthews S, Sauvage S, Grootemaat S, Hollis J, Kenny B, Fox-Hughes P (2019) 'Implementation of models and the forecast system for the Australian Fire Danger Rating System.'

McLauchlan KK, Higuera PE, Miesel J, Rogers BM, Schweitzer J, Shuman JK, Tepley AJ, Varner JM, Veblen TT, Adalsteinsson SA, Balch JK, Baker P, Batllori E, Bigio E, Brando P, Cattau M, Chipman ML, Coen J, Crandall R, Daniels L, Enright N, Gross WS, Harvey BJ, Hatten JA, Hermann S, Hewitt RE, Kobziar LN, Landesmann JB, Loranty MM, Maezumi SY, Mearns L, Moritz M, Myers JA, Pausas JG, Pellegrini AFA, Platt WJ, Roozeboom J, Safford H, Santos F, Scheller RM, Sherriff RL, Smith KG, Smith MD, Watts AC (2020) Fire as a fundamental ecological process: Research advances and frontiers. *Journal of Ecology* **108**, 2047–2069. doi:10.1111/1365-2745.13403.

Meng M, Gong D (2022) Winter North Atlantic SST as a Precursor of Spring Eurasian Wildfire. *Geophysical Research Letters* **49**, e2022GL099920. doi:10.1029/2022GL099920.

Met Office (2023) England and Wales Fire Severity Index. https://www.metoffice.gov.uk/public/weather/fire-severity-index.

Mickler RA (2021) Carbon emissions from a temperate coastal peatland wildfire: contributions from natural plant communities and organic soils. *Carbon Balance and Management* **16**, 26. doi:10.1186/s13021-021-00189-0.

Miller RL, Lackmann GM, Robinson WA (2020) A New Variable-Threshold Persistent Anomaly Index: Northern Hemisphere Anomalies in the ERA-Interim Reanalysis. *Monthly Weather Review* **148**, 43–62. doi:10.1175/MWR-D-19-0144.1.

Miller L, Zhu L, Yebra M, Rüdiger C, Webb GI (2022) Multi-modal temporal CNNs for live fuel moisture content estimation. *Environmental Modelling & Software* **156**, 105467. doi:10.1016/j.envsoft.2022.105467.

Minsavage-davis CD (2022) Evaluating the Performance of Fire Rate of Spread Models in Northern-European Calluna vulgaris Heathlands.

Miralles DG, Gentine P, Seneviratne SI, Teuling AJ (2019) Land-atmospheric feedbacks during droughts and heatwaves: state of the science and current challenges: Land feedbacks during droughts and heatwaves. *Annals of the New York Academy of Sciences* **1436**, 19–35. doi:10.1111/nyas.13912.

Monedero S, Ramirez J, Cardil A (2019) Predicting fire spread and behaviour on the fireline. Wildfire analyst pocket: A mobile app for wildland fire prediction. *Ecological Modelling* **392**, 103–107. doi:10.1016/j.ecolmodel.2018.11.016.

Moore PD (2002) The future of cool temperate bogs. *Environmental Conservation* **29**, 3–20. doi:10.1017/S0376892902000024.

Morrison LW (2016) Observer error in vegetation surveys: a review. *Journal of Plant Ecology* **9**, 367–379. doi:10.1093/jpe/rtv077.

Nakagawa S, Schielzeth H (2013) A general and simple method for obtaining R2 from generalized linear mixed-effects models (RB O'Hara, Ed.). *Methods in Ecology and Evolution* **4**, 133–142. doi:10.1111/j.2041-210x.2012.00261.x.

Natural Resources Canada (2021) An overview of the next generation of the Canadian Forest Fire Danger Rating System. Information Report GLC-X-26. http://cfs.nrcan.gc.ca/publications?id=40474.

Nolan RH, Boer MM, Resco De Dios V, Caccamo G, Bradstock RA (2016) Large-scale, dynamic transformations in fuel moisture drive wildfire activity across southeastern Australia. *Geophysical Research Letters* **43**, 4229–4238. doi:10.1002/2016GL068614.

Nolan RH, Foster B, Griebel A, Choat B, Medlyn BE, Yebra M, Younes N, Boer MM (2022) Drought-related leaf functional traits control spatial and temporal dynamics of live fuel moisture content. *Agricultural and Forest Meteorology* **319**, 108941. doi:10.1016/j.agrformet.2022.108941.

Nolan V, Gilbert F, Reader T (2022) Solving sampling bias problems in presence–absence or presence-only species data using zero-inflated models. *Journal of Biogeography* **49**, 215–232. doi:10.1111/jbi.14268.

Norum R a., Miller M (1984) Measuring Fuel Moisture Content in Alaska : Standard Methods and Protocols. *General Technical Report* 1–40. doi:10.1016/S0140-6701(02)85652-1.

NWCG (2022) NWCG Incident Response Pocket Guide (IRPG) | NWCG. https://www.nwcg.gov/publications/461.

NWCG (2023) Dead Fuel Moisture Content. https://www.nwcg.gov/publications/pms437/fuel-moisture/dead-fuel-moisture-content.

Nyman P, Baillie CC, Duff TJ, Sheridan GJ (2018) Eco-hydrological controls on microclimate and surface fuel evaporation in complex terrain. *Agricultural and Forest Meteorology* **252**, 49–61. doi:10.1016/j.agrformet.2017.12.255.

Nyman P, Metzen D, Noske PJ, Lane PNJ, Sheridan GJ (2015) Quantifying the effects of topographic aspect on water content and temperature in fine surface fuel. *International Journal of Wildland Fire* **24**, 1129–1142. doi:10.1071/WF14195.

Nyman P, Sherwin CB, Langhans C, Lane PNJ, Sheridan GJ (2014) Downscaling regional climate data to calculate the radiative index of dryness in complex terrain. *Australian Meteorological and Oceanographic Journal* **64**, 109–122. doi:10.22499/2.6402.003.

Ordnance S (2019) OS Terrain® 50 DTM. https://www.ordnancesurvey.co.uk/business-government/products/terrain-50.

Page SE, Baird AJ (2016) Peatlands and Global Change: Response and Resilience. *Annual Review of Environment and Resources* **41**, 35–57. doi:10.1146/annurev-environ-110615-085520.

Pandey P, Huidobro G, Lopes LF, Ganteaume A, Ascoli D, Colaco C, Xanthopoulos G, Giannaropoulos T, Gazzard R, Boustras G, Steelman T, Charlton V, Ferguson E, Kirschner J, Little K, Stoof C, Nikolakis W, Fernández-Blanco CR, Ribotta C, Lambrechts H, Fernandez M, Dossi S (2023) A global outlook on increasing wildfire risk: current policy situation and future pathways. *Trees, Forests and People* 100431. doi:10.1016/j.tfp.2023.100431.

Papavasileiou G, Giannaros TM (2023) The Predictability of the Synoptic-Scale Fire Weather Conditions during the 2018 Mati Wildfire. *Environmental Sciences Proceedings* **26**, 164. doi:10.3390/environsciproc2023026164.

Pepin A-C, Wotton M (2020) Fire Behaviour Observation in Shrublands in Nova Scotia, Canada and Assessment of Aids to Operational Fire Behaviour Prediction. *Fire* **3**, 34. doi:10.3390/fire3030034.

Perry MC, Vanvyve E, Betts RA, Palin EJ (2022) Past and future trends in fire weather for the UK. *Natural Hazards and Earth System Sciences* **22**, 559–575. doi:10.5194/nhess-22-559-2022.

Pfahl S, Wernli H (2012) Quantifying the relevance of atmospheric blocking for co-located temperature extremes in the Northern Hemisphere on (sub-)daily time scales. *Geophysical Research Letters* **39**,. doi:10.1029/2012GL052261.

Pimont F, Ruffault J, Martin-StPaul NK, Dupuy JL (2019) Why is the effect of live fuel moisture content on fire rate of spread underestimated in field experiments in shrublands? *International Journal of Wildland Fire* **28**, 127–137. doi:10.1071/WF18091.

Pivovaroff AL, Emery N, Sharifi MR, Witter M, Keeley JE, Rundel PW (2019) The Effect of Ecophysiological Traits on Live Fuel Moisture Content. *Fire* **2**, 12. doi:10.3390/fire2020028.

R Core Team (2022) 'R: A Language and Environment for Statistical Computing.' (R Foundation for Statistical Computing: Vienna, Austria) https://www.R-project.org/.

Rahimi E, Salman Mahini A (2018) Percolation Theory and its Applications in Landscape Ecology. *Environmental Researches* **9**, 47–61.

Rao K, Williams AP, Diffenbaugh NS, Yebra M, Konings AG (2022) Plant-water sensitivity regulates wildfire vulnerability. 332–339. doi:10.1038/s41559-021-01654-2.

Resco de Dios V, Cunill Camprubí À, Pérez-Zanón N, Peña JC, Martínez del Castillo E, Rodrigues M, Yao Y, Yebra M, Vega-García C, Boer MM (2022) Convergence in critical fuel moisture and fire weather thresholds associated with fire activity in the pyroregions of Mediterranean Europe. *Science of The Total Environment* **806**, 151462. doi:10.1016/j.scitotenv.2021.151462.

Rex DF (1950) Blocking Action in the Middle Troposphere and its Effect upon Regional Climate. *Tellus* **2**, 196–211. doi:10.1111/j.2153-3490.1950.tb00331.x.

Richardson D, Black AS, Monselesan DP, Risbey JS, Squire DT, Tozer CR, Canadell JG (2021) Increased extreme fire weather occurrence in southeast Australia and related atmospheric drivers. *Weather and Climate Extremes* **34**, 100397. doi:10.1016/j.wace.2021.100397.

Robine J-M, Cheung SLK, Le Roy S, Van Oyen H, Griffiths C, Michel J-P, Herrmann FR (2008) Death toll exceeded 70,000 in Europe during the summer of 2003. *Comptes Rendus Biologies* **331**, 171–178. doi:10.1016/j.crvi.2007.12.001.

Rodrigues M Identifying wildfire-prone atmospheric circulation weather types on mainland Spain. doi:10.1016/j.agrformet.2018.10.005. Accessed 1 September 2022.

Rodrigues M, Cunill Camprubí À, Balaguer-Romano R, Coco Megía CJ, Castañares F, Ruffault J, Fernandes PM, Resco de Dios V (2023) Drivers and implications of the extreme 2022 wildfire season in Southwest Europe. *Science of The Total Environment* **859**, 160320. doi:10.1016/j.scitotenv.2022.160320.

Rothermel RC (1972) A mathematical model for predicting fire spread in wildland fuels. *Res Pap INT-115 Ogden, UT: US Department of Agriculture, Intermountain Forest and Range Experiment Station 40 p* **115**,. http://www.fs.usda.gov/treesearch/pubs/32533.

Rousi E, Kornhuber K, Beobide-Arsuaga G, Luo F, Coumou D (2022) Accelerated western European heatwave trends linked to more-persistent double jets over Eurasia. *Nature Communications* **13**, 3851. doi:10.1038/s41467-022-31432-y.

Ruffault J, Curt T, Moron V, Trigo RM, Mouillot F, Koutsias N, Pimont F, Martin-StPaul N, Barbero R, Dupuy J-L, Russo A, Belhadj-Khedher C (2020) Increased likelihood of heat-induced large wildfires in the Mediterranean Basin. *Scientific Reports* **10**, 13790. doi:10.1038/s41598-020-70069-z.

Ruffault J, Limousin J-M, Pimont F, Dupuy J-L, De Càceres M, Cochard H, Mouillot F, Blackman CJ, Torres-Ruiz JM, Parsons RA, Moreno M, Delzon S, Jansen S, Olioso A, Choat B, Martin-StPaul N (2022) Plant hydraulic modelling of leaf and canopy fuel moisture content reveals increasing vulnerability of a Mediterranean forest to wildfires under extreme drought. *New Phytologist* **n/a**,. doi:10.1111/nph.18614.

Ruffault J, Moron V, Trigo RM, Curt T (2017) Daily synoptic conditions associated with large fire occurrence in Mediterranean France: evidence for a wind-driven fire regime. *International Journal of Climatology* **37**, 524–533. doi:10.1002/joc.4680.

Russo S, Dosio A, Graversen RG, Sillmann J, Carrao H, Dunbar MB, Singleton A, Montagna P, Barbola P, Vogt JV (2014) Magnitude of extreme heat waves in present climate and their projection in a warming world. *Journal of Geophysical Research: Atmospheres* **119**, 12,500-12,512. doi:10.1002/2014JD022098.

San-Miguel-Ayanz J, Durrant T, Boca R, Maianti P, Libertá G, Duarte O, Branco A, de Rigo D, Ferrari D, Roglia E, Scionti N (2023) Advance report on forest fires in Europe, Middle East and North Africa 2022. Publications Office of the European Union, Website https://op.europa.eu/en/publication-detail/-/publication/500b8dfa-de5e-11ed-a05c-01aa75ed71a1/language-en.

San-Miguel-Ayanz J, Schulte E, Schmuck G, Camia A, Strobl P, Liberta G, Giovando C, Boca R, Sedano F, Kempeneers P, McInerney D, Withmore C, de Oliveira SS, Rodrigues M, Durrant T, Corti P, Oehler F, Vilar L, Amatulli G (2012) Comprehensive Monitoring of Wildfires in Europe: The European Forest Fire Information System (EFFIS). 'Approaches to Managing Disaster - Assessing Hazards, Emergencies and Disaster Impacts'. (Ed J Tiefenbacher)(InTech) doi:10.5772/28441.

Santana VM, Marrs RH (2014) Flammability properties of British heathland and moorland vegetation: Models for predicting fire ignition. *Journal of Environmental Management* **139**, 88–96. doi:10.1016/j.jenvman.2014.02.027.

Scarff FR, Lenz T, Richards AE, Zanne AE, Wright IJ, Westoby M (2021) Effects of plant hydraulic traits on the flammability of live fine canopy fuels. *Functional Ecology* **35**, 835–846. doi:10.1111/1365-2435.13771.

Scholten RC, Coumou D, Luo F, Veraverbeke S (2022) Early snowmelt and polar jet dynamics co-influence recent extreme Siberian fire seasons. *Science* **0**, eabn4419. doi:10.1126/science.abn4419.

Scott JH, Burgan RE (2005) Standard fire behavior fuel models: A comprehensive set for use with Rothermel's surface fire spread model. *USDA Forest Service - General Technical Report RMRS-GTR* 1–76. doi:10.2737/RMRS-GTR-153.

Sharma AR, Jain P, Abatzoglou JT, Flannigan M (2022) Persistent Positive Anomalies in Geopotential Heights Promote Wildfires in Western North America. *Journal of Climate* **35**, 2867–2884. doi:10.1175/JCLI-D-21-0926.1.

Shepherd TG (2014) Atmospheric circulation as a source of uncertainty in climate change projections. *Nature Geoscience* **7**, 703–708. doi:10.1038/ngeo2253.

Shuman JK, Balch JK, Barnes RT, Higuera PE, Roos CI, Schwilk DW, Stavros EN, Banerjee T, Bela MM, Bendix J, Bertolino S, Bililign S, Bladon KD, Brando P, Breidenthal RE, Buma B, Calhoun D, Carvalho LMV, Cattau ME, Cawley KM, Chandra S, Chipman ML, Cobian-Iñiguez J, Conlisk E, Coop JD, Cullen A, Davis KT, Dayalu A, De Sales F, Dolman M, Ellsworth LM, Franklin S, Guiterman CH, Hamilton M, Hanan EJ, Hansen WD, Hantson S, Harvey BJ, Holz A, Huang T, Hurteau MD, Ilangakoon NT, Jennings M, Jones C, Klimaszewski-Patterson A, Kobziar LN, Kominoski J, Kosovic B, Krawchuk MA, Laris P, Leonard J, Loria-Salazar SM, Lucash M, Mahmoud H, Margolis E, Maxwell T, McCarty JL, McWethy DB, Meyer RS, Miesel JR, Moser WK, Nagy RC, Niyogi D, Palmer HM, Pellegrini A, Poulter B, Robertson K, Rocha AV, Sadegh M, Santos F, Scordo F, Sexton JO, Sharma AS, Smith AMS, Soja AJ, Still C, Swetnam T, Syphard AD, Tingley MW, Tohidi A, Trugman AT, Turetsky M, Varner JM, Wang Y, Whitman T, Yelenik S, Zhang X (2022) Reimagine fire science for the anthropocene. *PNAS Nexus* **1**, pgac115. doi:10.1093/pnasnexus/pgac115.

Sicacha-Parada J, Steinsland I, Cretois B, Borgelt J (2021) Accounting for spatial varying sampling effort due to accessibility in Citizen Science data: A case study of moose in Norway. *Spatial Statistics* **42**, 100446. doi:10.1016/j.spasta.2020.100446.

Simmons IG (1990) The Mid-Holocene Ecological History of the Moorlands of England and Wales and its Relevance for Conservation. *Environmental Conservation* **17**, 61–69. doi:10.1017/S0376892900017306.

Skinner WR, Flannigan MD, Stocks BJ, Martell DL, Wotton BM, Todd JB, Mason JA, Logan KA, Bosch EM (2002) A 500 hPa synoptic wildland fire climatology for large Canadian forest fires, 1959–1996. *Theoretical and Applied Climatology* **71**, 157–169. doi:10.1007/s007040200002.

Slijepcevic A, Anderson WR, Matthews S (2013) Testing existing models for predicting hourly variation in fine fuel moisture in eucalypt forests. *Forest Ecology and Management* **306**, 202–215. doi:10.1016/j.foreco.2013.06.033.

Slijepcevic A, Anderson WR, Matthews S, Anderson DH (2018) An analysis of the effect of aspect and vegetation type on fine fuel moisture content in eucalypt forest. *International Journal of Wildland Fire* **27**, 190–202. doi:10.1071/WF17049.

Sousa PM, Barriopedro D, García-Herrera R, Ordóñez C, Soares PMM, Trigo RM (2020) Distinct influences of large-scale circulation and regional feedbacks in two exceptional 2019 European heatwaves. *Communications Earth & Environment* **1**, 1–13. doi:10.1038/s43247-020-00048-9.

Stoof CR, Tapia VM, Marcotte AL, Stoorvogel JJ, Ribau MC (2020) Relatie tussen natuurbeheer en brandveiligheid in de Deurnese Peel : onderzoek naar aanleiding van de brand in de Deurnese Peel van 20 april 2020. doi:10.18174/533574.

Sweeney RE, Ulveling EF (1972) A Transformation for Simplifying the Interpretation of Coefficients of Binary Variables in Regression Analysis. *The American Statistician* **26**, 30–32. doi:10.2307/2683780.

Taylor A, Bruce M, Britton A, Owen I, Gagkas Z, Pohle I, Fielding D, Hadden R (2021) Scottish Fire Danger Rating System (FDRS) Report. The James Hutton Institute, (Scotland)

Thien SJ (1979) A flow diagram for teaching texture-by-feel analysis. *Journal of Agronomic Education* **8**, 54–55. doi:10.2134/jae.1979.0054.

Trigo RM, García-Herrera R, Díaz J, Trigo IF, Valente MA (2005) How exceptional was the early August 2003 heatwave in France? *Geophysical Research Letters* **32**,. doi:10.1029/2005GL022410.

Tromp-van Meerveld HJ, McDonnell JJ (2006) On the interrelations between topography, soil depth, soil moisture, transpiration rates and species distribution at the hillslope scale. *Advances in Water Resources* **29**, 293–310. doi:10.1016/j.advwatres.2005.02.016.

Trouet V, Babst F, Meko M (2018) Recent enhanced high-summer North Atlantic Jet variability emerges from three-century context. *Nature Communications* **9**, 180. doi:10.1038/s41467-017-02699-3.

Tuel A, Steinfeld D, Ali SM, Sprenger M, Martius O (2022) Large-Scale Drivers of Persistent Extreme Weather During Early Summer 2021 in Europe. *Geophysical Research Letters* **49**, e2022GL099624. doi:10.1029/2022GL099624.

Tyrlis E, Hoskins BJ (2008) Aspects of a Northern Hemisphere Atmospheric Blocking Climatology. *Journal of the Atmospheric Sciences* **65**, 1638–1652. doi:10.1175/2007JAS2337.1.

Van Wagner CE (1987) 'Development and structure of the Canadian forest fire weather index system.' doi:19927.

Walsh SF, Nyman P, Sheridan GJ, Baillie CC, Tolhurst KG, Duff TJ (2017) Hillslope-scale prediction of terrain and forest canopy effects on temperature and near-surface soil moisture deficit. *International Journal of Wildland Fire* **26**, 191–208. doi:10.1071/WF16106.

Wang X, Wotton BM, Cantin AS, Parisien MA, Anderson K, Moore B, Flannigan MD (2017) cffdrs: an R package for the Canadian Forest Fire Danger Rating System. *Ecological Processes* **6**, 11pp. doi:10.1186/s13717-017-0070-z.

Wehrli K, Luo F, Hauser M, Shiogama H, Tokuda D, Kim H, Coumou D, May W, Le Sager P, Selten F, Martius O, Vautard R, Seneviratne SI (2022) The ExtremeX global climate model experiment: investigating thermodynamic and dynamic processes contributing to weather and climate extremes. *Earth System Dynamics* **13**, 1167–1196. doi:10.5194/esd-13-1167-2022.

Yu ZC (2012) Northern peatland carbon stocks and dynamics: a review. *Biogeosciences* **9**, 4071–4085. doi:10.5194/bg-9-4071-2012.

Zacharakis I, Tsihrintzis VA (2023) Integrated wildfire danger models and factors: A review. *Science of The Total Environment* **899**, 165704. doi:10.1016/j.scitotenv.2023.165704.

Zhang Y, Sun P (2020) Study on the diurnal dynamic changes and prediction models of the moisture contents of two litters. *Forests* **11**, 1–15. doi:10.3390/f11010095.

Zhao F, Liu Y (2019) Atmospheric Circulation Patterns Associated With Wildfires in the Monsoon Regions of China. *Geophysical Research Letters* **46**, 4873–4882. doi:10.1029/2019GL081932.

8

8 SUPPLEMENTARY MATERIAL

CHAPTER 2: SUPPLEMENTARY MATERIAL

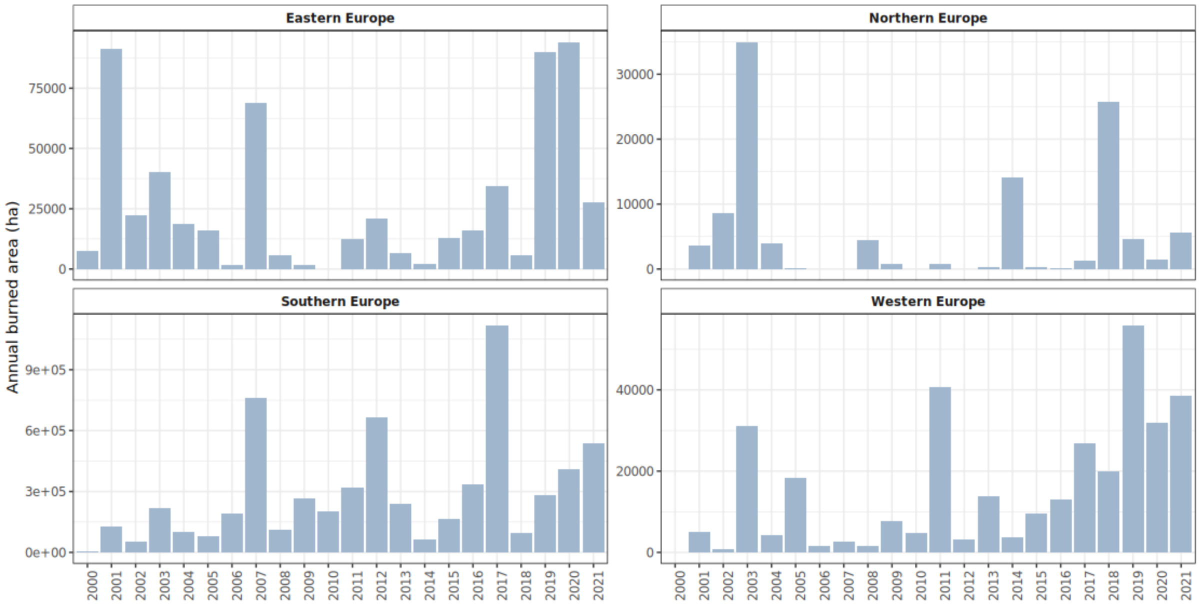

Figure S2.1 Annual burned area from 2000–2021 for each region.

Table S2.1 Annual number of PPAs detected using different size and duration thresholds.

	3 days			5 days		
year	20000 km^2	40000 km^2	80000 km^2	20000 km^2	40000 km^2	80000 km^2
2001	34	32	30	24	22	20
2002	33	33	30	23	20	19
2003	38	32	29	28	27	22
2004	35	34	29	29	23	21
2005	36	33	28	25	22	22
2006	35	34	32	27	26	21
2007	30	30	27	21	19	19
2008	35	33	31	28	26	24
2009	40	36	35	27	26	18
2010	31	31	28	26	26	25
2011	42	38	36	30	26	25
2012	33	30	29	21	21	20
2013	39	34	32	25	23	17
2014	33	30	28	25	24	21
2015	35	30	30	21	19	18
2016	35	35	34	30	29	23
2017	43	40	39	32	30	26
2018	36	37	30	24	22	19
2019	33	30	30	25	24	23
2020	44	39	34	31	28	25
2021	40	36	33	29	28	24
Average	36	34	31	26	24	22

Table S2.2 Comparison of mean and standard deviation (SD) of odds ratios summarised by region and month for Haldane Correction of 0.5 (HC 0.5) versus Haldane Correction of 2 (HC 2). Haldane Correction of 2 provides a more conservative odds ratio and reduced estimation bias.

Region	Month	HC0.5 (mean)	HC 0.5 (SD)	HC 2 (mean)	HC 2 (SD)
Eastern Europe	March	2.4	5.2	1.9	3.3
Eastern Europe	April	1.0	5.3	0.7	2.7
Eastern Europe	May	8.2	10.2	4.0	5.0
Eastern Europe	June	4.1	6.8	2.8	5.5
Eastern Europe	July	3.5	5.2	3.1	4.0
Eastern Europe	August	3.9	7.6	3.1	3.4
Northern Europe	March	1.4	3.8	0.8	1.9
Northern Europe	April	2.9	4.4	1.8	2.1
Northern Europe	May	6.8	4.7	3.6	2.2
Northern Europe	June	2.6	3.4	1.5	1.5
Northern Europe	July	3.6	2.6	1.9	1.1
Northern Europe	August	4.3	6.5	2.1	2.6
Southern Europe	March	4.3	7.2	3.2	3.6
Southern Europe	April	4.8	6.9	3.0	3.2
Southern Europe	May	3.4	6.3	2.1	2.9
Southern Europe	June	4.4	7.2	3.6	4.2
Southern Europe	July	3.4	6.0	3.7	5.6
Southern Europe	August	3.3	4.1	3.5	3.9
Western Europe	March	5.2	5.2	3.5	2.4
Western Europe	April	2.4	5.9	1.4	2.3
Western Europe	May	5.5	9.0	3.3	4.5
Western Europe	June	4.1	4.2	2.1	1.8
Western Europe	July	3.3	4.6	1.9	2.3
Western Europe	August	3.5	5.5	2.8	3.7

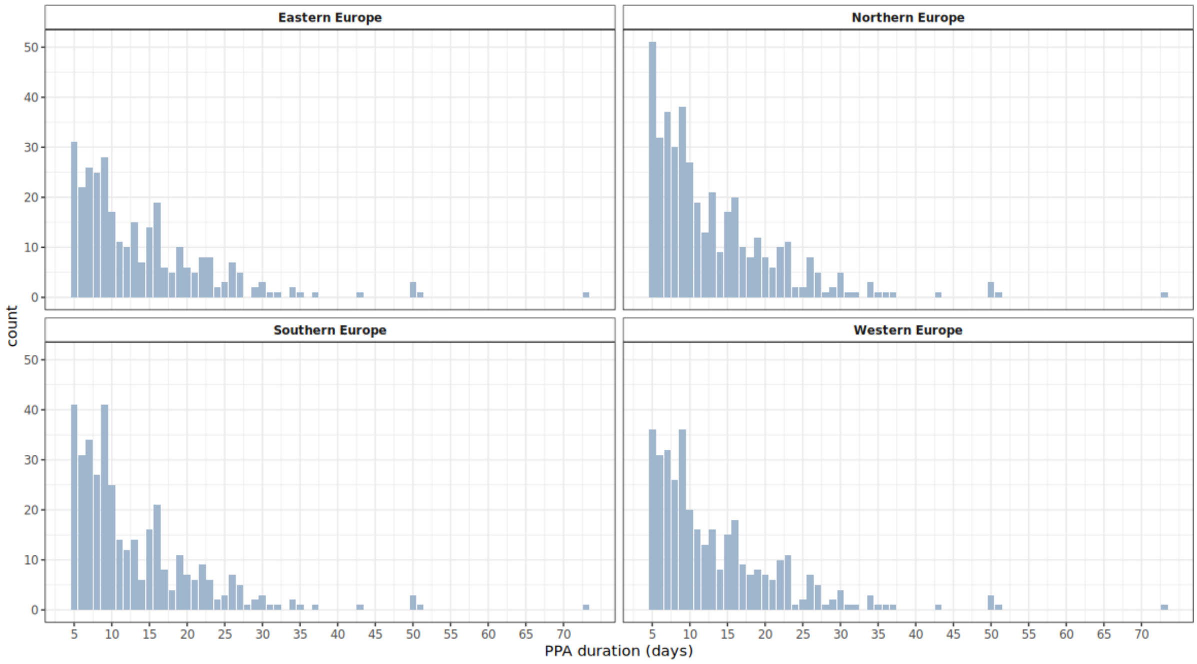

Figure S2.2 Distribution of PPA durations (days) for each region.

Figure S2.3 Test statistics for linear regression models of surface anomalies between PPA and non-PPA days by month (March (3)–August (8))

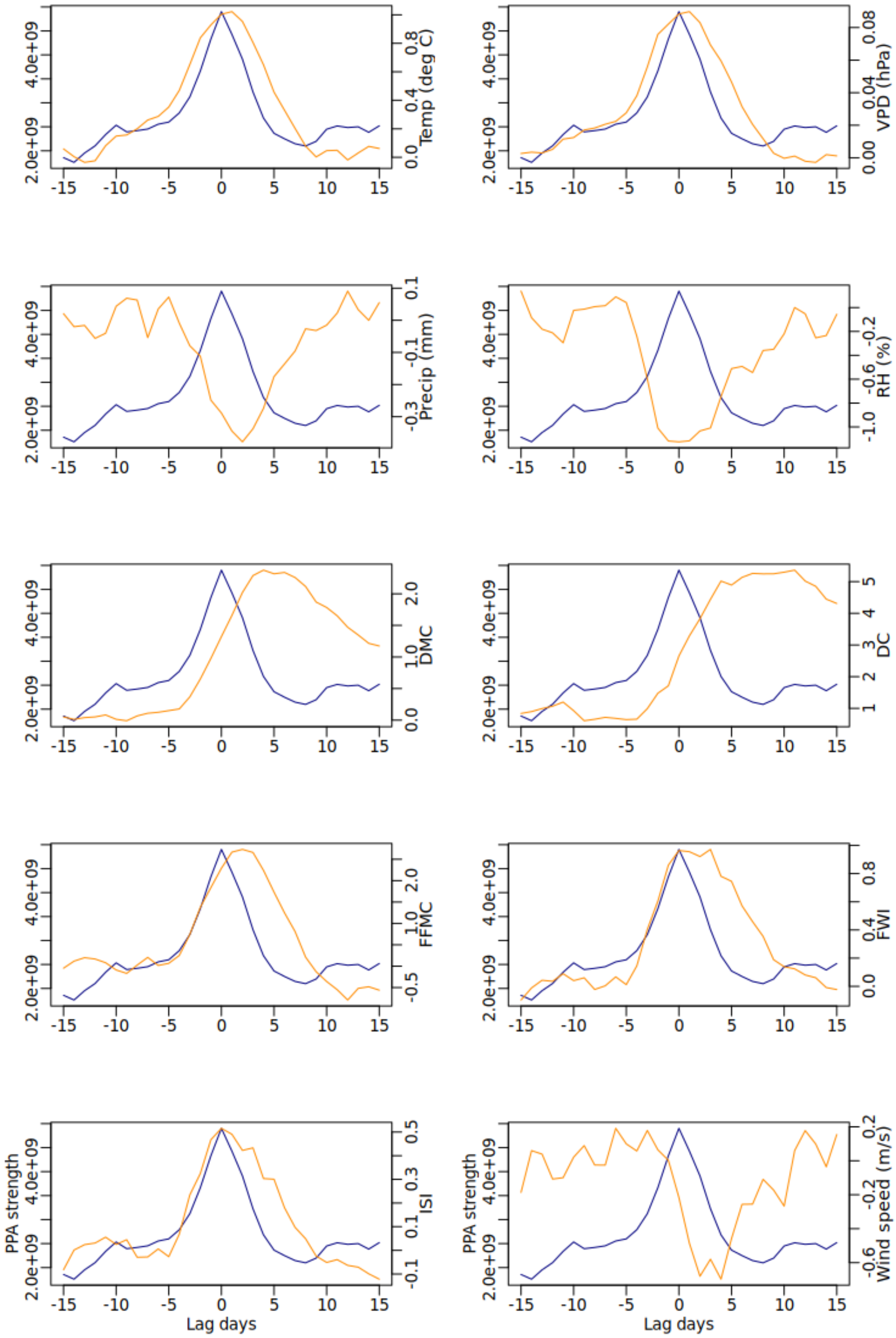

Figure S2.4 Lead-lag relationship between PPA strength and surface anomalies for Northern Europe. Blue line = PPA strength with maximum strength on day 0. Orange line = average surface anomalies for the maximum PPA strength area 15 days either side of maximum PPA strength.

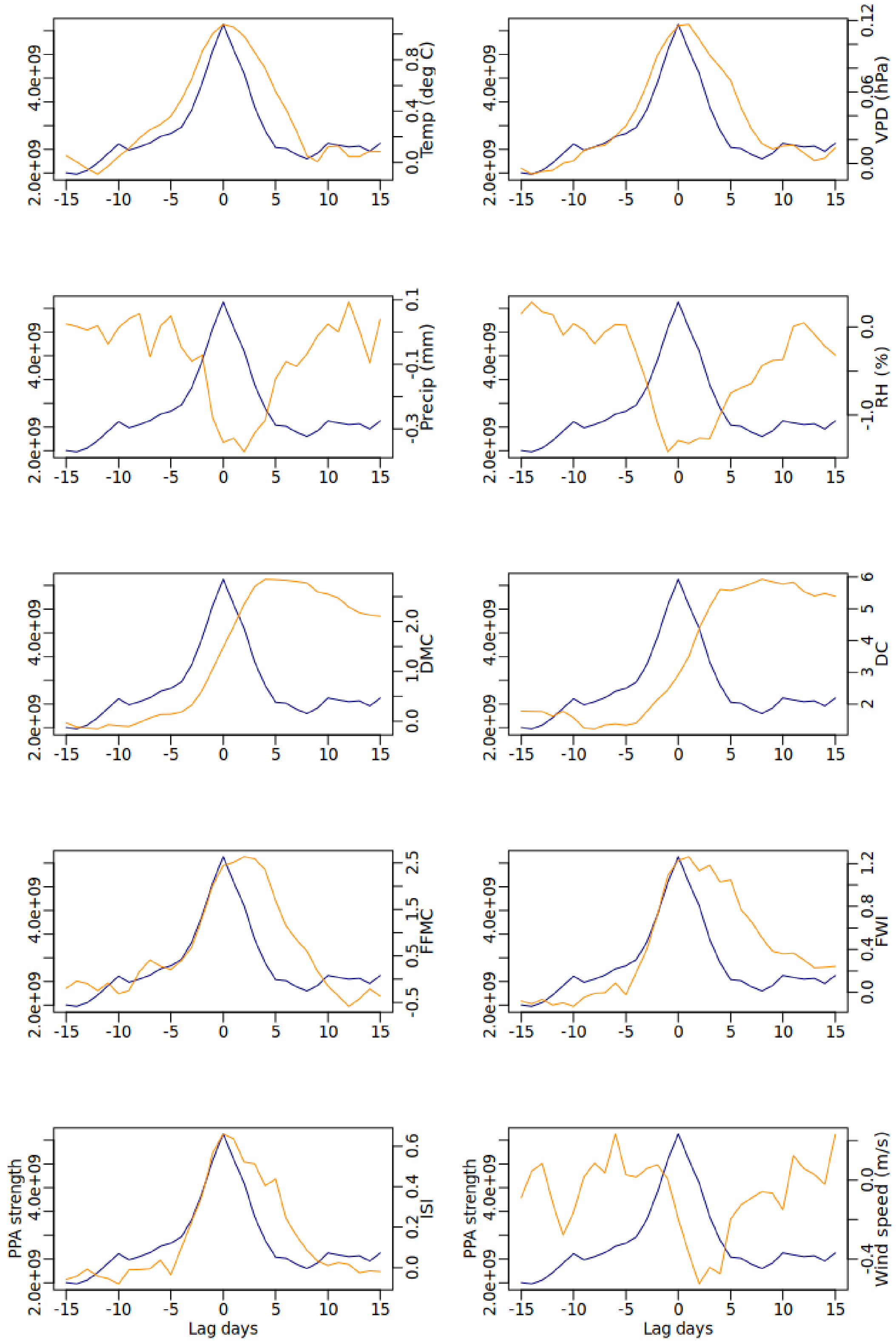

Figure S2.5 Lead-lag relationship between PPA strength and surface anomalies for Eastern Europe. Blue line = PPA strength with maximum strength on day 0. Orange line = average surface anomalies for the maximum PPA strength area 15 days either side of maximum PPA strength.

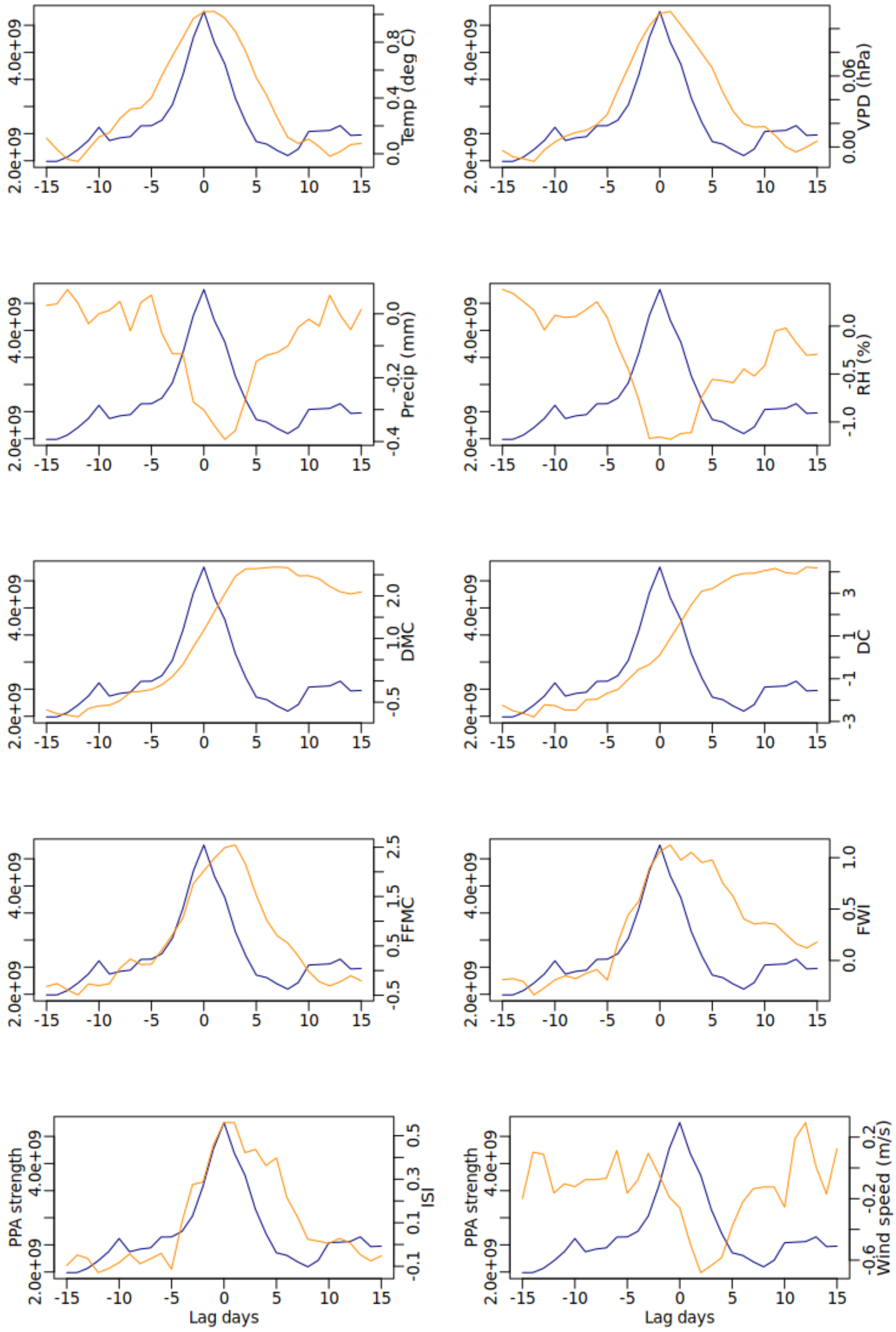

Figure S2.6 Lead-lag relationship between PPA strength and surface anomalies for Southern Europe. Blue line = PPA strength with maximum strength on day 0. Orange line = average surface anomalies for the maximum PPA strength area 15 days either side of maximum PPA strength.

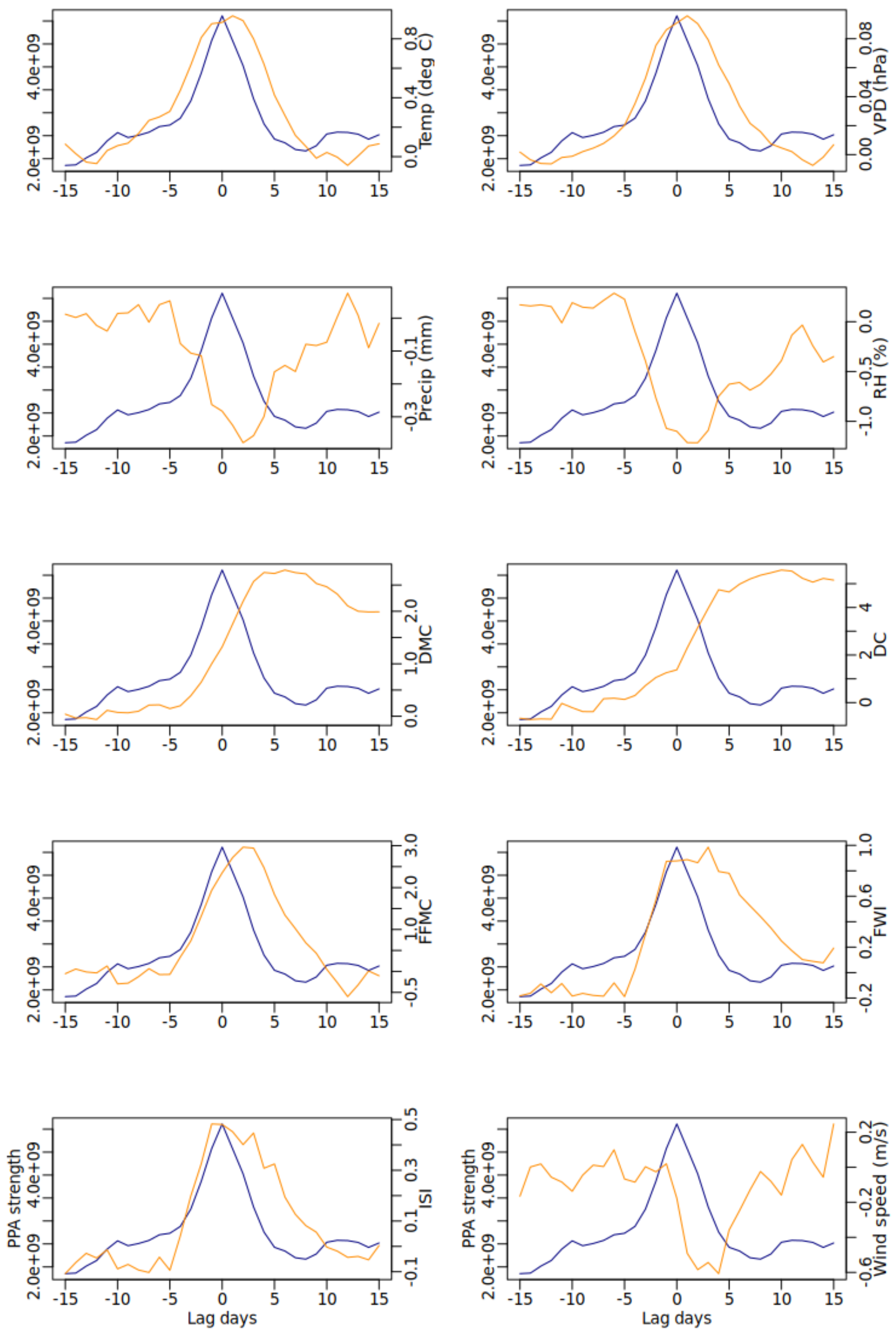

Figure S2.7 Lead-lag relationship between PPA strength and surface anomalies for Western Europe. Blue line = PPA strength with maximum strength on day 0. Orange line = average surface anomalies for the maximum PPA strength area 15 days either side of maximum PPA strength.

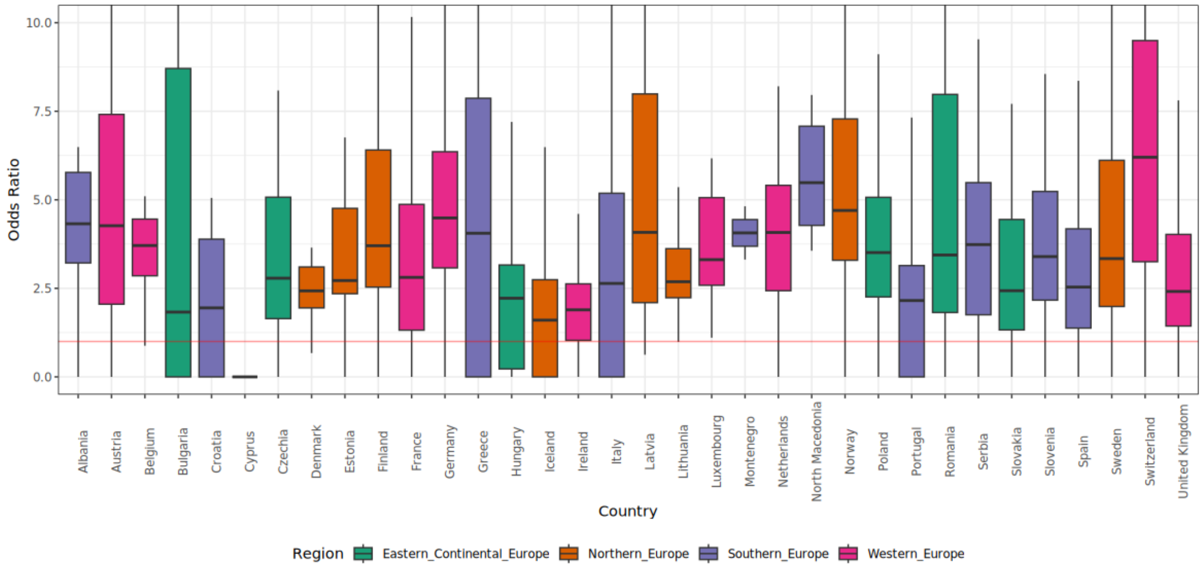

Figure S2.8 Odds ratio for likelihood of experiencing extreme fire weather (95th percentile FWI) during a PPA by country.

Table S2.3 Average odds ratio for the likelihood of experiencing extreme fire weather (95th percentile FWI) during a PPA by country and month.

Country	Mar	Apr	May	Jun	Jul	Aug	Sep
Albania			0.0	9.6	4.8	4.7	5.7
Austria	0.0	1.8	8.3	3.3	6.9	6.8	5.2
Belgium		1.0	4.2	3.4	4.1	5.1	3.6
Bulgaria	24.4	0.0	2.8	3.4	8.1	1.4	5.8
Croatia		0.0	12.8	0.2	2.8	3.1	3.4
Cyprus	0.0	0.0	0.0	0.0			0.0
Czechia		1.5	1.5	2.7	4.3	6.8	3.4
Denmark		1.2	9.7	1.7	2.7	2.4	3.5
Estonia		3.6	2.4	2.2	3.2	6.3	3.6
Finland		0.0	13.7	2.9	4.5	3.5	6.1
France	0.0	1.9	3.0	2.8	4.5	4.4	3.3
Germany	5.8	2.4	5.5	4.5	6.0	6.2	5.0
Greece		0.0	0.0	5.3	11.8	3.8	6.1
Hungary	0.0	0.9	3.4	1.7	3.0	2.9	2.2
Iceland			1.1	1.7	4.0	1.3	2.1
Ireland	0.0	1.2	1.6	2.2	5.4	1.7	2.2
Italy	0.0	0.9	3.8	2.8	4.9	4.6	3.6
Latvia		9.5	2.4	1.4	4.8	7.4	5.1
Lithuania		2.8	2.7	1.8	4.4	3.2	3.0
Luxembourg		1.1	2.6	3.3	5.1	6.2	3.6
Montenegro					4.8	3.3	4.1
Netherlands	0.0	3.0	2.3	4.0	6.6	6.1	4.0
North Macedonia			0.0	9.7	5.8	4.3	5.7
Norway	5.8	4.2	8.6	4.8	6.0	4.0	5.7
Poland		1.0	3.7	4.2	4.6	4.7	3.7
Portugal	0.3	0.0	2.0	2.5	3.2	2.2	2.1
Romania	16.5	5.3	9.3	4.0	3.2	2.5	5.9
Serbia		7.7	9.9	1.1	3.3	4.3	4.6
Slovakia		1.7	2.1	0.6	4.7	4.9	2.8
Slovenia	0.0	1.6	5.1	3.4	5.0	3.5	3.5
Spain	0.4	4.2	3.4	2.6	4.2	2.8	3.2
Sweden		2.7	11.4	2.3	4.8	2.5	5.1
Switzerland	1.9	4.6	8.6	4.0	9.9	8.8	6.6
United Kingdom	0.3	1.6	3.1	3.0	5.8	2.2	3.0

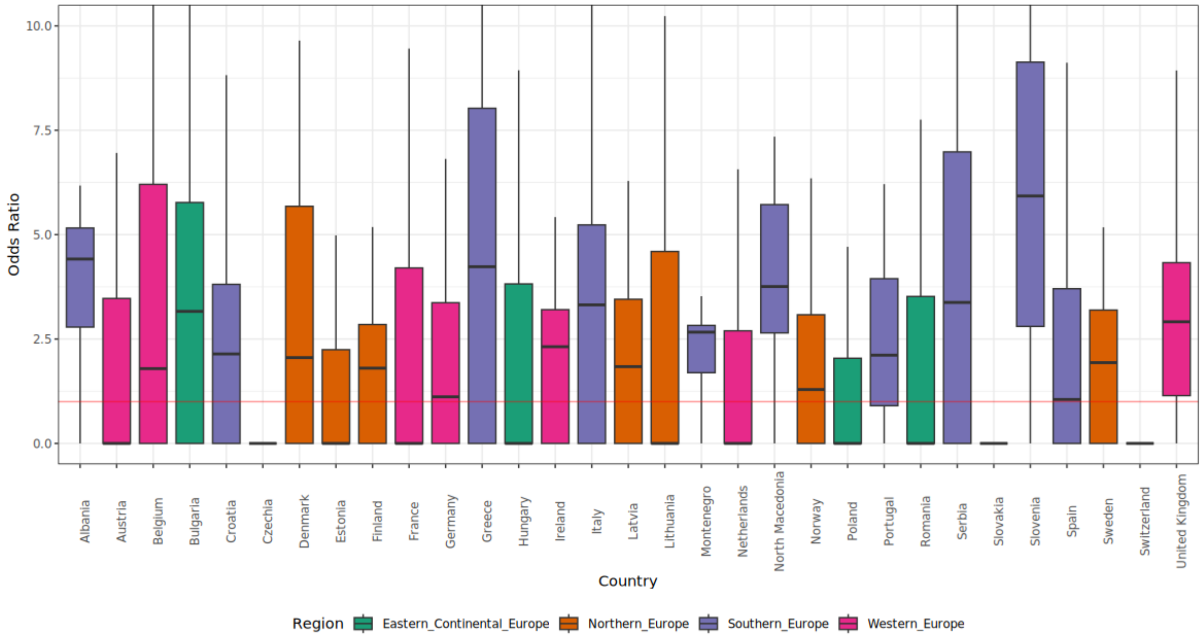

Figure S2.9 Odds ratio for likelihood of wildfires occurring concurrently with PPAs by country.

Table S2.4 Average odds ratio for likelihood of wildfires occurring concurrently with PPAs by country and month.

Country	Mar	Apr	May	Jun	Jul	Aug	Sep
Albania	4.1	3.2	5.8	9.1	6.1	2.7	5.2
Austria	1.6	0.0		3.0	1.4	1.5	1.6
Belgium		0.0	14.1		3.6		4.4
Bulgaria	4.3	2.3	0.0	2.1	6.0	4.1	4.0
Croatia	1.8	3.1	0.0	1.8	2.4	3.0	2.3
Czechia	0.7	0.0			0.0	0.0	0.3
Denmark	1.0	2.5	8.5	2.1	0.8	0.0	3.3
Estonia	0.6	0.9	0.0	0.0	1.6	5.0	1.2
Finland	0.0	1.5	3.0	1.9	1.4	0.6	1.7
France	4.2	1.8	2.8	1.8	1.7	3.2	2.5
Germany	2.3	0.9	2.5	2.0	1.6	2.5	1.9
Greece	3.3	0.0	4.1	7.4	7.7	3.2	5.3
Hungary	2.6	0.0		2.4	2.3	2.1	2.0
Ireland	3.1	0.8	2.6	1.6	3.2		2.2
Italy	3.3	3.9	4.6	2.9	2.4	4.5	3.5
Latvia	1.3	1.2	3.4	0.0	2.3	3.2	1.9
Lithuania	0.0	3.6	0.0	4.6	2.6	5.1	2.5
Montenegro	2.6	1.4	0.0	2.8	2.8	3.5	2.2
Netherlands	2.6	2.2	0.0		2.7		1.7
North Macedonia	2.8	2.9	2.2	9.9	4.8	3.0	4.3
Norway	5.0	0.5	4.5	0.7	1.4		1.9
Poland	0.1	0.0	2.8	2.9	2.5	2.3	1.2
Portugal	1.5	2.7	1.1	3.3	3.5	3.1	2.6
Romania	2.9	0.5	5.1	5.0	1.8	3.5	2.7
Serbia	7.3	3.5	1.6	4.3	5.3	3.6	4.7
Slovakia	1.1	0.0		0.0	0.0	2.4	0.9
Slovenia	6.1				3.7	8.1	6.0
Spain	2.4	2.8	1.2	2.4	3.2	3.2	2.7
Sweden	0.0	2.7	3.2	1.3	2.0	1.2	2.0
Switzerland	7.0	0.0	0.0		0.0		0.8
United Kingdom	3.5	1.9	4.3	2.8	2.6	1.9	3.0

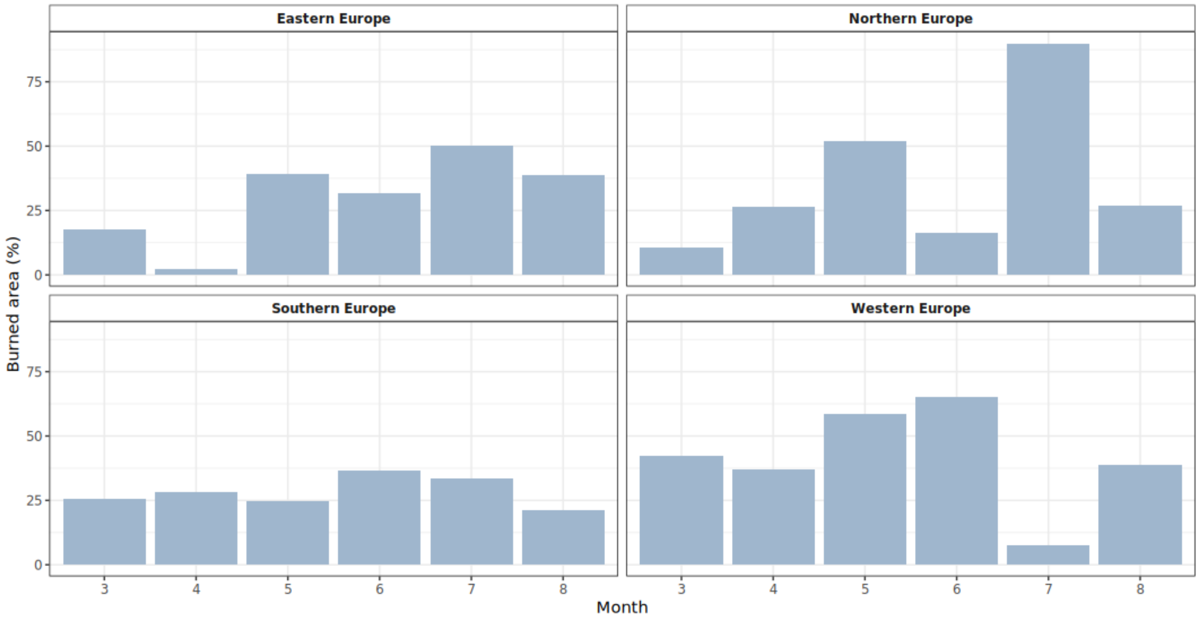

Figure S2.10 Percentage of PPA-related burned area by region and month.

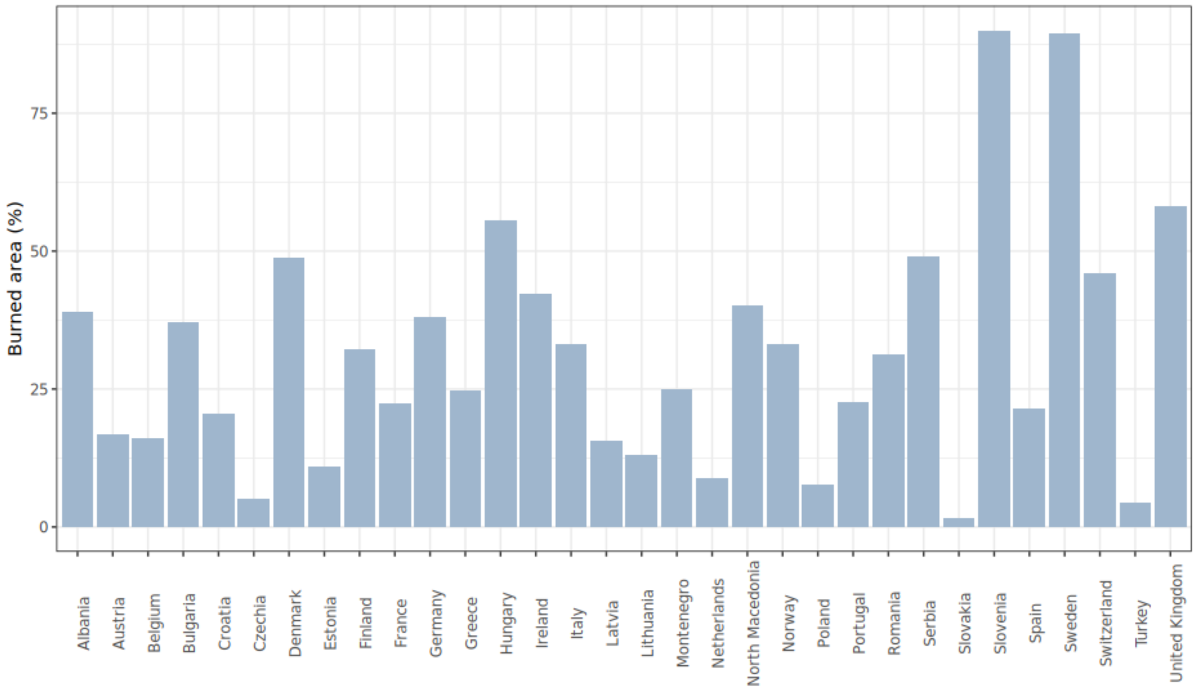

Figure S2.11 Percentage of PPA-related burned area by country.

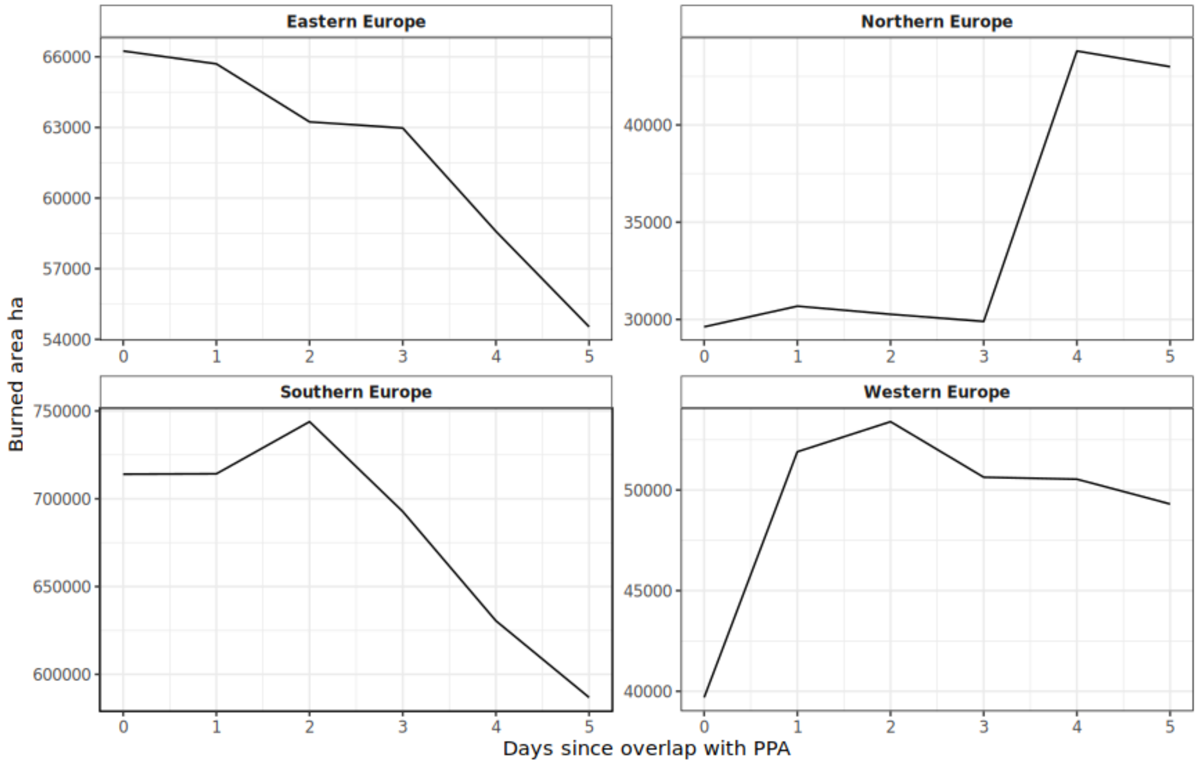

Figure S2.12 Total amount of burned area (ha) recorded when a PPA was present on the day of the fire event (0) or the 1–5 days preceding the fire event for each region.

CHAPTER 3: SUPPLEMENTARY MATERIAL

Weather conditions during sampling days

I collected samples during hot, dry conditions in the spring and summer of 2021. Fig S3.1 shows the sampling day weather conditions (vertical lines) within April, June, and July of a nearby weather station within North Yorkshire Moors National Park. I aimed to allow the greatest period of dry days prior to collection, unless logistics or forecast differences prevented this. No sampling was completed during May as there were no sufficiently dry windows for sampling.

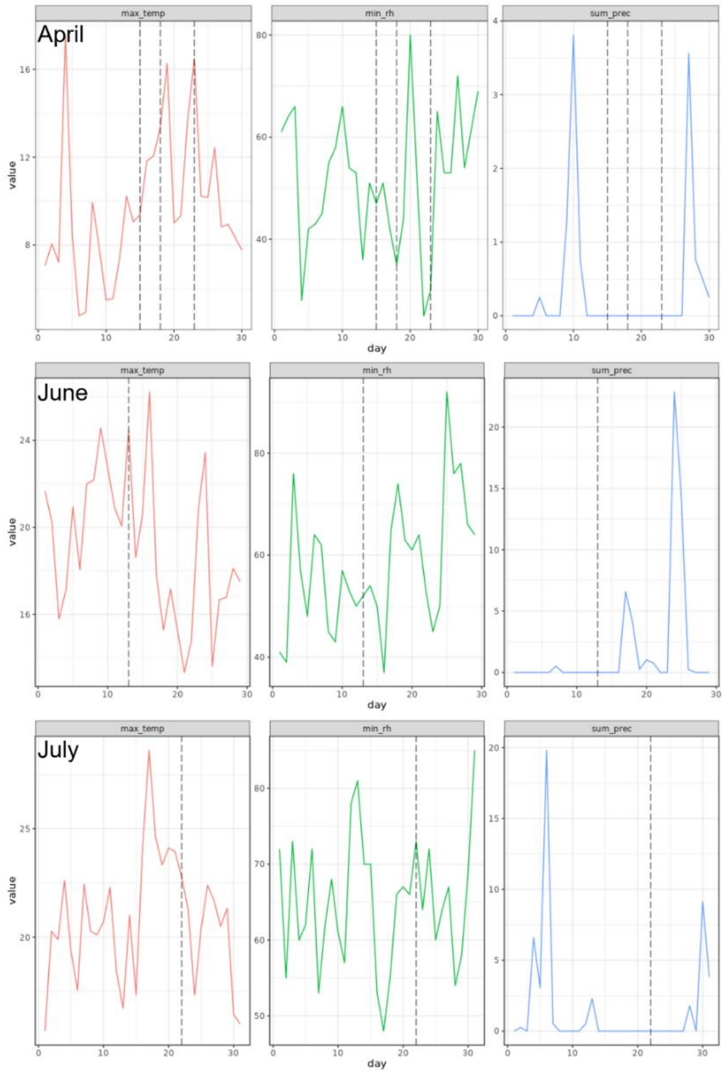

Figure S3.1 Time series of daily maximum temperature (degrees Celsius), minimum relative humidity (%) and accumulated precipitation (mm) for April, June and July from a weather station within the North Yorkshire Moors. Vertical dashed lines mark the sampling days within these months.

Micrometeorological model selection

I examined relationships between existing fire weather indices and fuel moisture variability using the Canadian Fire Weather Index System (CFWIS) (Fig S3.2). I calculated the components of the CFWIS at midday using the micrometeorological data from the weather stations installed at each pair of sites and initial input values from calculations for a nearby weather station in the 60 days prior to installation.

Fire weather indices are best correlated with fuel moisture in April, where there is largely a consistent negative relationship between fuel moisture and index value (i.e., index values are higher where fuels are drier). With the exception of April, it is difficult to discern consistent relationships between Canadian Fire Weather Indices and fuel moisture variation within a landscape. In particular, relationships between fuel moisture and fire weather indices in June largely indicate the opposite relationship to expected (i.e., increasing index values with increasing fuel moisture), apart from moss. This is consistent with my finding that landscape factors are more important drivers of fuel moisture variation in June for all fuel layers except moss. While the CFWIS is reasonably correlated with fuel moisture for individual fuel layers (dead Calluna and moss) and seasons (spring), I opted to exclude the CFWIS in favour of the micrometeorological variables themselves in the linear regression model because of their improved performance across all fuel layers and seasons.

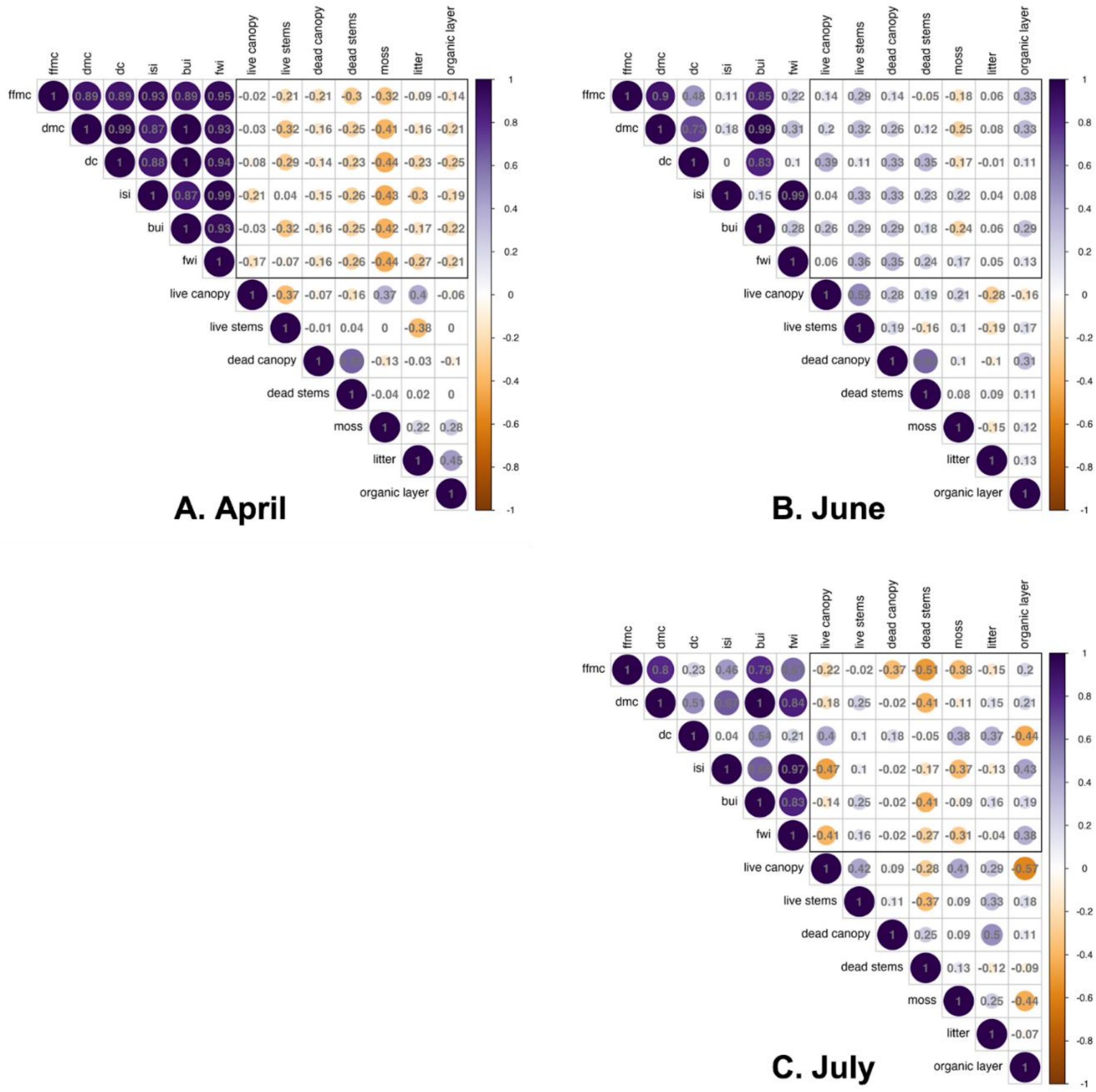

Figure S3.2 Pearson correlation matrices for components of the Canadian Fire Weather Index System calculated at midday using micrometeorological data recorded at each site and fuel moisture content collected in A. April, B. June, and C. July (within rectangle outline). Orange, negative coefficients indicate logical relationship direction.

I examined fuel moisture–micrometeorological relationships across different lag periods and parameters to derive the best relationships with observed fuel moisture, including: (1) maximum, (2) minimum, and (3) averages of variables (a) at the time of sampling, (b) lagged hourly back across the sampling window, and (c) lagged daily up to 1-week prior to sampling. Linear regression models using average micrometeorological variables on the day of sampling derived the best performing statistical models for the majority of fuel layers, thereby allowing simplicity and comparability of model outputs for making general conclusions on spatial fuel moisture–micrometeorological relationships. All models perform similarly well (maximum point difference of 0.05) when using meteorological inputs from time of sampling to 5 h prior averages. The 5 h-averaged micrometeorological model performed the best for the highest number of different fuel layers, so I opted to use this average to balance the differing response times of fuel layers into a simple micrometeorological model (Table S3.1).

Table S3.1 R^2 values from the micrometeorological model showing relationship between fuel moisture and micrometeorological variables (temperature, relative humidity, vapour pressure deficit, and wind speed) at the time of sampling (tos) and averaged 1–6 hours prior to the time of sampling for all sample dates combined.

Fuel layer	tos	1h	3h	5h	6 h
Live canopy	0.68	0.69	0.69	0.71	0.69
Live stems	0.48	0.5	0.49	0.47	0.51
Dead canopy	0.08	0.08	0.1	0.09	0.03
Dead stems	0.08	0.09	0.11	0.12	0.05
Moss	0.54	0.55	0.53	0.5	0.28
Litter	0.31	0.33	0.34	0.34	0.2
Organic layer	0.42	0.42	0.42	0.42	0.42

Landscape linear regression model outputs

Table S3.2 Linear models outputs for each landscape factor and fuel layer. Model intercepts show the overall sample mean estimate and deviations for each fuel layer within the landscape factor. Intercept estimate indicates an above (>0%) or below (<0%) average fuel moisture content. The difference between estimates (%) for each classified landscape factor shows the range of fuel moisture content in measured fuel layers. Statistically significant differences ($p < 0.05$) are indicated in bold.

Factor	Fuel layer	Landscape factor classification	April Estimate (%)	April Standard error	June Estimate (%)	June Standard error	July Estimate (%)	July Standard error
Soil texture	Live canopy	Intercept	56.8	1.0	93.1	2.8	114.4	3.2
		Coarse	**10.1**	1.4	**15.3**	3.9	**18.8**	4.6
		Fine	**-3.5**	1.3	**-13.3**	3.5	**-19.8**	4.0
		Peat	**-7.2**	1.6	0.3	4.4	5.2	5.2
	Live stems	Intercept	70.9	0.8	84.7	1.0	85.5	1.6
		Coarse	**-6.7**	1.1	**4.1**	1.4	1.4	2.2
		Fine	**3.9**	0.9	**-4.3**	1.3	-0.6	2.0
		Peat	**2.6**	1.2	1.2	1.7	-0.9	2.5
	Dead canopy	Intercept	12.9	0.7	11.8	0.2	13.1	0.6
		Coarse	-0.9	0.9	0.7	0.3	1.1	0.8
		Fine	-0.7	0.8	-0.3	0.3	0.2	0.7
		Peat	2.0	1.0	-0.4	0.4	-1.6	0.8
	Dead stems	Intercept	13.6	0.7	12.0	0.5	12.3	0.5
		Coarse	-0.8	1.0	1.3	0.7	**-1.7**	0.8
		Fine	-1.4	0.9	-0.6	0.6	**1.4**	0.7
		Peat	**3.0**	1.2	-0.8	0.7	0.0	0.9
	Moss	Intercept	56.8	4.5	16.3	0.8	18.0	1.1
		Coarse	**13.7**	6.4	-0.2	1.1	4.4	1.5
		Fine	**-11.8**	5.5	-1.2	1.0	-1.9	1.3
		Peat	0.1	7.3	2.0	1.3	-2.5	1.8
	Litter	Intercept	53.6	3.6	24.1	2.1	31.6	3.4
		Coarse	**17.4**	5.2	-4.7	3.0	17.6	4.9
		Fine	**-12.6**	4.4	**9.8**	2.7	-5.1	4.3
		Peat	-3.3	5.6	**-8.1**	3.4	-13.9	5.4
	Organic layer	Intercept	271.5	8.0	171.9	10.9	163.1	9.2
		Coarse	13.3	11.0	4.0	15.4	**-46.6**	13.0
		Fine	4.7	10.1	8.5	13.7	**28.2**	11.5
		Peat	-22.5	12.9	-16.7	17.6	16.5	14.8
Canopy age	Live canopy	Intercept	56.8	1.2	93.1	3.4	114.4	4.2
		Building	**3.1**	1.2	3.9	3.4	4.5	4.2
		Mature	**-3.1**	1.2	-3.9	3.4	-4.5	4.2
	Live stems	Intercept	70.8	0.9	84.7	1.2	85.5	1.5
		Building	0.9	0.9	1.6	1.2	2.3	1.5
		Mature	-0.9	0.9	-1.6	1.2	-2.3	1.5
	Dead canopy	Intercept	12.8	0.7	11.8	0.3	12.9	0.6
		Building	-1.1	0.7	-0.4	0.3	-0.4	0.6
		Mature	1.1	0.7	0.4	0.3	0.4	0.6
	Dead stems	Intercept	13.5	0.7	12.0	0.5	12.3	0.5
		Building	**-3.0**	0.7	-0.9	0.5	**-1.3**	0.5
		Mature	**3.0**	0.7	0.9	0.5	**1.3**	0.5
	Moss	Intercept	56.1	4.6	16.2	0.8	18.2	1.2
		Building	-4.5	4.6	-0.3	0.8	0.4	1.2
		Mature	4.5	4.6	0.3	0.8	-0.4	1.2
	Litter	Intercept	52.1	3.7	23.8	2.5	31.2	4.0
		Building	-7.1	3.7	-0.5	2.5	3.4	4.0
		Mature	7.1	3.7	0.5	2.5	-3.4	4.0
		Intercept	271.7	8.1	171.9	10.6	163.1	10.5

Organic layer	Building	-3.3	8.1	-14.8	10.6	-10.1	10.5
	Mature	3.3	8.1	14.8	10.6	10.1	10.5

Factor	Fuel layer	Landscape factor classification	April Estimate (%)	April Standard error	June Estimate (%)	June Standard error	July Estimate (%)	July Standard error
Aspect	Live canopy	Intercept	56.8	1.2	93.1	3.3	114.4	4.2
		North	0.1	1.2	-4.7	3.3	-2.8	4.2
		South	-0.1	1.2	4.7	3.3	2.8	4.2
	Live stems	Intercept	70.9	0.9	84.7	1.1	85.5	1.6
		North	**-2.2**	0.9	-1.8	1.1	0.2	1.6
		South	**2.2**	0.9	1.8	1.1	-0.2	1.6
	Dead canopy	Intercept	13.0	0.7	11.8	0.2	13.0	0.5
		North	-0.6	0.7	**-0.5**	0.2	**1.1**	0.5
		South	0.6	0.7	**0.5**	0.2	**-1.1**	0.5
	Dead stems	Intercept	13.5	0.7	12.0	0.5	12.2	0.6
		North	1.2	0.7	-0.8	0.5	0.4	0.6
		South	-1.2	0.7	0.8	0.5	-0.4	0.6
	Moss	Intercept	56.3	4.5	16.2	0.8	18.1	1.2
		North	7.5	4.5	**-1.8**	0.8	0.1	1.2
		South	-7.5	4.5	**1.8**	0.8	-0.1	1.2
	Litter	Intercept	52.3	3.8	23.8	2.5	31.7	3.9
		North	0.2	3.8	-1.6	2.5	7.1	3.9
		South	-0.2	3.8	1.6	2.5	-7.1	3.9
	Organic layer	Intercept	271.7	8.0	171.9	10.9	163.1	10.7
		North	6.3	8.0	-0.8	10.9	2.1	10.7
		South	-6.3	8.0	0.8	10.9	-2.1	10.7
Slope	Live canopy	Intercept	56.9	1.2	93.1	3.4	114.4	4.3
		Low	**4.0**	1.7	6.0	4.7	2.8	6.1
		Medium	-2.1	1.7	0.7	4.7	1.6	6.1
		High	-1.9	1.7	-6.7	4.7	-4.4	6.1
	Live stems	Intercept	70.8	0.9	84.7	1.1	85.5	1.6
		Low	**-3.3**	1.2	-2.8	1.6	-1.3	2.2
		Medium	2.3	1.2	2.2	1.6	1.8	2.2
		High	1.0	1.2	0.6	1.6	-0.6	2.2
	Dead canopy	Intercept	13.0	0.7	11.8	0.3	12.6	0.6
		Low	-0.3	0.9	0.3	0.4	1.3	0.8
		Medium	-0.4	0.9	-0.4	0.4	0.2	0.8
		High	0.6	1.0	0.2	0.4	-1.5	0.9
	Dead stems	Intercept	13.5	0.7	12.0	0.5	12.2	0.5
		Low	-0.9	1.1	**1.3**	0.7	**2.0**	0.7
		Medium	1.1	1.1	-0.6	0.7	-0.3	0.7
		High	-0.2	1.0	-0.8	0.7	-1.8	0.8
	Moss	Intercept	56.3	4.5	16.2	0.8	18.1	1.2
		Low	-5.3	6.5	1.8	1.1	0.8	1.7
		Medium	11.4	6.4	-0.7	1.2	-0.1	1.7
		High	-6.1	6.3	-1.1	1.1	-0.7	1.7
	Litter	Intercept	51.9	3.8	23.8	2.5	31.5	4.1
		Low	-2.7	5.8	-1.2	3.7	4.1	6.0
		Medium	-0.9	5.2	0.4	3.6	1.5	5.7
		High	3.6	5.2	0.8	3.6	-5.5	5.7
	Organic layer	Intercept	271.4	8.1	171.9	10.9	163.1	10.3
		Low	-7.6	11.8	-7.5	15.5	-25.5	14.6
		Medium	8.7	11.2	-6.0	15.5	20.9	14.6
		High	-1.2	11.5	13.6	15.5	4.6	14.6

Fig S3.3 The following figures show the results of the assumptions testing for the landscape, micrometeorological, and combined models. The model is described above each plot using the naming convention: *model type_fuel layer_month*. Full model = full_model; micrometeorological model = met_model; landscape model = lf_model. The lefthand plot is a Q-Q plot to check for normality. The righthand plot shows the residual v predicted plots to check for heteroscedasticity.

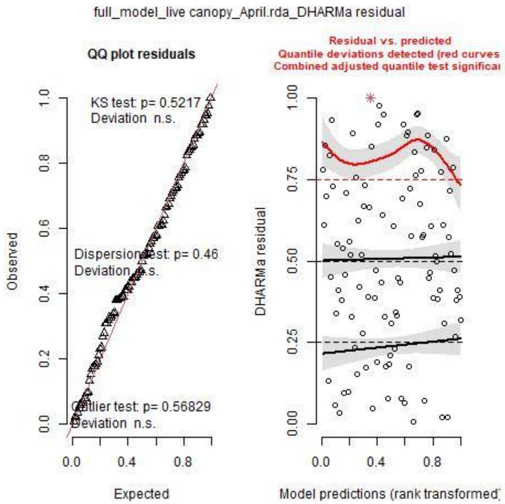
full_model_live canopy_April.rda_DHARMa residual
QQ plot residuals
KS test: p= 0.5217
Deviation n.s.
Dispersion test: p= 0.46
Deviation n.s.
Outlier test: p= 0.56829
Deviation n.s.
Observed
Expected
Residual vs. predicted
Quantile deviations detected (red curves
Combined adjusted quantile test significa
DHARMa residual
Model predictions (rank transformed)

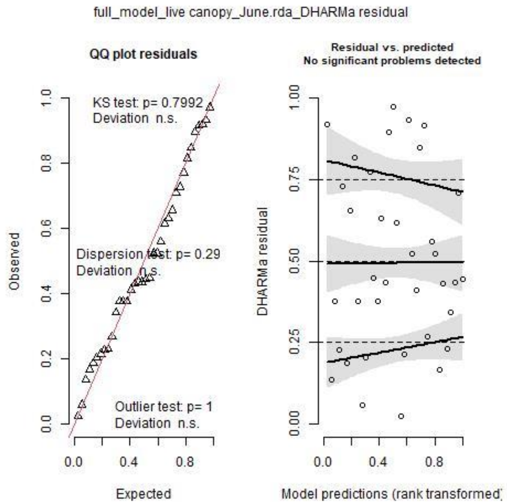
full_model_live canopy_June.rda_DHARMa residual
QQ plot residuals
KS test: p= 0.7992
Deviation n.s.
Dispersion test: p= 0.29
Deviation n.s.
Outlier test: p= 1
Deviation n.s.
Observed
Expected
Residual vs. predicted
No significant problems detected
DHARMa residual
Model predictions (rank transformed)

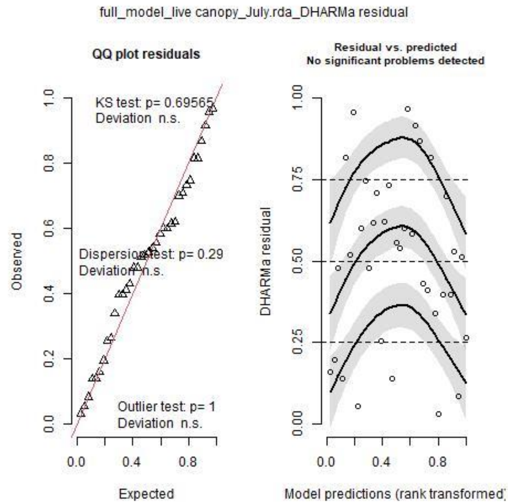
full_model_live canopy_July.rda_DHARMa residual
QQ plot residuals
KS test: p= 0.69565
Deviation n.s.
Dispersion test: p= 0.29
Deviation n.s.
Outlier test: p= 1
Deviation n.s.
Observed
Expected
Residual vs. predicted
No significant problems detected
DHARMa residual
Model predictions (rank transformed)

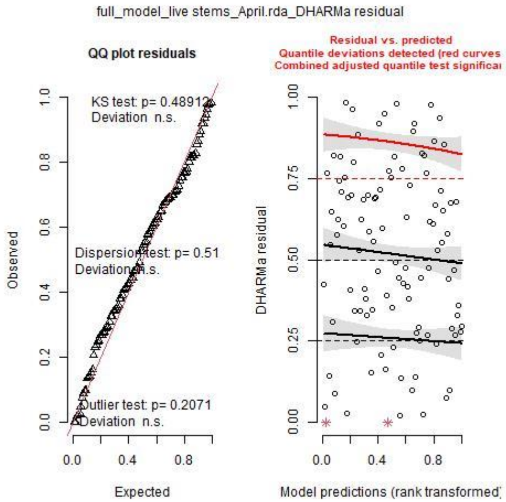
full_model_live stems_April.rda_DHARMa residual
QQ plot residuals
KS test: p= 0.48912
Deviation n.s.
Dispersion test: p= 0.51
Deviation n.s.
Outlier test: p= 0.2071
Deviation n.s.
Observed
Expected
Residual vs. predicted
Quantile deviations detected (red curves
Combined adjusted quantile test significa
DHARMa residual
Model predictions (rank transformed)

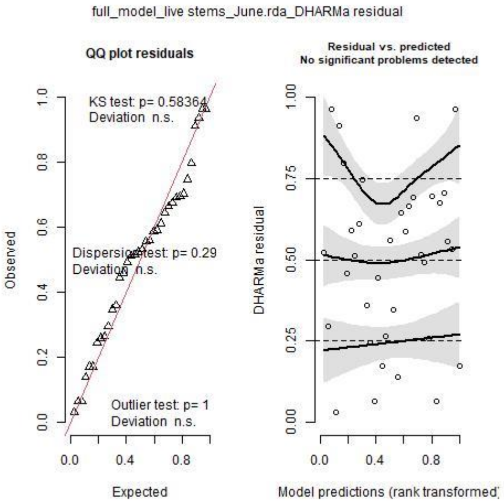
full_model_live stems_June.rda_DHARMa residual
QQ plot residuals
KS test: p= 0.58364
Deviation n.s.
Dispersion test: p= 0.29
Deviation n.s.
Outlier test: p= 1
Deviation n.s.
Observed
Expected
Residual vs. predicted
No significant problems detected
DHARMa residual
Model predictions (rank transformed)

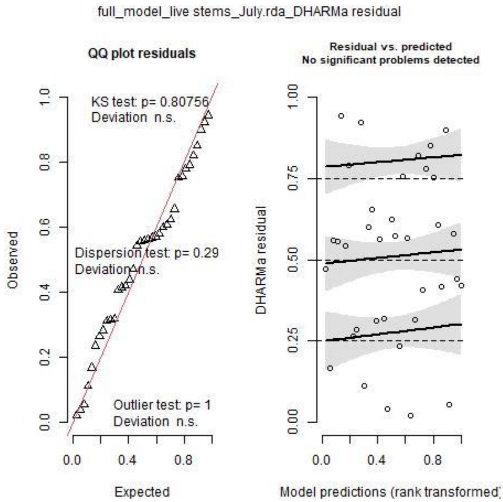
full_model_live stems_July.rda_DHARMa residual
QQ plot residuals
KS test: p= 0.80756
Deviation n.s.
Dispersion test: p= 0.29
Deviation n.s.
Outlier test: p= 1
Deviation n.s.
Observed
Expected
Residual vs. predicted
No significant problems detected
DHARMa residual
Model predictions (rank transformed)

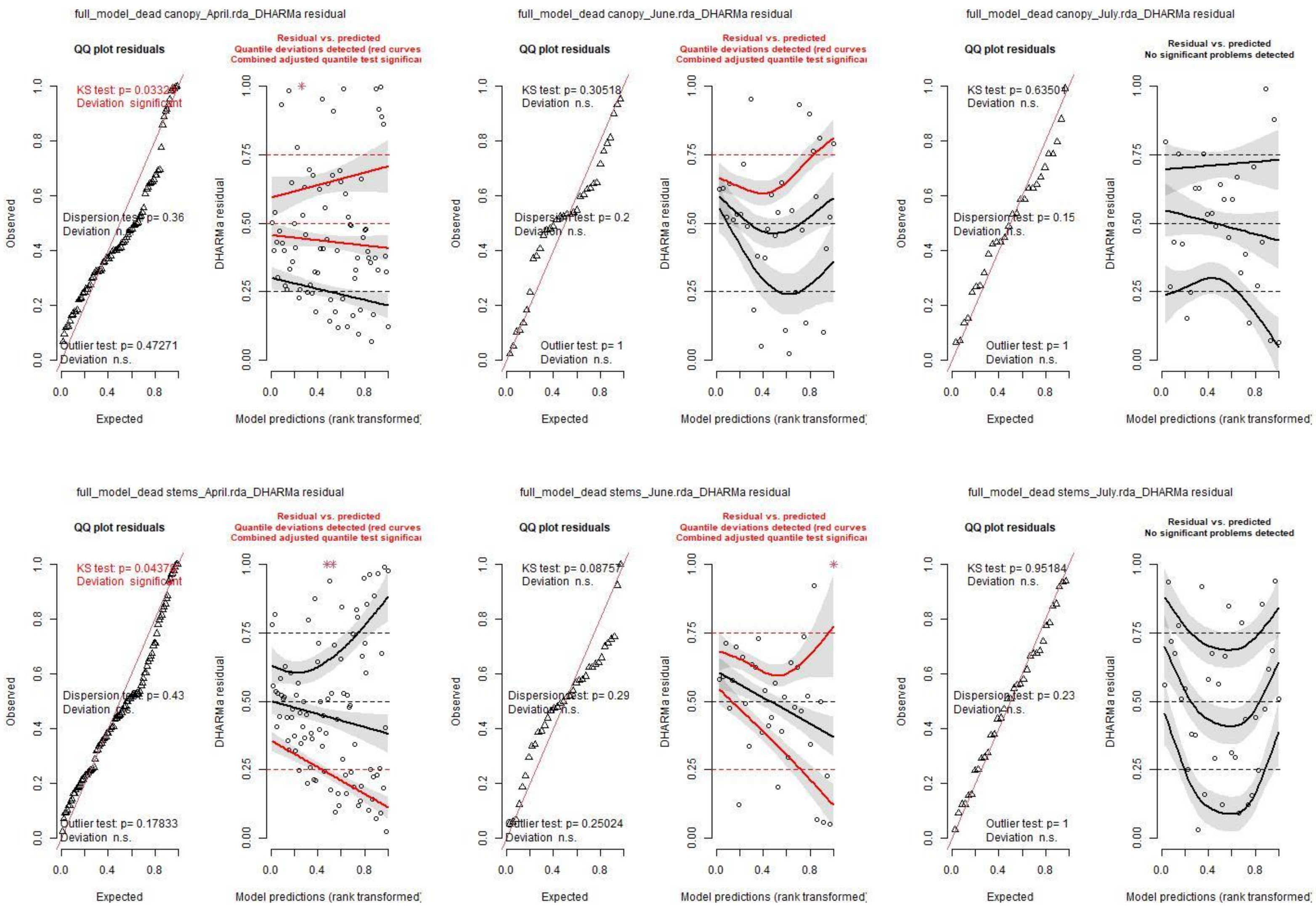
full_model_dead canopy_April.rda_DHARMa residual
QQ plot residuals
KS test: p= 0.0332
Deviation significant
Dispersion test: p= 0.36
Deviation n.s.
Outlier test: p= 0.47271
Deviation n.s.
Observed
Expected
Residual vs. predicted
Quantile deviations detected (red curves
Combined adjusted quantile test significa
DHARMa residual
Model predictions (rank transformed)
full_model_dead canopy_June.rda_DHARMa residual
QQ plot residuals
KS test: p= 0.30518
Deviation n.s.
Dispersion test: p= 0.2
Deviation n.s.
Outlier test: p= 1
Deviation n.s.
Residual vs. predicted
Quantile deviations detected (red curves
Combined adjusted quantile test significa
full_model_dead canopy_July.rda_DHARMa residual
QQ plot residuals
KS test: p= 0.6350
Deviation n.s.
Dispersion test: p= 0.15
Deviation n.s.
Outlier test: p= 1
Deviation n.s.
Residual vs. predicted
No significant problems detected
full_model_dead stems_April.rda_DHARMa residual
QQ plot residuals
KS test: p= 0.0437
Deviation significant
Dispersion test: p= 0.43
Deviation n.s.
Outlier test: p= 0.17833
Deviation n.s.
Residual vs. predicted
Quantile deviations detected (red curves
Combined adjusted quantile test significa
full_model_dead stems_June.rda_DHARMa residual
QQ plot residuals
KS test: p= 0.08757
Deviation n.s.
Dispersion test: p= 0.29
Deviation n.s.
Outlier test: p= 0.25024
Deviation n.s.
Residual vs. predicted
Quantile deviations detected (red curves
Combined adjusted quantile test significa
full_model_dead stems_July.rda_DHARMa residual
QQ plot residuals
KS test: p= 0.95184
Deviation n.s.
Dispersion test: p= 0.23
Deviation n.s.
Outlier test: p= 1
Deviation n.s.
Residual vs. predicted
No significant problems detected

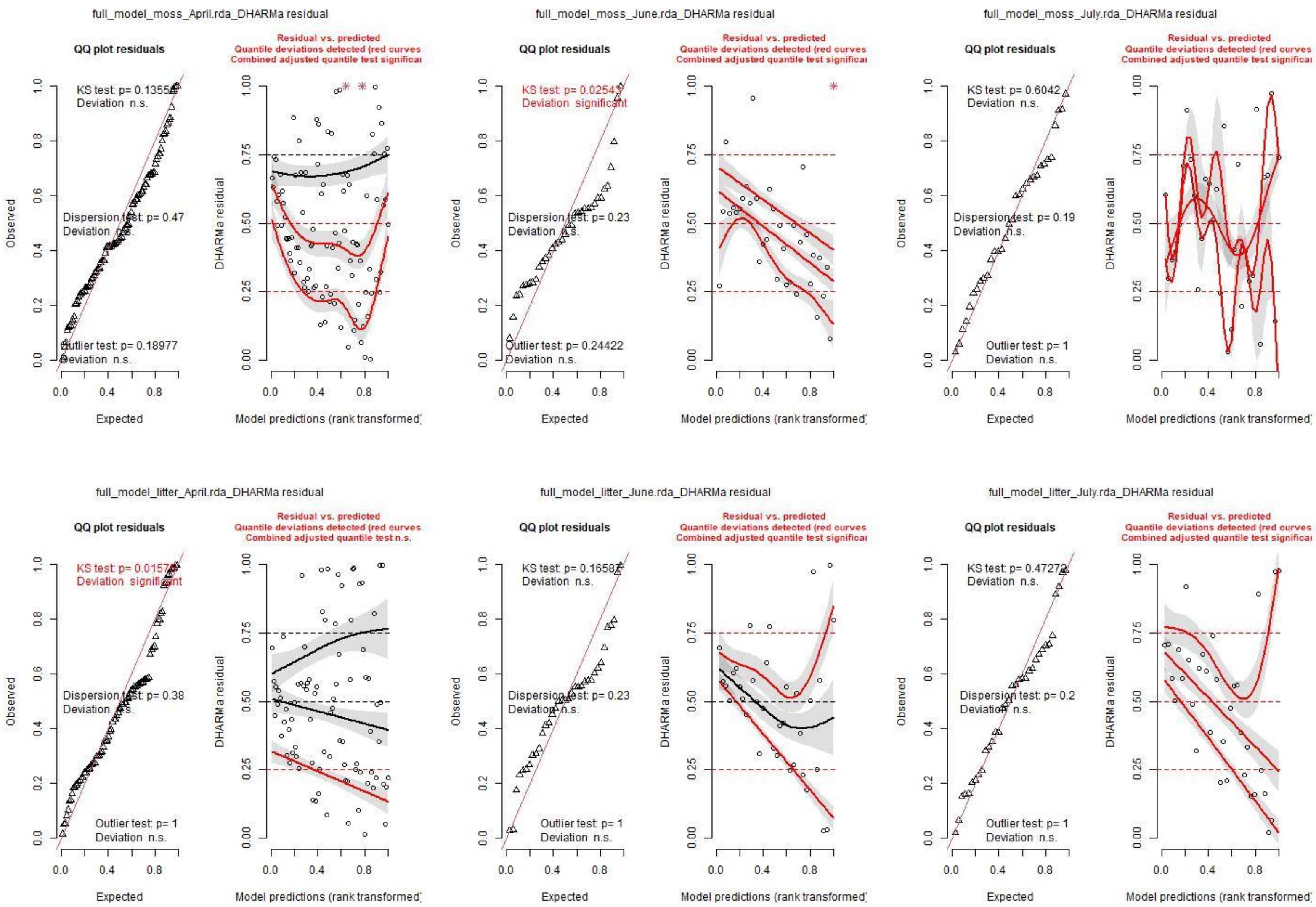
full_model_moss_April.rda_DHARMa residual
QQ plot residuals
KS test: p= 0.1355
Deviation n.s.
Dispersion test: p= 0.47
Deviation n.s.
Outlier test: p= 0.18977
Deviation n.s.
Observed
Expected
Residual vs. predicted
Quantile deviations detected (red curves
Combined adjusted quantile test significa
DHARMa residual
Model predictions (rank transformed)
full_model_moss_June.rda_DHARMa residual
QQ plot residuals
KS test: p= 0.0254
Deviation significant
Dispersion test: p= 0.23
Deviation n.s.
Outlier test: p= 0.24422
Deviation n.s.
Observed
Expected
Residual vs. predicted
Quantile deviations detected (red curves
Combined adjusted quantile test significa
DHARMa residual
Model predictions (rank transformed)
full_model_moss_July.rda_DHARMa residual
QQ plot residuals
KS test: p= 0.6042
Deviation n.s.
Dispersion test: p= 0.19
Deviation n.s.
Outlier test: p= 1
Deviation n.s.
Observed
Expected
Residual vs. predicted
Quantile deviations detected (red curves
Combined adjusted quantile test significa
DHARMa residual
Model predictions (rank transformed)
full_model_litter_April.rda_DHARMa residual
QQ plot residuals
KS test: p= 0.0157
Deviation significant
Dispersion test: p= 0.38
Deviation n.s.
Outlier test: p= 1
Deviation n.s.
Observed
Expected
Residual vs. predicted
Quantile deviations detected (red curves
Combined adjusted quantile test n.s.
DHARMa residual
Model predictions (rank transformed)
full_model_litter_June.rda_DHARMa residual
QQ plot residuals
KS test: p= 0.1658
Deviation n.s.
Dispersion test: p= 0.23
Deviation n.s.
Outlier test: p= 1
Deviation n.s.
Observed
Expected
Residual vs. predicted
Quantile deviations detected (red curves
Combined adjusted quantile test significa
DHARMa residual
Model predictions (rank transformed)
full_model_litter_July.rda_DHARMa residual
QQ plot residuals
KS test: p= 0.4727
Deviation n.s.
Dispersion test: p= 0.2
Deviation n.s.
Outlier test: p= 1
Deviation n.s.
Observed
Expected
Residual vs. predicted
Quantile deviations detected (red curves
Combined adjusted quantile test significa
DHARMa residual
Model predictions (rank transformed)

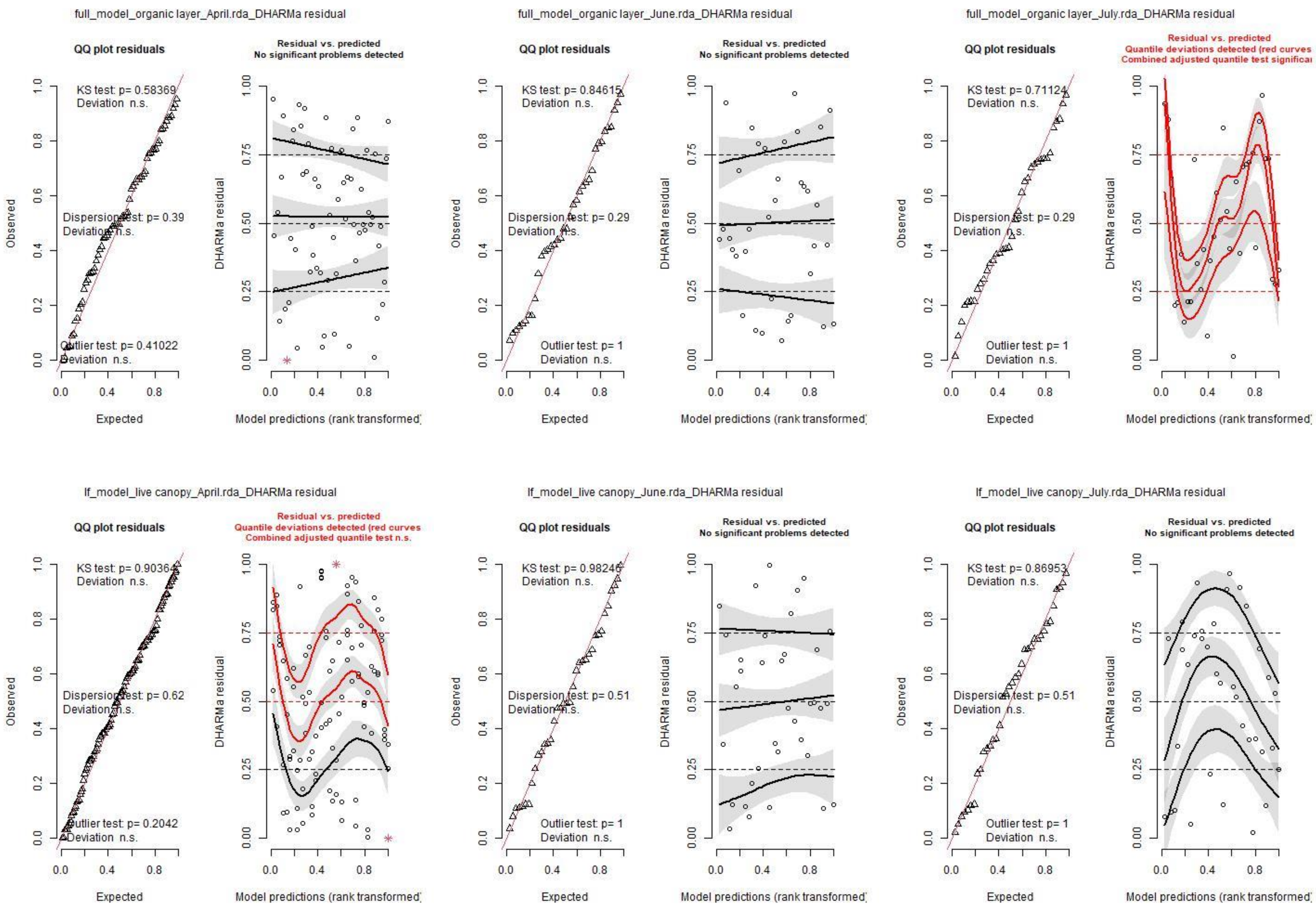
full_model_organic layer_April.rda_DHARMa residual
QQ plot residuals
KS test: p= 0.58369
Deviation n.s.
Dispersion test: p= 0.39
Deviation n.s.
Outlier test: p= 0.41022
Deviation n.s.
Residual vs. predicted
No significant problems detected
full_model_organic layer_June.rda_DHARMa residual
QQ plot residuals
KS test: p= 0.84615
Deviation n.s.
Dispersion test: p= 0.29
Deviation n.s.
Outlier test: p= 1
Deviation n.s.
Residual vs. predicted
No significant problems detected
full_model_organic layer_July.rda_DHARMa residual
QQ plot residuals
KS test: p= 0.71124
Deviation n.s.
Dispersion test: p= 0.29
Deviation n.s.
Outlier test: p= 1
Deviation n.s.
Residual vs. predicted
Quantile deviations detected (red curves
Combined adjusted quantile test significai
lf_model_live canopy_April.rda_DHARMa residual
QQ plot residuals
KS test: p= 0.90364
Deviation n.s.
Dispersion test: p= 0.62
Deviation n.s.
Outlier test: p= 0.2042
Deviation n.s.
Residual vs. predicted
Quantile deviations detected (red curves
Combined adjusted quantile test n.s.
lf_model_live canopy_June.rda_DHARMa residual
QQ plot residuals
KS test: p= 0.98246
Deviation n.s.
Dispersion test: p= 0.51
Deviation n.s.
Outlier test: p= 1
Deviation n.s.
Residual vs. predicted
No significant problems detected
lf_model_live canopy_July.rda_DHARMa residual
QQ plot residuals
KS test: p= 0.86953
Deviation n.s.
Dispersion test: p= 0.51
Deviation n.s.
Outlier test: p= 1
Deviation n.s.
Residual vs. predicted
No significant problems detected
Observed
Expected
DHARMa residual
Model predictions (rank transformed)

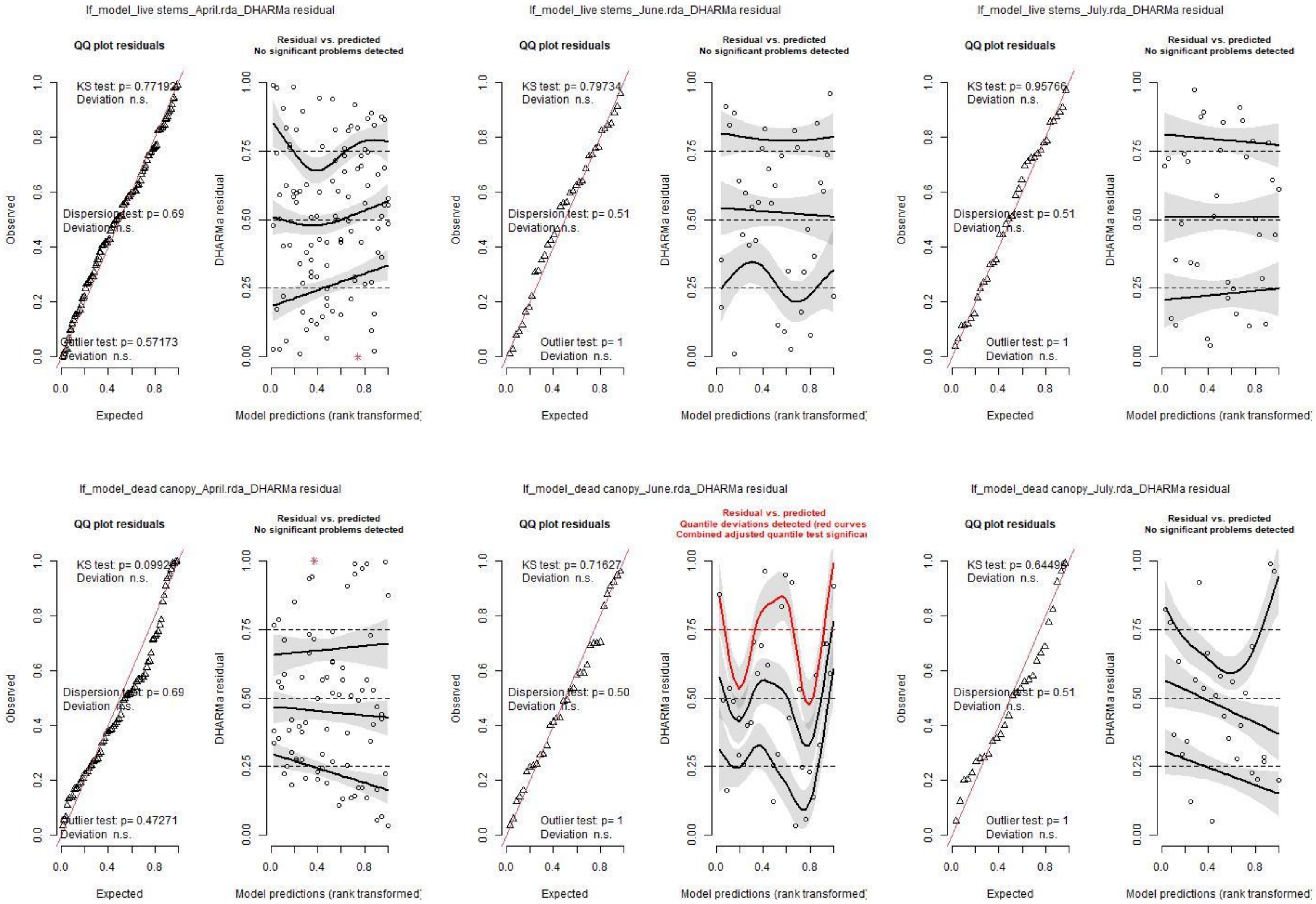

lf_model_live stems_April.rda_DHARMa residual
QQ plot residuals
KS test: p= 0.77192
Deviation n.s.
Dispersion test: p= 0.69
Deviation n.s.
Outlier test: p= 0.57173
Deviation n.s.
Residual vs. predicted
No significant problems detected
lf_model_live stems_June.rda_DHARMa residual
QQ plot residuals
KS test: p= 0.79734
Deviation n.s.
Dispersion test: p= 0.51
Deviation n.s.
Outlier test: p= 1
Deviation n.s.
Residual vs. predicted
No significant problems detected
lf_model_live stems_July.rda_DHARMa residual
QQ plot residuals
KS test: p= 0.95766
Deviation n.s.
Dispersion test: p= 0.51
Deviation n.s.
Outlier test: p= 1
Deviation n.s.
Residual vs. predicted
No significant problems detected
lf_model_dead canopy_April.rda_DHARMa residual
QQ plot residuals
KS test: p= 0.09926
Deviation n.s.
Dispersion test: p= 0.69
Deviation n.s.
Outlier test: p= 0.47271
Deviation n.s.
Residual vs. predicted
No significant problems detected
lf_model_dead canopy_June.rda_DHARMa residual
QQ plot residuals
KS test: p= 0.71627
Deviation n.s.
Dispersion test: p= 0.50
Deviation n.s.
Outlier test: p= 1
Deviation n.s.
Residual vs. predicted
Quantile deviations detected (red curves
Combined adjusted quantile test significa
lf_model_dead canopy_July.rda_DHARMa residual
QQ plot residuals
KS test: p= 0.64496
Deviation n.s.
Dispersion test: p= 0.51
Deviation n.s.
Outlier test: p= 1
Deviation n.s.
Residual vs. predicted
No significant problems detected
Observed
Expected
DHARMa residual
Model predictions (rank transformed)

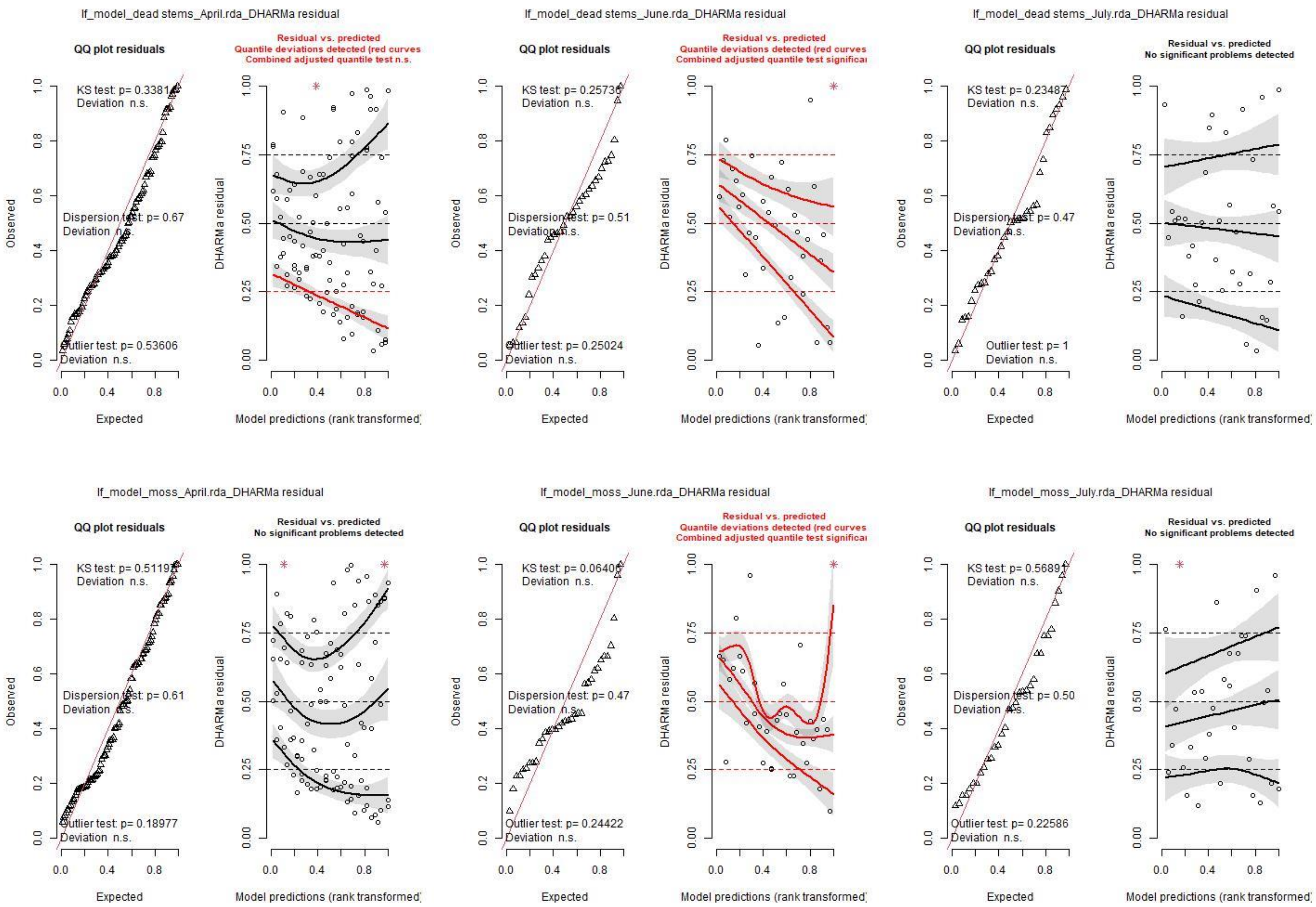

lf_model_dead stems_April.rda_DHARMa residual
QQ plot residuals
KS test: p= 0.3381
Deviation n.s.
Dispersion test: p= 0.67
Deviation n.s.
Outlier test: p= 0.53606
Deviation n.s.
Observed
Expected
Residual vs. predicted
Quantile deviations detected (red curves
Combined adjusted quantile test n.s.
DHARMa residual
Model predictions (rank transformed)
lf_model_dead stems_June.rda_DHARMa residual
QQ plot residuals
KS test: p= 0.25736
Deviation n.s.
Dispersion test: p= 0.51
Deviation n.s.
Outlier test: p= 0.25024
Deviation n.s.
Residual vs. predicted
Quantile deviations detected (red curves
Combined adjusted quantile test significa
lf_model_dead stems_July.rda_DHARMa residual
QQ plot residuals
KS test: p= 0.23487
Deviation n.s.
Dispersion test: p= 0.47
Deviation n.s.
Outlier test: p= 1
Deviation n.s.
Residual vs. predicted
No significant problems detected
lf_model_moss_April.rda_DHARMa residual
QQ plot residuals
KS test: p= 0.51193
Deviation n.s.
Dispersion test: p= 0.61
Deviation n.s.
Outlier test: p= 0.18977
Deviation n.s.
Residual vs. predicted
No significant problems detected
lf_model_moss_June.rda_DHARMa residual
QQ plot residuals
KS test: p= 0.06406
Deviation n.s.
Dispersion test: p= 0.47
Deviation n.s.
Outlier test: p= 0.24422
Deviation n.s.
Residual vs. predicted
Quantile deviations detected (red curves
Combined adjusted quantile test significa
lf_model_moss_July.rda_DHARMa residual
QQ plot residuals
KS test: p= 0.56893
Deviation n.s.
Dispersion test: p= 0.50
Deviation n.s.
Outlier test: p= 0.22586
Deviation n.s.
Residual vs. predicted
No significant problems detected

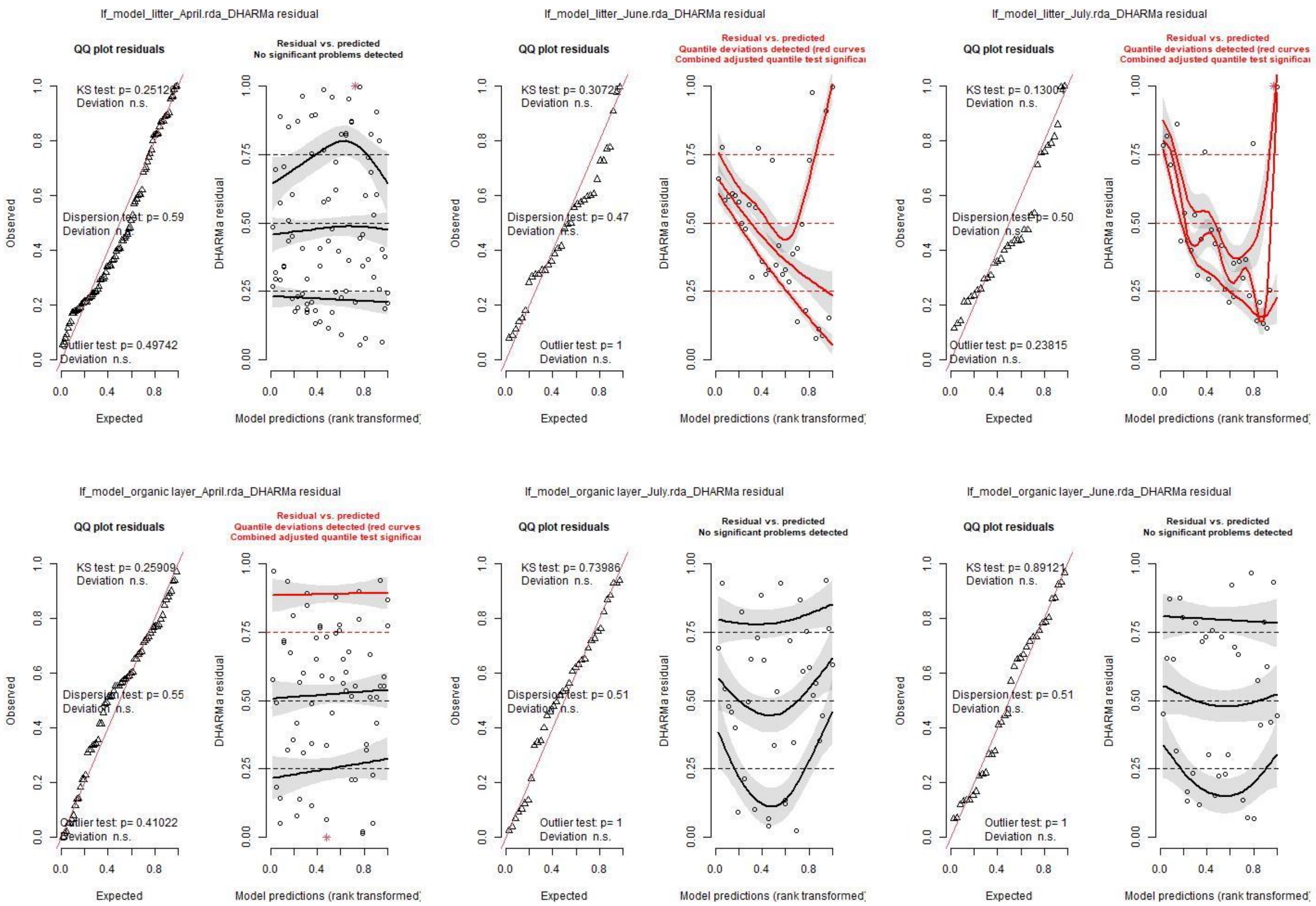
lf_model_litter_April.rda_DHARMa residual
QQ plot residuals
KS test: p= 0.25126
Deviation n.s.
Dispersion test: p= 0.59
Deviation n.s.
Outlier test: p= 0.49742
Deviation n.s.
Observed
Expected
Residual vs. predicted
No significant problems detected
DHARMa residual
Model predictions (rank transformed)
lf_model_litter_June.rda_DHARMa residual
QQ plot residuals
KS test: p= 0.30728
Deviation n.s.
Dispersion test: p= 0.47
Deviation n.s.
Outlier test: p= 1
Deviation n.s.
Observed
Expected
Residual vs. predicted
Quantile deviations detected (red curves
Combined adjusted quantile test significa
DHARMa residual
Model predictions (rank transformed)
lf_model_litter_July.rda_DHARMa residual
QQ plot residuals
KS test: p= 0.13004
Deviation n.s.
Dispersion test: p= 0.50
Deviation n.s.
Outlier test: p= 0.23815
Deviation n.s.
Observed
Expected
Residual vs. predicted
Quantile deviations detected (red curves
Combined adjusted quantile test significa
DHARMa residual
Model predictions (rank transformed)
lf_model_organic layer_April.rda_DHARMa residual
QQ plot residuals
KS test: p= 0.25909
Deviation n.s.
Dispersion test: p= 0.55
Deviation n.s.
Outlier test: p= 0.41022
Deviation n.s.
Observed
Expected
Residual vs. predicted
Quantile deviations detected (red curves
Combined adjusted quantile test significa
DHARMa residual
Model predictions (rank transformed)
lf_model_organic layer_July.rda_DHARMa residual
QQ plot residuals
KS test: p= 0.73986
Deviation n.s.
Dispersion test: p= 0.51
Deviation n.s.
Outlier test: p= 1
Deviation n.s.
Observed
Expected
Residual vs. predicted
No significant problems detected
DHARMa residual
Model predictions (rank transformed)
lf_model_organic layer_June.rda_DHARMa residual
QQ plot residuals
KS test: p= 0.89121
Deviation n.s.
Dispersion test: p= 0.51
Deviation n.s.
Outlier test: p= 1
Deviation n.s.
Observed
Expected
Residual vs. predicted
No significant problems detected
DHARMa residual
Model predictions (rank transformed)

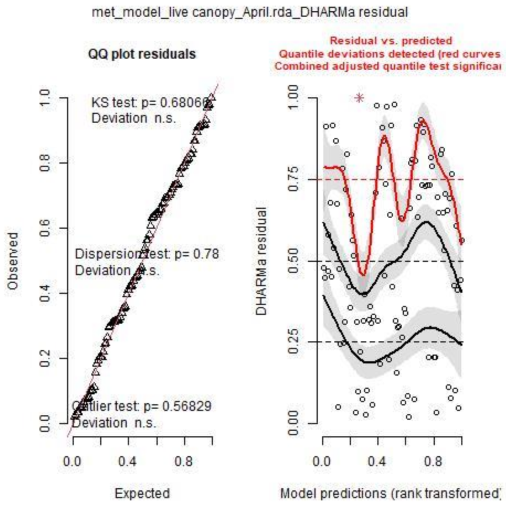
met_model_live canopy_April.rda_DHARMa residual
QQ plot residuals
KS test: p= 0.68066
Deviation n.s.
Dispersion test: p= 0.78
Deviation n.s.
Outlier test: p= 0.56829
Deviation n.s.
Observed
Expected
Residual vs. predicted
Quantile deviations detected (red curves
Combined adjusted quantile test significa
DHARMa residual
Model predictions (rank transformed)

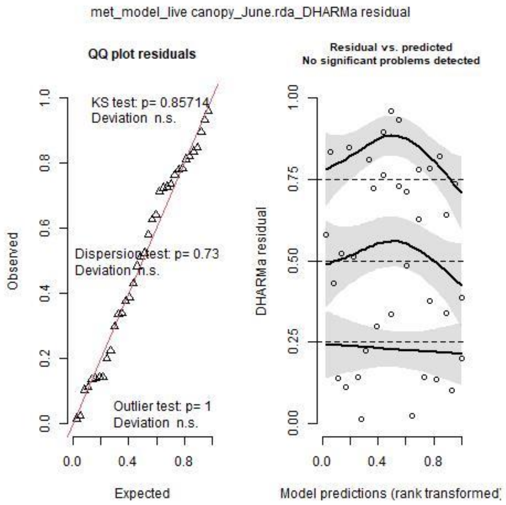
met_model_live canopy_June.rda_DHARMa residual
QQ plot residuals
KS test: p= 0.85714
Deviation n.s.
Dispersion test: p= 0.73
Deviation n.s.
Outlier test: p= 1
Deviation n.s.
Observed
Expected
Residual vs. predicted
No significant problems detected
DHARMa residual
Model predictions (rank transformed)

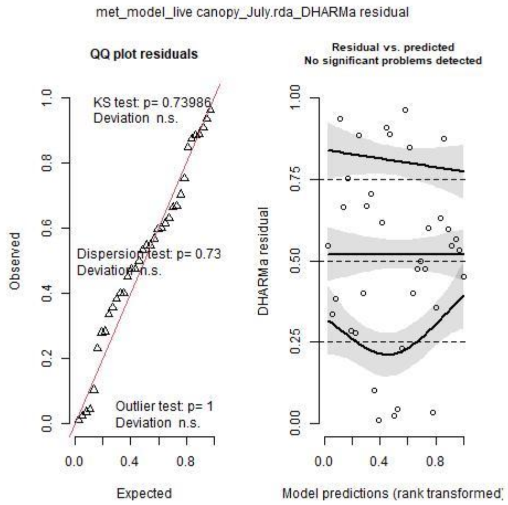
met_model_live canopy_July.rda_DHARMa residual
QQ plot residuals
KS test: p= 0.73986
Deviation n.s.
Dispersion test: p= 0.73
Deviation n.s.
Outlier test: p= 1
Deviation n.s.
Observed
Expected
Residual vs. predicted
No significant problems detected
DHARMa residual
Model predictions (rank transformed)

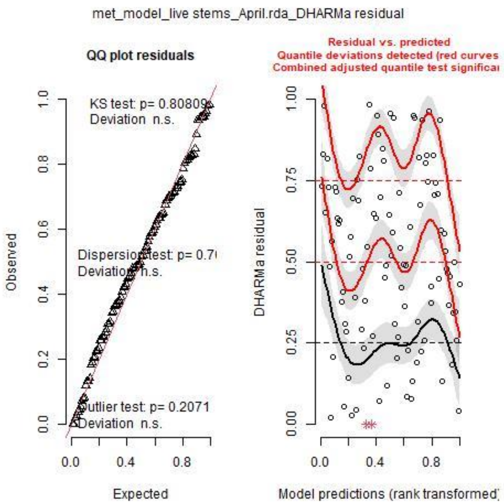
met_model_live stems_April.rda_DHARMa residual
QQ plot residuals
KS test: p= 0.80809
Deviation n.s.
Dispersion test: p= 0.7
Deviation n.s.
Outlier test: p= 0.2071
Deviation n.s.
Observed
Expected
Residual vs. predicted
Quantile deviations detected (red curves
Combined adjusted quantile test significa
DHARMa residual
Model predictions (rank transformed)

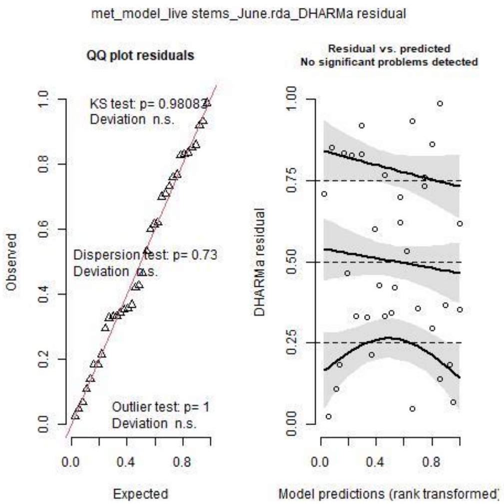
met_model_live stems_June.rda_DHARMa residual
QQ plot residuals
KS test: p= 0.98087
Deviation n.s.
Dispersion test: p= 0.73
Deviation n.s.
Outlier test: p= 1
Deviation n.s.
Observed
Expected
Residual vs. predicted
No significant problems detected
DHARMa residual
Model predictions (rank transformed)

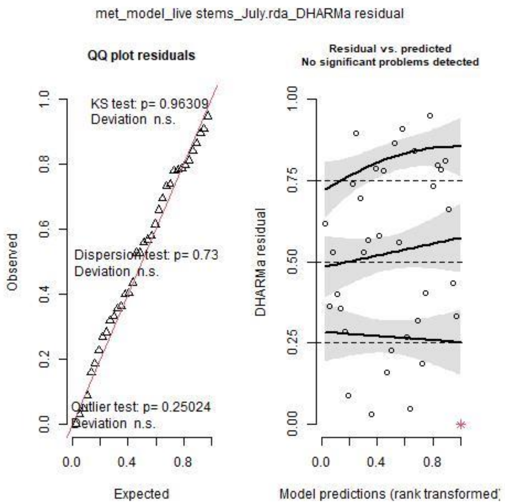
met_model_live stems_July.rda_DHARMa residual
QQ plot residuals
KS test: p= 0.96309
Deviation n.s.
Dispersion test: p= 0.73
Deviation n.s.
Outlier test: p= 0.25024
Deviation n.s.
Observed
Expected
Residual vs. predicted
No significant problems detected
DHARMa residual
Model predictions (rank transformed)

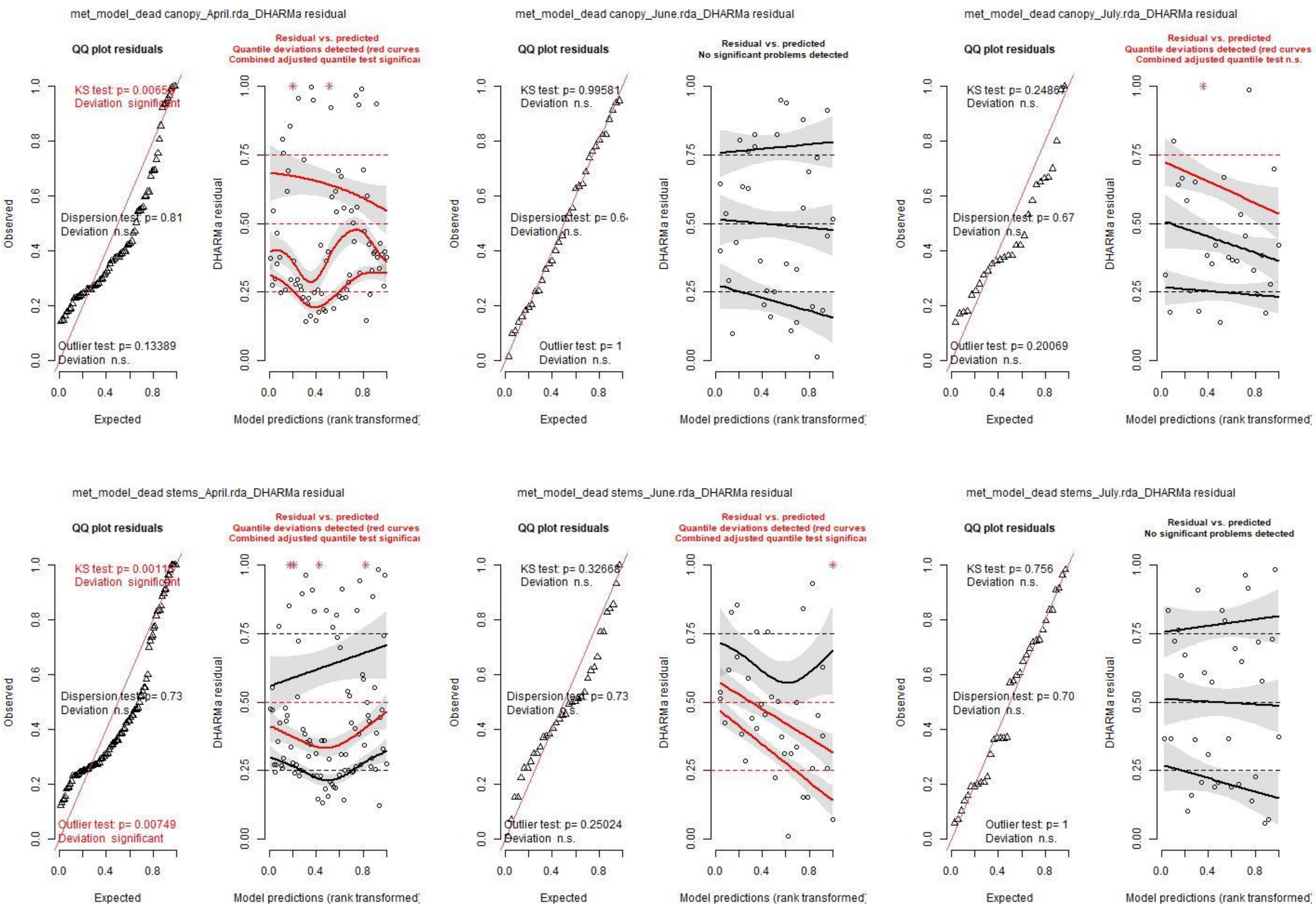
met_model_dead canopy_April.rda_DHARMa residual
QQ plot residuals
KS test: p= 0.0065
Deviation significant
Dispersion test: p= 0.81
Deviation n.s.
Outlier test: p= 0.13389
Deviation n.s.
Residual vs. predicted
Quantile deviations detected (red curves
Combined adjusted quantile test significa
met_model_dead canopy_June.rda_DHARMa residual
QQ plot residuals
KS test: p= 0.99581
Deviation n.s.
Dispersion test: p= 0.6
Deviation n.s.
Outlier test: p= 1
Deviation n.s.
Residual vs. predicted
No significant problems detected
met_model_dead canopy_July.rda_DHARMa residual
QQ plot residuals
KS test: p= 0.2486
Deviation n.s.
Dispersion test: p= 0.67
Deviation n.s.
Outlier test: p= 0.20069
Deviation n.s.
Residual vs. predicted
Quantile deviations detected (red curves
Combined adjusted quantile test n.s.
met_model_dead stems_April.rda_DHARMa residual
QQ plot residuals
KS test: p= 0.0011
Deviation significant
Dispersion test: p= 0.73
Deviation n.s.
Outlier test: p= 0.00749
Deviation significant
Residual vs. predicted
Quantile deviations detected (red curves
Combined adjusted quantile test significa
met_model_dead stems_June.rda_DHARMa residual
QQ plot residuals
KS test: p= 0.3266
Deviation n.s.
Dispersion test: p= 0.73
Deviation n.s.
Outlier test: p= 0.25024
Deviation n.s.
Residual vs. predicted
Quantile deviations detected (red curves
Combined adjusted quantile test significa
met_model_dead stems_July.rda_DHARMa residual
QQ plot residuals
KS test: p= 0.756
Deviation n.s.
Dispersion test: p= 0.70
Deviation n.s.
Outlier test: p= 1
Deviation n.s.
Residual vs. predicted
No significant problems detected
Observed
Expected
DHARMa residual
Model predictions (rank transformed)

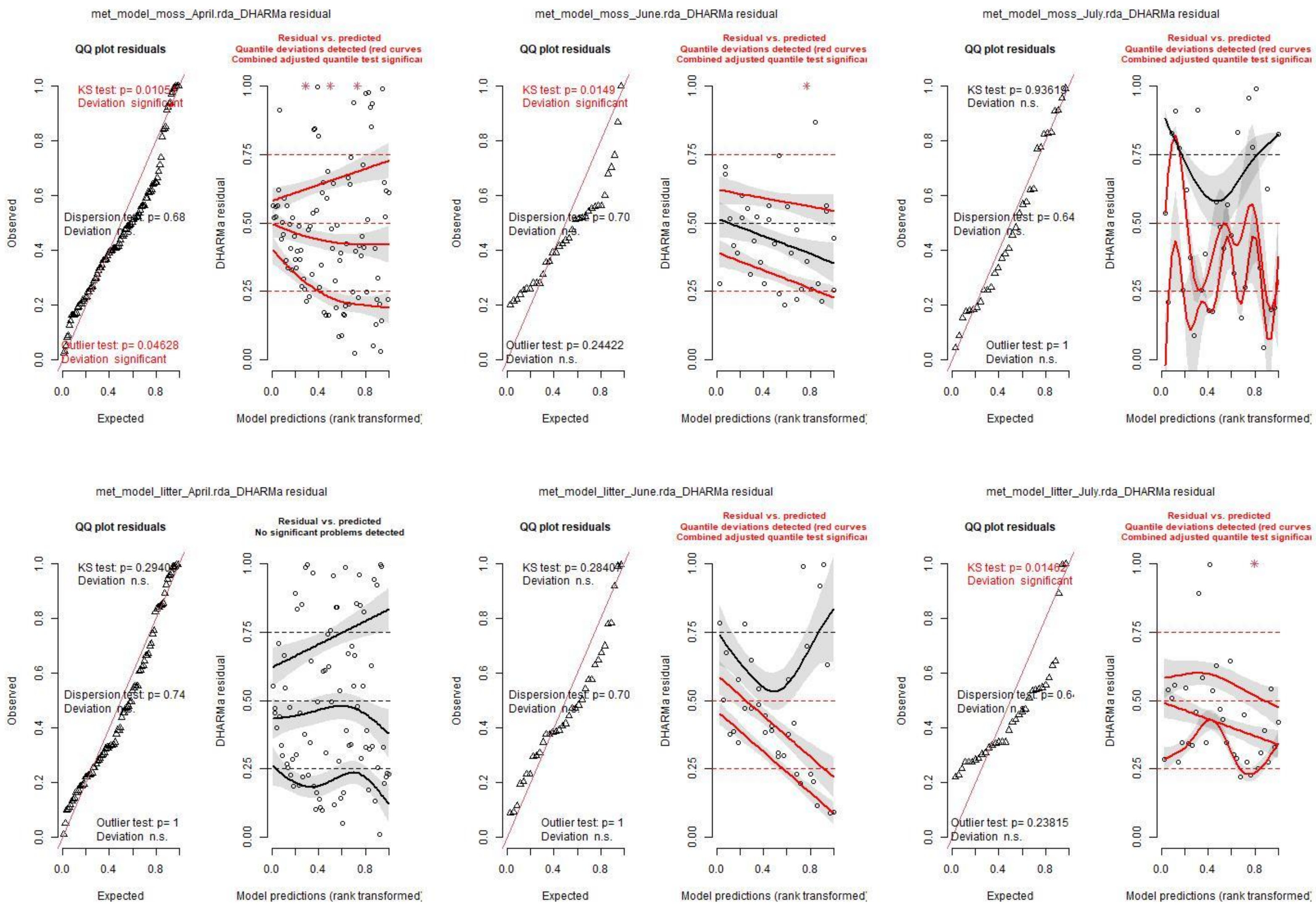
met_model_moss_April.rda_DHARMa residual
QQ plot residuals
KS test: p= 0.0105
Deviation significant
Dispersion test: p= 0.68
Deviation n.s.
Outlier test: p= 0.04628
Deviation significant
Observed
Expected
Residual vs. predicted
Quantile deviations detected (red curves
Combined adjusted quantile test significa
DHARMa residual
Model predictions (rank transformed)
met_model_moss_June.rda_DHARMa residual
QQ plot residuals
KS test: p= 0.0149
Deviation significant
Dispersion test: p= 0.70
Deviation n.s.
Outlier test: p= 0.24422
Deviation n.s.
Observed
Expected
Residual vs. predicted
Quantile deviations detected (red curves
Combined adjusted quantile test significa
DHARMa residual
Model predictions (rank transformed)
met_model_moss_July.rda_DHARMa residual
QQ plot residuals
KS test: p= 0.9361
Deviation n.s.
Dispersion test: p= 0.64
Deviation n.s.
Outlier test: p= 1
Deviation n.s.
Observed
Expected
Residual vs. predicted
Quantile deviations detected (red curves
Combined adjusted quantile test significa
DHARMa residual
Model predictions (rank transformed)
met_model_litter_April.rda_DHARMa residual
QQ plot residuals
KS test: p= 0.2940
Deviation n.s.
Dispersion test: p= 0.74
Deviation n.s.
Outlier test: p= 1
Deviation n.s.
Observed
Expected
Residual vs. predicted
No significant problems detected
DHARMa residual
Model predictions (rank transformed)
met_model_litter_June.rda_DHARMa residual
QQ plot residuals
KS test: p= 0.2840
Deviation n.s.
Dispersion test: p= 0.70
Deviation n.s.
Outlier test: p= 1
Deviation n.s.
Observed
Expected
Residual vs. predicted
Quantile deviations detected (red curves
Combined adjusted quantile test significa
DHARMa residual
Model predictions (rank transformed)
met_model_litter_July.rda_DHARMa residual
QQ plot residuals
KS test: p= 0.0146
Deviation significant
Dispersion test: p= 0.6
Deviation n.s.
Outlier test: p= 0.23815
Deviation n.s.
Observed
Expected
Residual vs. predicted
Quantile deviations detected (red curves
Combined adjusted quantile test significa
DHARMa residual
Model predictions (rank transformed)

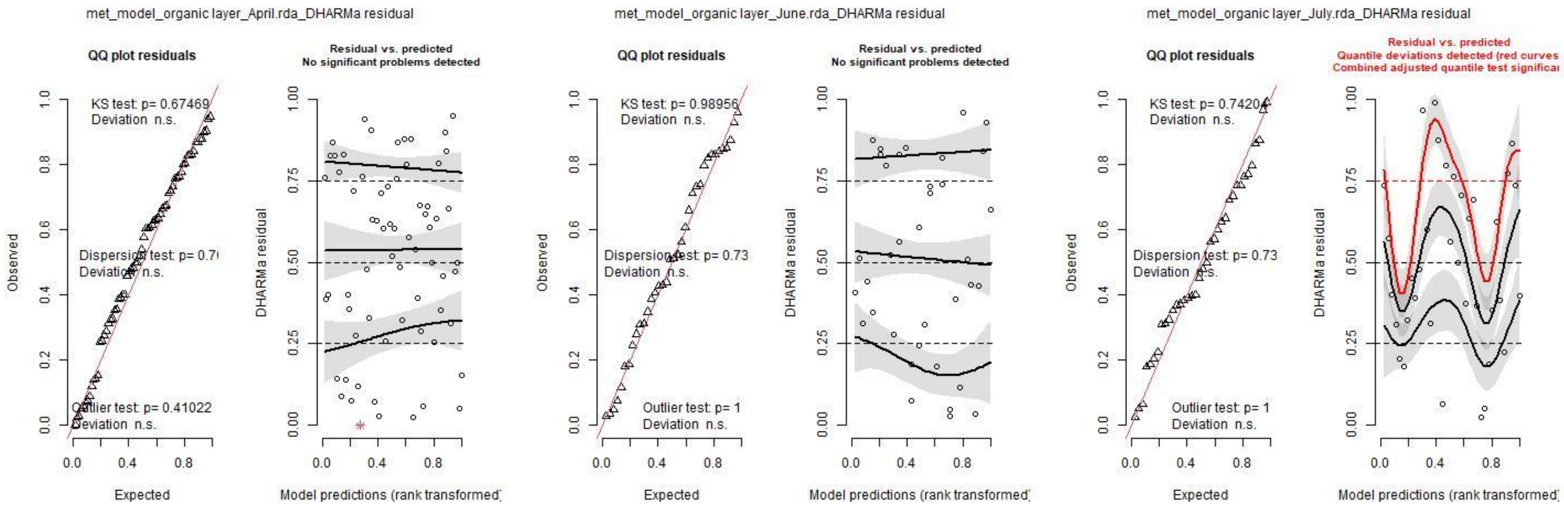

Table S3.3. Moran's I statistic for testing spatial autocorrelation in the landscape, micrometeorological, and combined full linear regression models. Significant p-values (<0.05) are indicated in bold. Number of nearest neighbours = 10 (number of sites included to calculate the weights).

Morans.I	Expected.I	Z resampling	Z randomisation	p.value resampling	p.value randomisation	model type	neighbours	model fuel layer	model month
-0.052	-0.013	-0.957	-0.976	0.339	0.329	full	10	dead canopy	April
-0.097	-0.037	-0.981	-1.008	0.326	0.313	full	10	dead canopy	July
-0.096	-0.030	-1.132	-1.142	0.258	0.253	full	10	dead canopy	June
-0.019	-0.011	-0.221	-0.225	0.825	0.822	full	10	dead stems	April
-0.099	-0.029	-1.186	-1.184	0.236	0.236	full	10	dead stems	July
-0.083	-0.029	-0.918	-0.988	0.359	0.323	full	10	dead stems	June
-0.027	-0.012	-0.399	-0.401	0.690	0.688	full	10	litter	April
-0.095	-0.030	-1.047	-1.052	0.295	0.293	full	10	litter	July
-0.092	-0.029	-1.032	-1.080	0.302	0.280	full	10	litter	June
0.077	-0.010	2.303	2.315	**0.021**	**0.021**	full	10	live canopy	April

-0.071	-0.029	-0.712	-0.709	0.477	0.479	full	10	live canopy	July
-0.096	-0.029	-1.142	-1.142	0.253	0.254	full	10	live canopy	June
-0.026	-0.010	-0.447	-0.451	0.655	0.652	full	10	live stems	April
-0.061	-0.029	-0.549	-0.552	0.583	0.581	full	10	live stems	July
-0.103	-0.029	-1.255	-1.255	0.210	0.210	full	10	live stems	June
-0.059	-0.010	-1.275	-1.300	0.202	0.194	full	10	moss	April
-0.078	-0.032	-0.742	-0.743	0.458	0.457	full	10	moss	July
-0.031	-0.029	-0.025	-0.029	0.980	0.976	full	10	moss	June
0.012	-0.015	0.619	0.623	0.536	0.534	full	10	organic layer	April
-0.032	-0.029	-0.066	-0.066	0.948	0.947	full	10	organic layer	July
-0.097	-0.029	-1.157	-1.145	0.247	0.252	full	10	organic layer	June
-0.058	-0.013	-1.104	-1.119	0.270	0.263	landscape	10	dead canopy	April
-0.061	-0.037	-0.388	-0.396	0.698	0.692	landscape	10	dead canopy	July
-0.048	-0.030	-0.308	-0.308	0.758	0.758	landscape	10	dead canopy	June
-0.036	-0.011	-0.638	-0.647	0.524	0.518	landscape	10	dead stems	April
-0.003	-0.029	0.456	0.456	0.648	0.649	landscape	10	dead stems	July
-0.077	-0.029	-0.817	-0.883	0.414	0.377	landscape	10	dead stems	June
-0.031	-0.012	-0.481	-0.483	0.631	0.629	landscape	10	litter	April
-0.077	-0.030	-0.761	-0.799	0.446	0.424	landscape	10	litter	July
-0.079	-0.029	-0.822	-0.864	0.411	0.388	landscape	10	litter	June
0.195	-0.010	5.405	5.418	**6.5E-08**	**6.0E-08**	landscape	10	live canopy	April
-0.063	-0.029	-0.575	-0.569	0.565	0.570	landscape	10	live canopy	July
-0.059	-0.029	-0.521	-0.521	0.603	0.603	landscape	10	live canopy	June
0.009	-0.010	0.497	0.501	0.619	0.616	landscape	10	live stems	April
0.038	-0.029	1.118	1.110	0.264	0.267	landscape	10	live stems	July
-0.064	-0.029	-0.595	-0.593	0.552	0.553	landscape	10	live stems	June
-0.043	-0.010	-0.858	-0.864	0.391	0.388	landscape	10	moss	April
-0.091	-0.032	-0.955	-0.989	0.340	0.323	landscape	10	moss	July
-0.006	-0.029	0.389	0.472	0.698	0.637	landscape	10	moss	June
0.066	-0.015	1.843	1.858	0.065	0.063	landscape	10	organic layer	April
0.142	-0.029	2.882	2.875	**0.004**	**0.004**	landscape	10	organic layer	July
0.013	-0.029	0.709	0.701	0.478	0.484	landscape	10	organic layer	June
-0.015	-0.013	-0.047	-0.048	0.963	0.962	micromet	10	dead canopy	April
0.052	-0.037	1.463	1.609	0.144	0.108	micromet	10	dead canopy	July
-0.095	-0.030	-1.113	-1.113	0.266	0.266	micromet	10	dead canopy	June
0.021	-0.011	0.781	0.794	0.435	0.427	micromet	10	dead stems	April
-0.021	-0.029	0.135	0.134	0.892	0.893	micromet	10	dead stems	July
-0.086	-0.029	-0.962	-1.043	0.336	0.297	micromet	10	dead stems	June
0.171	-0.012	4.639	4.644	**3.5E-06**	**3.4E-06**	micromet	10	litter	April
0.232	-0.030	4.263	4.947	**2.0E-05**	**7.5E-07**	micromet	10	litter	July
-0.040	-0.029	-0.183	-0.194	0.855	0.846	micromet	10	litter	June
0.253	-0.010	6.946	6.945	**3.8E-12**	**3.8E-12**	micromet	10	live canopy	April
0.313	-0.029	5.760	5.783	**8.4E-09**	**7.3E-09**	micromet	10	live canopy	July

-0.038	-0.029	-0.152	-0.151	0.879	0.880	micromet	10	live canopy	June
0.059	-0.010	1.837	1.849	0.066	0.064	micromet	10	live stems	April
0.003	-0.029	0.539	0.542	0.590	0.588	micromet	10	live stems	July
-0.063	-0.029	-0.581	-0.578	0.561	0.563	micromet	10	live stems	June
0.170	-0.010	4.717	4.799	**2.4E-06**	**1.6E-06**	micromet	10	moss	April
0.000	-0.032	0.527	0.527	0.598	0.598	micromet	10	moss	July
-0.017	-0.029	0.198	0.288	0.843	0.773	micromet	10	moss	June
0.211	-0.015	5.139	5.157	**2.8E-07**	**2.5E-07**	micromet	10	organic layer	April
0.214	-0.029	4.086	4.154	**4.4E-05**	**3.3E-05**	micromet	10	organic layer	July
-0.090	-0.029	-1.028	-1.021	0.304	0.307	micromet	10	organic layer	June

Table S3.4. Moran's I statistic for testing spatial autocorrelation in the landscape, micrometeorological, and combined full linear regression models. Significant p-values (<0.05) are indicated in bold. Number of nearest neighbours = 5 (number of sites included to calculate the weights)

Morans.I	Expected.I	Z resampling	Z randomisation	p.value resampling	p.value randomisation	model type	neighbours	model fuel layer	model month
-0.089	-0.013	-1.267	-1.293	0.205	0.196	full	5	dead canopy	April
-0.184	-0.037	-1.486	-1.528	0.137	0.127	full	5	dead canopy	July
-0.190	-0.030	-1.765	-1.782	0.078	0.075	full	5	dead canopy	June
0.005	-0.011	0.288	0.293	0.773	0.770	full	5	dead stems	April
-0.198	-0.029	-1.884	-1.882	0.060	0.060	full	5	dead stems	July
-0.133	-0.029	-1.180	-1.271	0.238	0.204	full	5	dead stems	June
-0.002	-0.012	0.151	0.152	0.880	0.879	full	5	litter	April
-0.074	-0.030	-0.489	-0.491	0.625	0.623	full	5	litter	July
-0.118	-0.029	-0.999	-1.046	0.318	0.296	full	5	litter	June
0.127	-0.010	2.384	2.396	**0.017**	**0.017**	full	5	live canopy	April
-0.094	-0.029	-0.734	-0.731	0.463	0.465	full	5	live canopy	July
-0.092	-0.029	-0.716	-0.715	0.474	0.474	full	5	live canopy	June
-0.083	-0.010	-1.265	-1.275	0.206	0.202	full	5	live stems	April
-0.102	-0.029	-0.831	-0.837	0.406	0.403	full	5	live stems	July
-0.173	-0.029	-1.632	-1.631	0.103	0.103	full	5	live stems	June
-0.036	-0.010	-0.458	-0.467	0.647	0.641	full	5	moss	April
-0.145	-0.032	-1.203	-1.205	0.229	0.228	full	5	moss	July
-0.061	-0.029	-0.351	-0.422	0.725	0.673	full	5	moss	June
0.164	-0.015	2.634	2.647	**0.008**	**0.008**	full	5	organic layer	April
-0.033	-0.029	-0.046	-0.046	0.963	0.963	full	5	organic layer	July
-0.120	-0.029	-1.028	-1.017	0.304	0.309	full	5	organic layer	June
-0.101	-0.013	-1.473	-1.493	0.141	0.135	landscape	5	dead canopy	April
-0.118	-0.037	-0.817	-0.836	0.414	0.403	landscape	5	dead canopy	July

-0.130	-0.030	-1.105	-1.106	0.269	0.269	landscape	5	dead canopy	June
-0.013	-0.011	-0.039	-0.039	0.969	0.969	landscape	5	dead stems	April
0.006	-0.029	0.397	0.397	0.691	0.692	landscape	5	dead stems	July
-0.128	-0.029	-1.121	-1.212	0.262	0.226	landscape	5	dead stems	June
-0.055	-0.012	-0.691	-0.695	0.489	0.487	landscape	5	litter	April
0.015	-0.030	0.505	0.530	0.613	0.596	landscape	5	litter	July
-0.120	-0.029	-1.025	-1.078	0.305	0.281	landscape	5	litter	June
0.269	-0.010	4.856	4.867	**1.2E-06**	**1.1E-06**	landscape	5	live canopy	April
-0.091	-0.029	-0.705	-0.698	0.481	0.485	landscape	5	live canopy	July
-0.029	-0.029	-0.005	-0.005	0.996	0.996	landscape	5	live canopy	June
-0.030	-0.010	-0.354	-0.357	0.723	0.721	landscape	5	live stems	April
0.061	-0.029	1.016	1.009	0.310	0.313	landscape	5	live stems	July
-0.047	-0.029	-0.210	-0.209	0.834	0.834	landscape	5	live stems	June
-0.059	-0.010	-0.876	-0.881	0.381	0.378	landscape	5	moss	April
-0.067	-0.032	-0.372	-0.386	0.710	0.700	landscape	5	moss	July
-0.030	-0.029	-0.008	-0.010	0.994	0.992	landscape	5	moss	June
0.201	-0.015	3.163	3.190	**0.002**	**0.001**	landscape	5	organic layer	April
0.291	-0.029	3.609	3.600	**0.000**	**0.000**	landscape	5	organic layer	July
0.058	-0.029	0.976	0.964	0.329	0.335	landscape	5	organic layer	June
-0.017	-0.013	-0.064	-0.066	0.949	0.948	micromet	5	dead canopy	April
0.088	-0.037	1.268	1.398	0.205	0.162	micromet	5	dead canopy	July
-0.149	-0.030	-1.316	-1.316	0.188	0.188	micromet	5	dead canopy	June
0.077	-0.011	1.601	1.629	0.109	0.103	micromet	5	dead stems	April
-0.071	-0.029	-0.461	-0.457	0.645	0.648	micromet	5	dead stems	July
-0.095	-0.029	-0.750	-0.814	0.453	0.416	micromet	5	dead stems	June
0.190	-0.012	3.191	3.194	**0.001**	**0.001**	micromet	5	litter	April
0.262	-0.030	3.249	3.766	**0.001**	**0.000**	micromet	5	litter	July
-0.024	-0.029	0.059	0.062	0.953	0.950	micromet	5	litter	June
0.256	-0.010	4.619	4.618	**3.9E-06**	**3.9E-06**	micromet	5	live canopy	April
0.344	-0.029	4.215	4.233	**2.5E-05**	**2.3E-05**	micromet	5	live canopy	July
0.095	-0.029	1.400	1.385	0.162	0.166	micromet	5	live canopy	June
0.013	-0.010	0.391	0.393	0.696	0.694	micromet	5	live stems	April
-0.014	-0.029	0.170	0.171	0.865	0.864	micromet	5	live stems	July
-0.037	-0.029	-0.098	-0.098	0.922	0.922	micromet	5	live stems	June
0.238	-0.010	4.414	4.491	**1.0E-05**	**7.1E-06**	micromet	5	moss	April
0.068	-0.032	1.068	1.067	0.286	0.286	micromet	5	moss	July
0.047	-0.029	0.849	1.235	0.396	0.217	micromet	5	moss	June
0.313	-0.015	4.816	4.833	**1.5E-06**	**1.3E-06**	micromet	5	organic layer	April
0.245	-0.029	3.094	3.146	**0.002**	**0.002**	micromet	5	organic layer	July
-0.066	-0.029	-0.428	-0.425	0.669	0.671	micromet	5	organic layer	June

Table S3.5. Moran's I statistic for testing spatial autocorrelation in the landscape, micrometeorological, and combined full linear regression models. Significant p-values (<0.05) are indicated in bold. Number of nearest neighbours = 2 (number of sites included to calculate the weights).

Morans.I	Expected.I	Z resampling	Z randomisation	p.value resampling	p.value randomisation	model type	neighbours	model fuel layer	model month
-0.038	-0.013	-0.259	-0.264	0.796	0.792	full	2	dead canopy	April
-0.330	-0.037	-1.779	-1.830	0.075	0.067	full	2	dead canopy	July
-0.405	-0.030	-2.465	-2.489	**0.014**	**0.013**	full	2	dead canopy	June
0.141	-0.011	1.714	1.740	0.087	0.082	full	2	dead stems	April
-0.386	-0.029	-2.374	-2.372	**0.018**	**0.018**	full	2	dead stems	July
-0.337	-0.029	-2.052	-2.213	**0.040**	**0.027**	full	2	dead stems	June
0.099	-0.012	1.147	1.153	0.251	0.249	full	2	litter	April
0.009	-0.030	0.249	0.250	0.803	0.802	full	2	litter	July
-0.136	-0.029	-0.693	-0.726	0.488	0.468	full	2	litter	June
0.208	-0.010	2.314	2.326	**0.021**	**0.020**	full	2	live canopy	April
0.162	-0.029	1.269	1.263	0.205	0.206	full	2	live canopy	July
-0.231	-0.029	-1.349	-1.349	0.177	0.177	full	2	live canopy	June
-0.105	-0.010	-1.006	-1.014	0.314	0.311	full	2	live stems	April
-0.050	-0.029	-0.142	-0.143	0.887	0.886	full	2	live stems	July
-0.273	-0.029	-1.626	-1.625	0.104	0.104	full	2	live stems	June
0.103	-0.010	1.245	1.269	0.213	0.204	full	2	moss	April
-0.079	-0.032	-0.290	-0.291	0.772	0.771	full	2	moss	July
-0.198	-0.029	-1.109	-1.337	0.268	0.181	full	2	moss	June
0.582	-0.015	5.975	6.006	**2E-09**	**0.000**	full	2	organic layer	April
0.045	-0.029	0.493	0.497	0.622	0.619	full	2	organic layer	July
-0.172	-0.029	-0.955	-0.945	0.340	0.345	full	2	organic layer	June
-0.043	-0.013	-0.303	-0.307	0.762	0.759	landscape	2	dead canopy	April
-0.102	-0.037	-0.395	-0.404	0.693	0.686	landscape	2	dead canopy	July
-0.220	-0.030	-1.248	-1.249	0.212	0.212	landscape	2	dead canopy	June

0.097	-0.011	1.217	1.234	0.224	0.217	landscape	2	dead stems	April
0.092	-0.029	0.809	0.808	0.419	0.419	landscape	2	dead stems	July
-0.213	-0.029	-1.227	-1.329	0.220	0.184	landscape	2	dead stems	June
-0.083	-0.012	-0.734	-0.738	0.463	0.461	landscape	2	litter	April
0.266	-0.030	1.895	1.989	**0.058**	**0.047**	landscape	2	litter	July
-0.078	-0.029	-0.318	-0.335	0.751	0.738	landscape	2	litter	June
0.305	-0.010	3.346	3.354	**0.001**	**0.001**	landscape	2	live canopy	April
0.268	-0.029	1.976	1.955	**0.048**	**0.051**	landscape	2	live canopy	July
-0.052	-0.029	-0.154	-0.154	0.878	0.878	landscape	2	live canopy	June
-0.120	-0.010	-1.160	-1.171	0.246	0.242	landscape	2	live stems	April
0.144	-0.029	1.148	1.141	0.251	0.254	landscape	2	live stems	July
-0.021	-0.029	0.049	0.049	0.961	0.961	landscape	2	live stems	June
-0.140	-0.010	-1.425	-1.434	0.154	0.152	landscape	2	moss	April
-0.052	-0.032	-0.123	-0.127	0.902	0.899	landscape	2	moss	July
-0.193	-0.029	-1.077	-1.314	0.281	0.189	landscape	2	moss	June
0.531	-0.015	5.460	5.506	**4.8E-08**	**3.7E-08**	landscape	2	organic layer	April
0.487	-0.029	3.432	3.423	**0.001**	**0.001**	landscape	2	organic layer	July
0.172	-0.029	1.335	1.319	0.182	0.187	landscape	2	organic layer	June
0.040	-0.013	0.530	0.542	0.596	0.588	micromet	2	dead canopy	April
0.180	-0.037	1.319	1.456	0.187	0.145	micromet	2	dead canopy	July
-0.356	-0.030	-2.144	-2.145	**0.032**	**0.032**	micromet	2	dead canopy	June
0.343	-0.011	3.985	4.055	**6.7E-05**	**5.0E-05**	micromet	2	dead stems	April
-0.213	-0.029	-1.221	-1.209	0.222	0.227	micromet	2	dead stems	July
-0.291	-0.029	-1.749	-1.899	0.080	0.058	micromet	2	dead stems	June
0.413	-0.012	4.402	4.406	**1.1E-05**	**1.1E-05**	micromet	2	litter	April
0.552	-0.030	3.722	4.331	**0.000**	**1.5E-05**	micromet	2	litter	July
-0.023	-0.029	0.045	0.048	0.964	0.962	micromet	2	litter	June
0.335	-0.010	3.665	3.664	**0.000**	**0.000**	micromet	2	live canopy	April
0.646	-0.029	4.490	4.509	**7.1E-06**	**6.5E-06**	micromet	2	live canopy	July

0.033	-0.029	0.412	0.408	0.680	0.684	micromet	2	live canopy	June
0.043	-0.010	0.554	0.558	0.579	0.577	micromet	2	live stems	April
0.058	-0.029	0.580	0.583	0.562	0.560	micromet	2	live stems	July
-0.038	-0.029	-0.066	-0.066	0.947	0.948	micromet	2	live stems	June
0.294	-0.010	3.336	3.395	**0.001**	**0.001**	micromet	2	moss	April
0.153	-0.032	1.145	1.144	0.252	0.253	micromet	2	moss	July
0.038	-0.029	0.445	0.654	0.656	0.513	micromet	2	moss	June
0.659	-0.015	6.737	6.761	**1.6E-11**	**1.4E-11**	micromet	2	organic layer	April
0.415	-0.029	2.951	3.002	**0.003**	**0.003**	micromet	2	organic layer	July
-0.106	-0.029	-0.518	-0.514	0.605	0.607	micromet	2	organic layer	June

CHAPTER 4: SUPPLEMENTARY MATERIAL

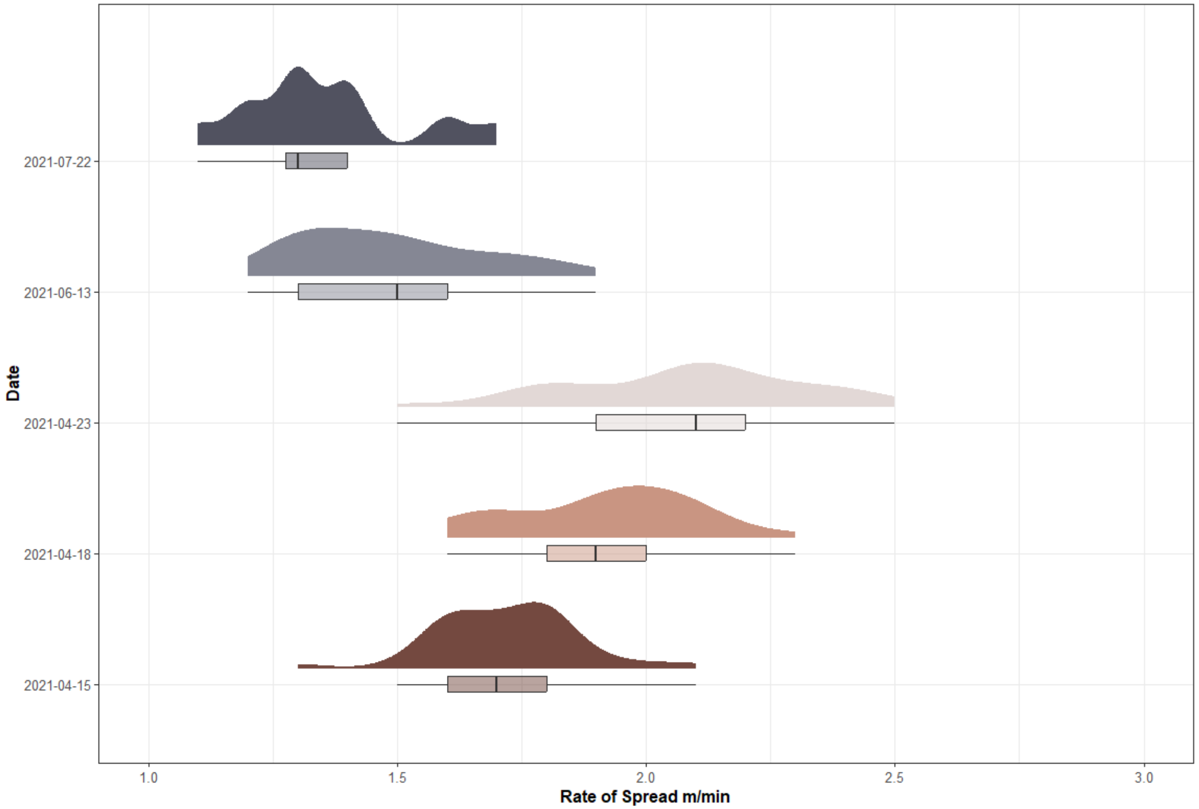

Figure S4.1. Cross-landscape predicted rate of spread (m/min) variation from observed fuel moisture content inputs for five days during the spring and summer of 2021.

Table S4.1. Kruskall-Wallis (KW) test for differences in predicted rate of spread between different fuel layer fuel moisture inputs for each of the five dates. P < 0.05 differences are indicated in bold. Table S2 examines specific fuel layer differences for significant Kruskal-Wallis outcomes.

fuel layer	**date**	**KW chi-squared**	**p-value**
Live	15/04/2021	38.134	**0.000**
Live	18/04/2021	25.827	**0.000**
Live	23/04/2021	18.928	**0.000**
Live	13/06/2021	5.127	0.077
Live	22/07/2021	37.089	**0.000**
Dead	15/04/2021	0.269	0.874
Dead	18/04/2021	0.629	0.730
Dead	23/04/2021	0.015	0.993
Dead	13/06/2021	0.063	0.969
Dead	22/07/2021	1.908	0.385
Predicted dead	23/04/2021	6.546	**0.038**
Predicted dead	22/07/2021	0.756	0.685

Table S4.2. Wilcoxon rank sum test pairwise comparisons for differences in predicted rate of spread calculated using different fuel layer fuel moisture content inputs. Statistically significant differences (p < 0.05) are indicated in bold.

Pairwise fuel layers	15/04/2021	18/04/2021	23/04/2021	13/06/2021	22/07/2021
Live combined X live canopy	**0.001**	**0.013**	**0.016**	**0.357**	**0.0025**
Live combined X live stems	**0.000**	**0.000**	**0.006**	**0.289**	**0.000**
Live stems X live canopy	**0.000**	**0.000**	**0.000**	**0.089**	**0.000**
Dead combined X Fosberg dead shaded	-	-	0.270	-	0.570
Dead combined X Fosberg dead unshaded	-	-	**0.000**	-	**0.000**
Fosberg dead unshaded X Fosberg dead shaded	-	-	**0.000**	-	**0.000**

Table S4.3. Spearman Rank correlation coefficients for dead fuel moisture content predicted using the shaded and unshaded versions of Fosberg's model and observed combined dead fuel moisture content (average of canopy and stems for each site) on 23/04/2021. Significant correlations ($p < 0.01$) are indicated in bold.

	Fosberg dead unshaded	Fosberg dead shaded	Dead combined fmc
Fosberg dead unshaded	1.000	**0.880**	-0.070
Fosberg dead shaded	**0.880**	1.000	0.010
Dead combined fmc	-0.070	0.010	1.000

Table S4.4. Spearman Rank correlation coefficients for dead fuel moisture content predicted using the shaded and unshaded versions of Fosberg's model and observed combined dead fuel moisture content (average of canopy and stems for each site) on the 22/07/2021. Significant correlations ($p < 0.01$) are indicated in bold.

	Fosberg dead unshaded	Fosberg dead shaded	Dead combined fmc
Fosberg dead unshaded	1.000	**0.980**	**0.460**
Fosberg dead shaded	**0.980**	1.000	**0.480**
Dead combined fmc	**0.460**	**0.480**	1.000

CHAPTER 5: SUPPLEMENTARY MATERIAL

Field Course Sampling Protocol

Sampling strategy adapted from Norum and Miller (1984)

1. Equipment

- 2 pairs secateurs (one for cutting dead material, one for cutting live material)
- Aluminium, rust proof sampling containers with tight-fitting screw lids
- Masking tape for sealing tins
- Pen/clipboard/recording sheets
- Gardening gloves

2. *Calluna vulgaris* sampling strategy

Samples will be collected from the following fuel layers:

1. Live canopy
2. Live stems (<2 mm diameter)
3. Dead canopy
4. Dead stems (<2 mm diameter)
5. Moss layer (top 2 cm)
6. Litter layer (top 2 cm)

2.1 Set out a 25 m transect covering a representative area of the site. Starting with the live *Calluna,* walk along the transect taking the same size sample from each plant, collecting sprigs from approximately 10 plants (Figure S1). Clip the sprigs into small one-inch segments, separating the top shoots and canopy into one tin and the lower canopy and stems into another. Aim to take the same approximate mass for each sample of the same material and fill the tin ¾ full.
Nb. Live heather may look brown or grey early in spring. If you are unsure if it is live heather or dead bend the stem. Dead heather stems should easily break and be brown inside. Live heather stems will bend and be harder to break. The inside of the stem will be green.

2.2 Repeat step 1 but for dead heather plants.
Nb. You may find completely dead plants, sections of dead heather or sprigs that have been pulled out from grazing sheep.

2.3 In the same haphazard manner, collect moss along the transect by grasping the top 2 cm of moss and pulling it up from the moss layer. Clip off the highly decomposed dark brown moss from the base of the layer.
2.4 Collect litter in the same manner underneath *Calluna* plants, grasping the top 2 cm of litter above the organic soil layer.
2.5 As soon as you have collected the material for one tin, replace the lid tightly and seal it with masking tape.
2.6 Record the following details on your sampling sheet: the tin number for each fuel layer, sampling time, date and sampler name.

3. Laboratory protocol

3.1 Preheat drying oven to 80 ˚C.

3.2 Remove masking tape from tin lid, ensure no tape or debris is stuck to the tin.

3.3 Weigh sample, with the lid still on, to 3 dp and record this as the wet weight. Repeat for all samples.

3.4 Remove the lid and place it under the tin as you put the sample in the drying oven. Space the samples evenly in the oven so air can circulate.

3.5 Record the date and time the samples were put in the oven.

3.6 Dry samples for at least 48 hours at 80 ˚C.

3.7 Remove samples from the oven in batches, quickly replacing the lid tightly as each tin is removed to prevent absorption of moisture. Close the oven door in between batches.

3.8 Allow the tins to cool to room temperature before weighing them and record the dry weight (following step 3).

3.9 Calculate fuel moisture content (%) as mass of water as a percentage of the mass of the dried sample (Equation 1).

$$\text{Fuel moisture content} = \frac{(\text{sample wet weight} - \text{sample dry weight})}{(\text{sample dry weight} - \text{container tare weight})} * 100 \qquad \text{[Eq.1]}$$

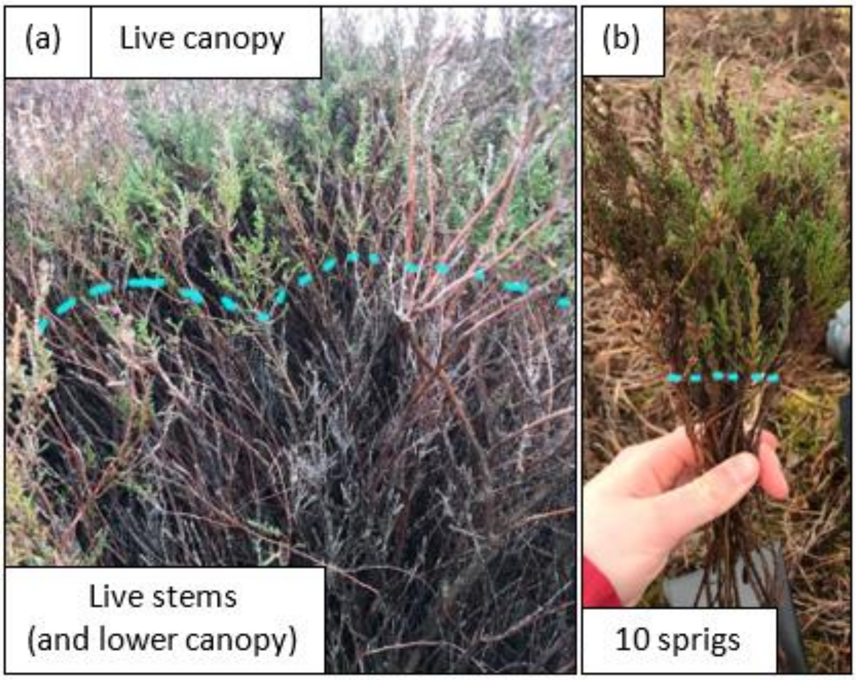

Figure S5.1 (a) Identifying live canopy material from live stems (and grey lower canopy material). (b) Collecting 10 sprigs as per step 2.1.

References

Norum R a., Miller M (1984) Measuring Fuel Moisture Content in Alaska: Standard Methods and Protocols. *General Technical Report* 1–40. doi:10.1016/S0140-6701(02)85652-1.

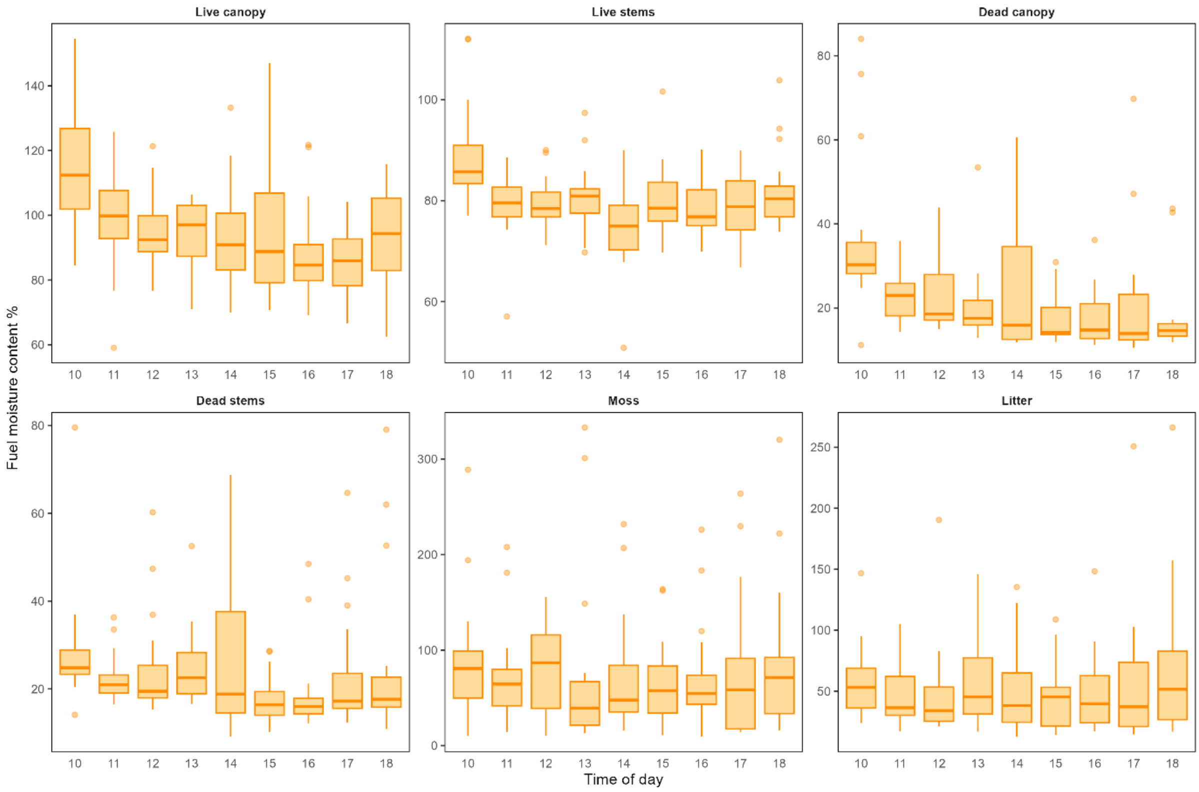

Figure S5.2 Measurement variability in fuel moisture content measurements for each fuel layer hourly from 10:00 to 18:00. Each y-axis is scaled independently to clearly visualise within-fuel layer measurement variability.